nature mental health

Supplementary information https://doi.org/10.1038/s44220-025-00493-5

An umbrella review of neuroimaging studies and conceptual framework linking pathophysiology and psychopathology in schizophrenia

In the format provided by the authors and unedited

TABLE OF CONTENTS

Umbrella review of neuroimaging data in schizophrenia

Additional data on brain alterations in schizophrenia

Alterations in task-based brain activation

Early-onset schizophrenia was associated with decreased task-based brain activation in the occipital cortex and precuneus (belonging to the visual network (VN) and dorsal attention network (DAN)), as well as increased task-based brain activation in the dorsolateral prefrontal cortex and precuneus (belonging to the central executive network (CEN) and default-mode network (DMN)) and in the cerebellum, during cognitive processing.

Chronic-stage schizophrenia was associated with decreased task-based brain activation primarily in the thalamus and dorsolateral prefrontal cortex (mainly belonging to the CEN), along with heterogeneous changes across other subcortical and cortical areas during perception, emotion, and cognitive processing. However, when considering specific tasks, some differentiated patterns of alterations emerged.

Perception. During perception processing (of auditory stimuli), schizophrenia was associated with decreased task-based activation in the superior temporal gyrus, frontal areas, thalamus, and hippocampus.

Emotion processing. During emotion processing, schizophrenia was associated with: decreased task-based activation in the dorsolateral prefrontal cortex, superior temporal gyrus, fusiform gyrus, thalamus, hippocampus, and cerebellum; increased activation in the postcentral gyrus/posterior parietal cortex; and decreased or increased activation in the precentral gyrus, occipital cortex, temporal pole, midline structures, insula, basal ganglia, amygdala, and brainstem.

More specifically, during emotion processing of neutral stimuli, schizophrenia was associated with decreased activation in the dorsolateral prefrontal cortex and fusiform gyrus, as well as increased activation in the striatum (extending to the amygdala and insula) and precentral gyrus.

During emotion processing of negative stimuli, schizophrenia was associated with decreased activation in the dorsolateral prefrontal cortex, fusiform gyrus, thalamus, amygdala, and cerebellum, alongside increased activation in the anterior cingulate cortex/medial prefrontal cortex.

Finally, during emotion processing of positive stimuli, schizophrenia was associated with: decreased activation in the dorsolateral prefrontal cortex, anterior cingulate cortex/medial prefrontal cortex, precentral gyrus, superior temporal gyrus, and thalamus; increased activation in the postcentral gyrus, middle cingulate cortex, and amygdala; and decreased or increased activation in the striatum and brainstem.

Cognitive processing. During cognitive processing, schizophrenia was associated with decreased task-based activation primarily in the dorsolateral prefrontal cortex, thalamus, basal ganglia, and cerebellum, while also showing decreased or increased activation in midline structures, the insula, precentral/postcentral gyri, posterior parietal cortex, temporal cortex, and occipital cortex.

More specifically, during cognitive processing of episodic memory, schizophrenia was associated with: decreased activation in the dorsolateral prefrontal cortex, posterior cingulate cortex/precuneus and angular gyrus, thalamus, and cerebellum; increased activation in the postcentral gyrus and posterior parietal cortex; and decreased or increased activation in the anterior cingulate cortex/medial prefrontal cortex, precentral gyrus, temporal cortex, and occipital cortex.

During cognitive processing of working memory, schizophrenia was associated with decreased activation in the dorsolateral prefrontal cortex, precuneus, insula, basal ganglia, and cerebellum, as well as increased activation in the anterior cingulate cortex/medial prefrontal cortex, posterior cingulate cortex/precuneus, angular gyrus, temporal pole, precentral gyrus, and occipital cortex.
During cognitive processing of timing, schizophrenia was associated with decreased activation in the dorsolateral prefrontal cortex, superior temporal gyrus, thalamus, and basal ganglia, while also showing decreased or increased activation in the anterior cingulate cortex/medial prefrontal cortex and occipital cortex.
During cognitive processing of executive functions, schizophrenia was associated with: decreased activation in the dorsolateral prefrontal cortex, thalamus, and basal ganglia; increased activation in the posterior parietal cortex, middle temporal gyrus, and amygdala; and decreased or increased activation in the anterior cingulate cortex/medial prefrontal cortex, insula, precentral gyrus, and occipital cortex.
Finally, during cognitive processing of theory of mind, schizophrenia was associated with decreased activation in the medial prefrontal cortex, angular gyrus, posterior cingulate cortex, superior temporal gyrus, precentral/postcentral gyri, and occipital cortex, as well as increased activation in the posterior parietal cortex, dorsolateral prefrontal cortex, and precuneus.
See **Supplementary Figures 3–14** and **Supplementary Table 3**.

Brain correlates of symptoms
Positive symptomatology in schizophrenia correlated with: increases in intrinsic brain activity in the precuneus, inferior parietal lobule, medial prefrontal cortex, and superior frontal gyrus (belonging to the DMN and CEN)[1]; and increases in task-based brain activation in the inferior frontal gyrus (belonging to the DMN) during cognitive processing of theory of mind[2], as well as decreased task-based activation in the amygdala during emotion processing of negative stimuli[3].
On the other hand, negative symptomatology in schizophrenia correlated with: deficits in grey matter in the insula and medial prefrontal cortex[4]; alterations in white matter in the insular area and uncinate fasciculus[5]; decreases in intrinsic brain activity in the striatum[1]; and decreases in task-based brain activation in the striatum during emotion processing of positive stimuli[6], as well as decreased task-based activation in the supramarginal gyrus during cognitive processing of theory of mind[2].
See **Supplementary Table 2**.

Relationship of brain alterations between schizophrenia and other psychiatric disorders

The spatiotemporal pattern of brain alterations in prototypical schizophrenia notably overlaps with features observed in other major psychiatric disorders, such as bipolar disorder and major depressive disorder, while also exhibiting key distinctive features. These comparisons may further help delineate the specific roles of brain alterations in the pathophysiology and psychopathology of schizophrenia.
At the structural level, a substantial profile of shared brain alterations has been reported across schizophrenia, bipolar disorder, and major depressive disorder[7-12]. These overlapping deficits span multiple distributed brain regions, complicating efforts to disentangle the disorders or to identify smaller, yet potentially relevant, disorder-specific abnormalities.
In particular, grey matter alterations have been consistently observed across major psychiatric disorders in a set of brain regions, including decreased volume in midline structures (anterior

cingulate cortex, medial and orbital prefrontal cortex), opercular regions (insula, inferior frontal gyrus/frontal operculum, parietal operculum, and superior temporal gyrus/temporal pole), inferomedial temporal regions (hippocampus, amygdala, parahippocampal area, and fusiform gyrus), and the thalamus; increased volume in the basal ganglia; and possible reductions in the dorsolateral prefrontal and occipital cortices[7-11]. Among these regions, grey matter loss in the anterior insula and anterior cingulate cortex has emerged as a core alteration robustly shared across schizophrenia, bipolar disorder, and major depressive disorder; damage to these areas, which are part of the salience network (SN), is likely involved in disruptions of interoception, affectivity, salience detection, and related cognitive processes across conditions[7,13]. Furthermore, reductions in grey matter in the hippocampus and amygdala are also consistently shared across these disorders and have been dimensionally linked to stress system activation[8,10]. Increased basal ganglia volume has been associated with medication effects[7,10]. Lastly, grey matter reductions in the thalamus (and subcortical regions more broadly), as well as in the dorsolateral prefrontal cortex (and occipital cortex), appear most prominent in the chronic stage of schizophrenia (as reported in the present work), and may thus contribute to cognitive deterioration.

In contrast, key differences in grey matter alterations between major psychiatric disorders are also evident. Beyond the widely accepted notion of earlier onset and more severe structural alterations, schizophrenia is associated with more extensive and pronounced grey matter deficits, including reductions in grey matter volume, cortical thickness, and cortical surface area, compared to the other disorders[7-8,10-11]. Interestingly, while cortical thickness deficits are shared across disorders, cortical surface area reductions appear to be shared between schizophrenia and major depressive disorder, but not bipolar disorder[11]. On a regional level, grey matter loss in opercular regions—particularly the superior temporal gyrus—appears to be unique to schizophrenia and is detectable from the first-episode/early psychosis stage, as it is less commonly observed in bipolar disorder and major depressive disorder[7-8]. Notably, deficits in these opercular areas have been robustly linked to hallucinations[14].

White matter abnormalities are also broadly shared among major psychiatric disorders. However, white matter deficits in core limbic tracts—namely the fornix and cingulum—are shared between schizophrenia and bipolar disorder and emerge early in the illness course; by contrast, white matter alterations in major depressive disorder tend to be inconsistent[9,12].

At the functional level, abnormalities in the DMN**,** CEN, and SN are widely observed across major psychiatric disorders, although the directionality and specific features of these changes may differ. Decreased intrinsic activity in the DMN appears to be shared between the first-episode/early psychosis stage of schizophrenia and the manic state of bipolar disorder, as well as certain forms of dementia (whereas increased DMN activity is more commonly associated with the depressive state in both bipolar disorder and major depressive disorder)[15-19]. Notably, DMN dysfunction has been linked to positive symptoms, and may reflect a common ground of thought deficits that predisposes to psychotic symptomatology under specific conditions[1,15,20]. On the other hand, reduced task-based activation in CEN areas is commonly found across major psychiatric disorders, while functional alterations in the SN appear more heterogeneous[15]. These functional alterations, including changes in network activity and network imbalances, may play distinct roles in the expression of psychopathologic symptoms[15-16,21-22].

In summary, both shared and distinctive patterns of brain alterations are evident across major psychiatric disorders. While caution is warranted—especially since some regional or microstructural features may not be fully captured by standard neuroimaging techniques—

structural similarities, such as grey matter loss in the insula, anterior cingulate, and hippocampal regions (across major psychiatric disorders), as well as white matter deficits in limbic tracts (in schizophrenia and bipolar disorder), may reflect shared pathophysiological mechanisms. Conversely, distinctive abnormalities—such as opercular damage (specific to schizophrenia) and DMN alterations (showing distinct patterns across conditions)—may reflect the additional contribution of distinct pathophysiological mechanisms and, when considered alongside the prototypical clinical features of each disorder, may suggest that these alterations play a critical role in psychotic symptomatology—central to schizophrenia but more peripheral in bipolar disorder and major depressive disorder.

Models of psychosis

According to the reported data, a defined set of brain alterations is closely linked to psychosis in prototypical schizophrenia—namely, damage to the opercular region (particularly the superior temporal gyrus and insula), which is associated with auditory hallucinations, and DMN dysfunction, which is associated with positive symptoms. However, while these findings establish clear brain-symptom associations, the mechanisms through which these alterations give rise to psychotic symptoms, such as hallucinations and delusions, remain unclear. Several models have been proposed to explain psychosis, among which the aberrant salience model and the predictive coding model are two of the most well-established biological frameworks, providing insight into potential mechanisms.

The aberrant salience model posits that psychosis arises from an excessive attribution of salience and meaning to neutral stimuli[23]. This process leads to hallucinations, which reflect internal representations associated with aberrant salience, and delusions, which serve as cognitive explanations for these anomalous experiences[23]. Aberrant salience is thought to be mediated by dysregulated dopaminergic signaling, increased activation of the insula, and abnormal activity within the SN[23-24]. This model has been combined with the triple-network framework into an integrative model proposing that schizophrenia stems from a core deficit in the SN, which disrupts the dynamic switching between the DMN and the CEN[21,25]. As a result, the CEN is under-engaged while the DMN is over-engaged, leading to cognitive and negative symptoms such as difficulty disengaging from internal mental processes and withdrawal from the external environment and its rewarding stimuli[21,25]. This framework may align with the observed relationship between insular dysfunction and hallucinations. Specifically, abnormal affective processing within the insula may lead to the erroneous attribution of salience to otherwise low-relevance sensory inputs, thereby contributing to hallucinations.

The predictive coding theory posits that the brain is a machine that continuously generates inferences and predictions about the current state of the world (the causal structure of the sensorium) by modulating prior (top-down) beliefs with incoming (bottom-up) sensory signals[26-28]. Mismatches between these predictions and sensory input constitute prediction errors, which drive new learning aimed at minimizing prediction error and optimizing the system[26-28]. In this model, psychosis results from disruptions in these predictive mechanisms, leading to maladaptive inferences about the causes of sensory stimuli—such as erroneously attributing self-caused experiences or actions to external sources[28]. Thus, psychosis has been linked to decreased precision of prior beliefs relative to sensory data, making inferences more strongly driven by the sensory input itself[28]. In particular, corollary discharges serve as predictions of the sensory consequences of action, contributing to the feeling that such actions are self-caused (i.e., the sense of intentionality or agency)[28-29]. When the precision of predictions regarding the sensory consequences of internally generated speech or thoughts is reduced, these experiences become surprising (i.e., they are not accounted for by the sense of intentionality) and are therefore erroneously attributed to external sources, generating hallucinations and delusions[28-29]. However, hallucinations have also been associated with stronger beliefs, where inferences are abnormally driven more by beliefs than by sensory inputs[28]. This can lead to the recognition of speech or visual objects from noisy signals; in such cases, deficits in corollary discharges might give rise to aberrant inferences about agency and intentions[28]. This framework may align with the observed relationship between DMN dysfunction and positive symptoms. Specifically, abnormal cognitive processing associated with DMN deficits could reduce the precision of prior beliefs, impairing the sense of intentionality or agency. This, in turn, may lead to the erroneous attribution of internal actions or representations to external sources, thereby promoting both hallucinations and delusions.

Alongside these models, we recently proposed a three-dimensional neurophenomenal framework, which we applied to mania, depression, and psychosis[15-16,20], potentially offering a complementary perspective to these established models. This framework links the structure of neural activity to phenomenal experience across three complementary modes of organism-environment interaction: interaction with the outer environment—primarily mediated by activity in the primary/secondary sensorimotor areas, subserving exteroception and psychomotricity; interaction with the inner/body environment—primarily mediated by activity in the insular areas, subserving interoception and affectivity; and detachment from the environment—primarily mediated by activity in higher-order associative areas, subserving imagery and thought. According to this framework, imbalances among these neurophenomenal dimensions give rise to distinct psychopathological states. A pathological tilt toward lower-order sensorimotor areas (at the expense of higher-order associative areas), leading to the predominance of perception and psychomotor-affective responses (over imagery), manifests as mania—characterized by immediate interaction with the current environment[16-17]. Conversely, a pathological tilt toward higher-order associative areas (at the expense of lower-order sensorimotor areas), leading to the predominance of imagery (over perception and psychomotor-affective responses), manifests as depression—characterized by detachment from the current environment[16-18]. Finally, a pathological flattening between sensorimotor and associative areas, leading to the flattening between perception and imagery, manifests as psychosis—characterized by a destructuration of the interaction with the environment[20].

In this framework[20], more specifically, a key assumption (rooted in classical phenomenology[30]) is that phenomenal experience has an intrinsic structure based on the *primacy of perception*—that is, perception is fundamental, representing the essential unity of the organism and its environment, while imagery is derived from perception both evolutionarily and developmentally. Importantly, phenomenal intensity (or vividness), which is intrinsically higher in perception than in imagery, is thought to serve as the fundamental reality criterion (as demonstrated in recent robust work[29]): during ongoing phenomenal experience, elements with higher intensity are attributed to perception (directly related to the current environment, i.e., felt as real), whereas elements with lower intensity are attributed to imagery (not directly related to the current environment, i.e., felt as imaginary). A complementary assumption (in line with a neurophenomenal approach) is that the intrinsic structure of phenomenal experience is traceable to the structure of neural activity. Accordingly, phenomenal intensity may be traced to the

density of neural activation in sensory areas, which is physiologically higher when driven by receptor stimulation than when driven by activity in associative areas (this distinction accounts for the inherently greater vividness of perception compared to imagery, as imagery is presumed to originate from perception and later undergo modification and recombination).
Based on this framework[20], we hypothesize that the primary alteration in psychosis consists of a blurring of phenomenal intensity between perception and imagery (and a corresponding loss of the physiological primacy of perception), which impairs reality monitoring. This alteration is traceable to a corresponding neural change in the sensory cortex during the interplay between receptor-driven and association-driven activity. More specifically, any deficit in perception that results in a similar and indistinguishable phenomenal intensity between perception and imagery may give rise to hallucinatory experiences. In turn, this core phenomenal alteration may stem from any functional or structural disruption in the sensory systems (from receptors to sensory cortices) that critically reduces the density of sensory cortex activation driven by receptor stimulation, making it indistinguishable from activation driven by associative processing. On the other hand, severe thought deficits—impairing the manipulation of complex ideas or their updating by sensory inputs—may promote the formation of delusional ideas (fixed ideas misaligned with the changing environment), which may be traceable to either abnormally decreased or increased activity in associative areas. Finally, the superimposition of these thought alterations onto perception-imagery blurring, arising from corresponding neural dysfunctions, may intimately link delusions and hallucinations (as imagery mistaken for perception may lead to the formation of related delusional ideas, while delusional thought may trigger imagery mistaken for perception) and may ultimately lead to a severe dissociation of phenomenal experience from the changing environment, resulting in a global loss of contact with reality.
This model may align with the reported data showing a robust relationship between damage to the opercular region, including the superior temporal gyrus and the insula, and hallucinations in prototypical schizophrenia. Specifically, structural damage to the auditory cortex in the superior temporal gyrus, which induces a critical reduction in neural units and/or synaptic connections, may result in a corresponding decrease in the maximal density of neural activation that can be elaborated in such sensory cortices. This damage might primarily affect the intrinsically dense neuronal activation of the auditory cortex driven by receptor stimulation, rather than the typically sparse neuronal activation of the same cortex driven by associative processing. Thus, structural damage could ultimately lead to a density of neuronal activation in the auditory cortex that is equally sparse, whether driven by associative processing or receptor stimulation. This may manifest as a stable reduction in the phenomenal intensity of auditory perception, with auditory imagery then having an intensity indistinguishable from perception, and thus felt as real—i.e., auditory hallucinations. Analogously, structural damage to the interoceptive cortex in the insula might give rise to "interoceptive hallucinations", which could account for abnormal affective experiences in the disorder (even if less specific to schizophrenia, as damage to the insula appears to be shared across major psychiatric disorders[7]). Accordingly, damage to the opercular region may help explain the dominance of auditory hallucinations over other modalities, as well as their association with affective alterations in prototypical schizophrenia. At the same time, this model allows for the dissociation of brain alterations underlying hallucinations and delusions across different neuropsychiatric conditions. Alterations in DMN activity are well documented across various psychopathological states, ranging from predominant hyperactivity in depressive states to predominant hypoactivity in manic states and dementias[15-19]. These alterations may correspond to a wide spectrum of thought disturbances, from rumination to thought deficits that

can verge on or culminate in delusional thinking[15,20]. On the other hand, the combination of DMN dysfunction with sensory damage may strongly link delusions and hallucinations in the prototypical form of psychosis in schizophrenia.

Thus, this model shifts the focus from affective or cognitive disturbances to the phenomenology of perceptual alterations and their potential biological basis in sensory area damage. This may align with evidence showing a close relationship between sensory deficits and hallucinations across neuropsychiatric conditions[20]. Moreover, it aligns with recent research robustly supporting the vividness of experience—rather than intention or sense of agency—as the primary criterion for distinguishing reality from imagination[29]. It may also be consistent with recent studies demonstrating the dominant role of alterations in low-order sensorimotor areas within the large-scale gradients of cortical organization in schizophrenia[31]. However, this model and its hypotheses have yet to be specifically tested, necessitating dedicated investigation in future research.

Taken together, while existing models have made significant contributions to understanding psychosis, our model offers a potentially complementary framework that may help explain the specific neural alterations associated with hallucinations, particularly those arising from sensory cortex damage. This approach can be explored alongside current models, offering an integrative perspective that incorporates sensory deficits as a key factor in psychotic experience. Future research should specifically test the various biological models of psychosis and explore their potential integration to explain different aspects of the condition, including affective, cognitive, and sensory dimensions, as well as computational and phenomenological components. Additionally, these models could be applied to investigate potential subtypes across neuropsychiatric conditions or among individuals.

Future directions

The synthesis from the umbrella review of neuroimaging studies provides the empirical foundation for an emerging conceptual framework linking the pathophysiology and psychopathology of schizophrenia, which in turn generates specific hypotheses to be empirically tested in future research.

Key hypotheses concern the relationship between grey matter deficits in the superior temporal gyrus/auditory cortex, alterations in neuronal activation density during auditory perception, blurring of phenomenal intensity between perception and imagery, and the occurrence of auditory hallucinations. Additionally, testable hypotheses address the relationship between inflammatory/immune dysregulation and the spatial pattern of structural brain damage (such as the spread of pathological processes via cerebrospinal fluid, white matter damage to the fornix and tracts near the ventricular horns, and grey matter damage to regions in the opercular space and interhemispheric fissure) along with its link to functional brain alterations (including damage to the fornix and altered intrinsic activity in the DMN).

These observations also suggest the involvement and interplay of potential etiological factors in the pathological process, such as neurodevelopmental and immune factors. While the discussion of these factors is beyond the scope of the present work, they should be more thoroughly characterized and specifically investigated in future studies.

References

1 Gong, J. *et al.* Abnormalities of intrinsic regional brain activity in first-episode and chronic schizophrenia: a meta-analysis of resting-state functional MRI. *J Psychiatry Neurosci*. **45**, 55-68 (2020).

2 Jani, M. & Kasparek, T. Emotion recognition and theory of mind in schizophrenia: A meta-analysis of neuroimaging studies. *World J Biol Psychiatry*. **19**, S86-S96 (2018).

3 Dong, D. *et al.* Abnormal brain activation during threatening face processing in schizophrenia: A meta-analysis of functional neuroimaging studies. *Schizophr Res*. **197**, 200-208 (2018).

4 Bora, E. *et al.* Neuroanatomical abnormalities in schizophrenia: a multimodal voxelwise meta-analysis and meta-regression analysis. *Schizophr Res*. **127**, 46-57 (2011).

5 Zhao, G. *et al.* A Comparative Multimodal Meta-analysis of Anisotropy and Volume Abnormalities in White Matter in People Suffering From Bipolar Disorder or Schizophrenia. *Schizophr Bull*. **48**, 69-79 (2022).

6 Zeng, J. *et al.* Neural substrates of reward anticipation and outcome in schizophrenia: a meta-analysis of fMRI findings in the monetary incentive delay task. *Transl Psychiatry*. **12**, 448 (2022).

7 Goodkind, M. *et al.* Identification of a common neurobiological substrate for mental illness. *JAMA Psychiatry*. **72**, 305-315 (2015).

8 Brosch, K. *et al.* Reduced hippocampal gray matter volume is a common feature of patients with major depression, bipolar disorder, and schizophrenia spectrum disorders. *Mol Psychiatry*. **27**, 4234-4243 (2022).

9 Chang, M. *et al.* Neurobiological Commonalities and Distinctions Among Three Major Psychiatric Diagnostic Categories: A Structural MRI Study. *Schizophr Bull*. **44**, 65-74 (2018).

10 McCutcheon, R. *et al.* Shared and separate patterns in brain morphometry across transdiagnostic dimensions. *Nat. Mental Health*. **1**, 55-65 (2023).

11 Matsumoto, J. *et al.* Cerebral cortical structural alteration patterns across four major psychiatric disorders in 5549 individuals. *Mol Psychiatry*. **28**, 4915-4923 (2023).

12 Koshiyama, D. *et al.* White matter microstructural alterations across four major psychiatric disorders: mega-analysis study in 2937 individuals. *Mol Psychiatry*. **25**, 883-895 (2020).

13 Craig, A. D. How do you feel? Interoception: the sense of the physiological condition of the body. *Nature reviews. Neuroscience*. **3**, 655-666 (2002).

14 Palaniyappan, L., Balain, V., Radua, J. & Liddle, P. F. Structural correlates of auditory hallucinations in schizophrenia: a meta-analysis. *Schizophr Res*. **137**, 169-173 (2012).

15 Martino, M. & Magioncalda, P. A three-dimensional model of neural activity and phenomenal-behavioral patterns. *Mol Psychiatry*. **29**, 639-652 (2024).

16 Martino, M. & Magioncalda, P. Tracing the psychopathology of bipolar disorder to the functional architecture of intrinsic brain activity and its neurotransmitter modulation: a three-dimensional model. *Mol Psychiatry*. **27**, 793-802 (2022).

17 Martino, M. *et al.* Contrasting variability patterns in the default mode and sensorimotor networks balance in bipolar depression and mania. *Proceedings of the National Academy of Sciences of the United States of America*. **113**, 4824-4829 (2016).

18 Zhang, Y. *et al.* Dysfunction in sensorimotor and default mode networks in major depressive disorder with insights from global brain connectivity. *Nat. Mental Health*. **2**, 1371–1381 (2024).
19 Darby, R. R., Joutsa, J. & Fox, M. D. Network localization of heterogeneous neuroimaging findings. *Brain*. **142**, 70-79 (2019).
20 Martino, M. & Magioncalda, P. A working model of neural activity and phenomenal experience in psychosis. *Mol Psychiatry*. **29**, 3814-3825 (2024).
21 Menon, V. Large-scale brain networks and psychopathology: a unifying triple network model. *Trends Cogn Sci*. **15**, 483-506 (2011).
22 Magioncalda, P. & Martino, M. A unified model of the pathophysiology of bipolar disorder. *Mol Psychiatry*. **27**, 202-211 (2022).
23 Kapur, S. Psychosis as a state of aberrant salience: a framework linking biology, phenomenology, and pharmacology in schizophrenia. *Am J Psychiatry*. **160**, 13-23 (2003).
24 Palaniyappan, L. & Liddle, P. F. Does the salience network play a cardinal role in psychosis? An emerging hypothesis of insular dysfunction. *J Psychiatry Neurosci*. **37**, 17-27 (2012).
25 Menon, V., Palaniyappan, L. & Supekar, K. Integrative Brain Network and Salience Models of Psychopathology and Cognitive Dysfunction in Schizophrenia. *Biol Psychiatry*. **94**, 108-120 (2023).
26 Friston, K. & Kiebel, S. Predictive coding under the free-energy principle. *Philos Trans R Soc Lond B Biol Sci*. **364**, 1211-1221 (2009).
27 Friston, K. The free-energy principle: a unified brain theory? *Nat Rev Neurosci*. **11**, 127-138 (2010).
28 Sterzer, P. *et al.* The Predictive Coding Account of Psychosis. *Biol Psychiatry*. **84**, 634-643 (2018).
29 Dijkstra, N. & Fleming, S. M. Subjective signal strength distinguishes reality from imagination. *Nat Commun*. **14**, 1627 (2023).
30 Hume, D. A Treatise of Human Nature. Oxford: Clarendon Press (1740).
31 Huang, Z., Mashour, G. A. & Hudetz, A. G. Functional geometry of the cortex encodes dimensions of consciousness. *Nat Commun*. **14**, 72 (2023).

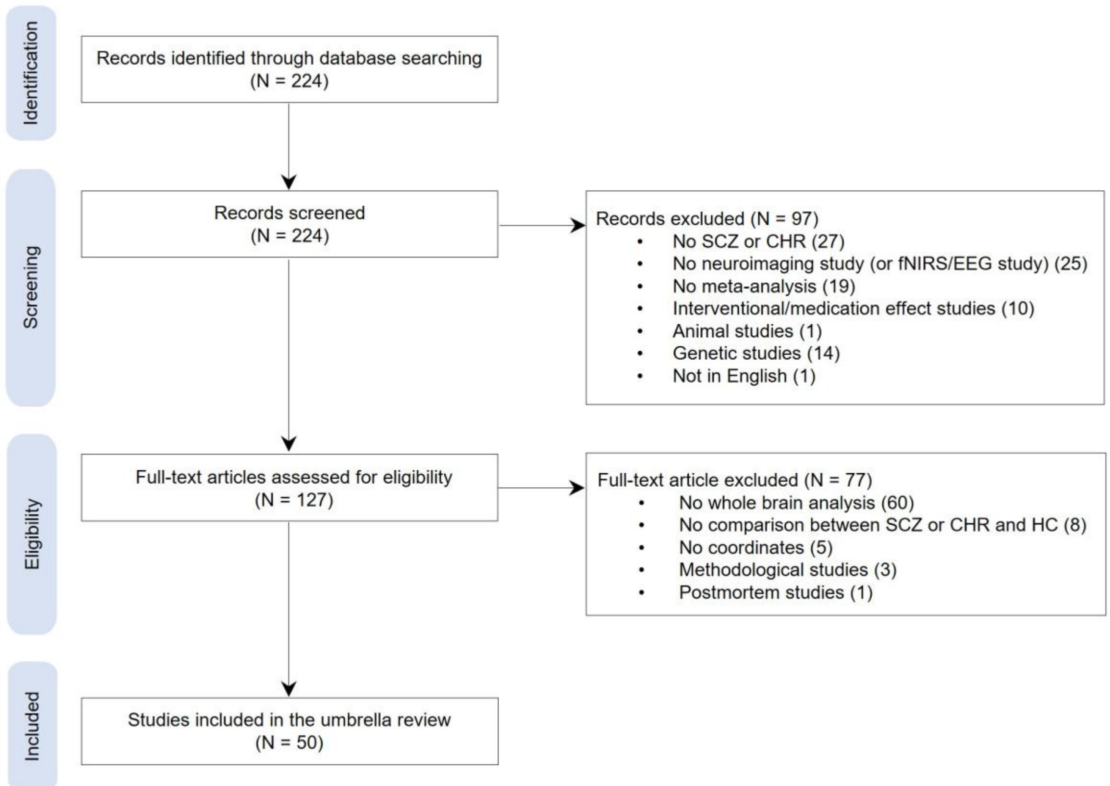

Supplementary Figure 1. PRISMA chart

Abbreviations: SCZ, schizophrenia; CHR, clinical high risk for schizophrenia.

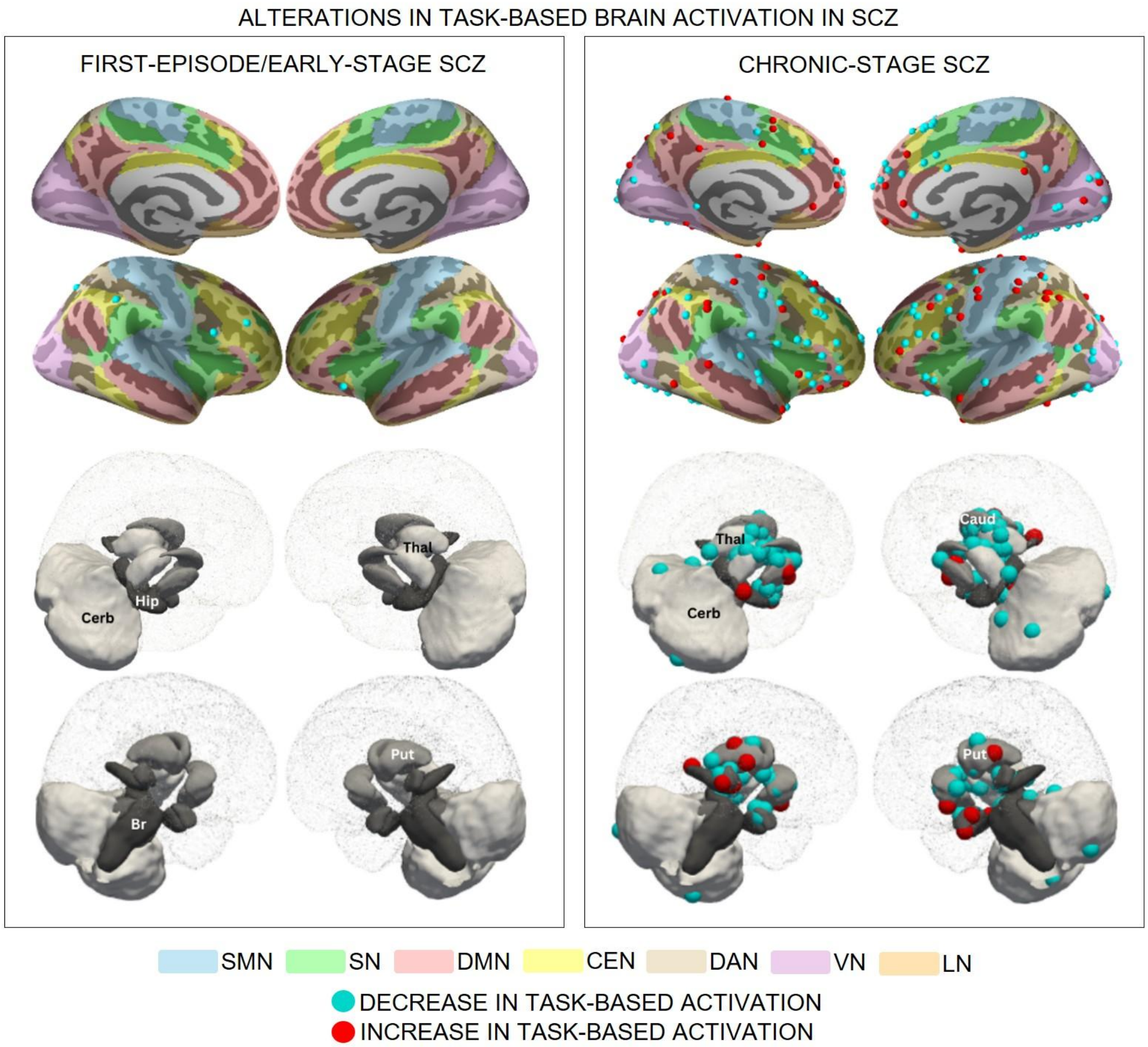

Supplementary Figure 2. Alterations in task-based brain activation in schizophrenia

Results of the systematic umbrella review of neuroimaging studies investigating task-based brain activation in schizophrenia. All peak coordinates of brain activation alterations—during perception, emotion, or cognitive tasks—as reported in all whole-brain voxelwise meta-analyses on this topic comparing schizophrenia patients and healthy controls, are mapped onto the brain, including both cortical and subcortical structures. Blue spheres indicate decreases in task-based brain activation, and red spheres indicate increases in task-based brain activation in patients relative to controls. Cortical background colors represent the seven large-scale brain networks defined by Yeo *et al*. (2011).

Abbreviations: SCZ, schizophrenia; SMN, somatomotor network; SN, salience network; DMN, default-mode network; CEN, central executive network; DAN, dorsal attention network; VN, visual network; LN, limbic network; Thal, thalamus; Caud, caudate; Put, putamen; Hip, hippocampus; Br, brainstem; Cerb, cerebellum.

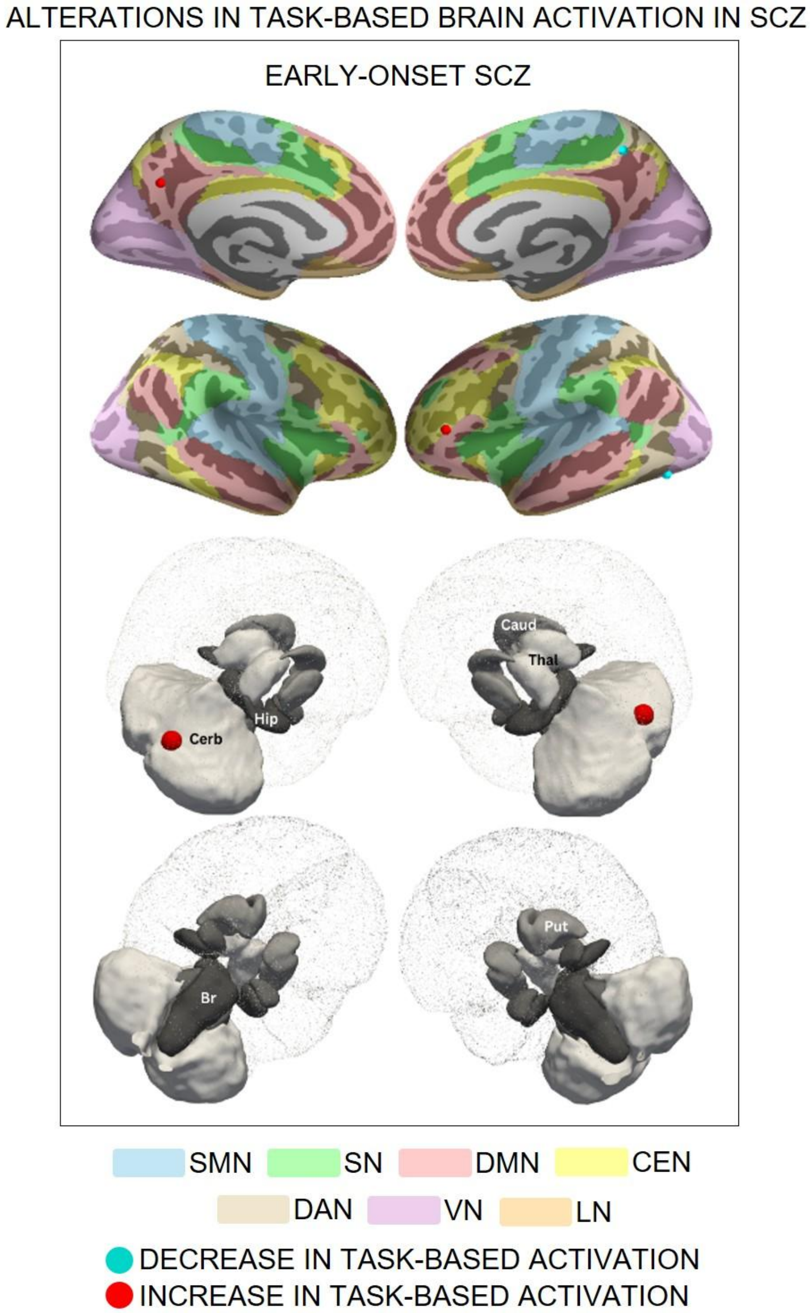

Supplementary Figure 3. Alterations in task-based brain activation in schizophrenia (early-onset)

Results of the systematic umbrella review of neuroimaging studies investigating task-based brain activation in early-onset schizophrenia. All peak coordinates of brain activation alterations (during cognitive tasks), as reported in all whole-brain voxelwise meta-analyses on this topic comparing early-onset schizophrenia patients and healthy controls, are mapped onto the brain, including both cortical and subcortical structures. Blue spheres indicate decreases in task-based brain activation, and red spheres indicate increases in task-based brain activation in patients relative to controls. Cortical background colors represent the seven large-scale brain networks defined by Yeo *et al*. (2011).

Abbreviations: SCZ, schizophrenia; SMN, somatomotor network; SN, salience network; DMN, default-mode network; CEN, central executive network; DAN, dorsal attention network; VN, visual network; LN, limbic network; Thal, thalamus; Caud, caudate; Put, putamen; Hip, hippocampus; Br, brainstem; Cerb, cerebellum.

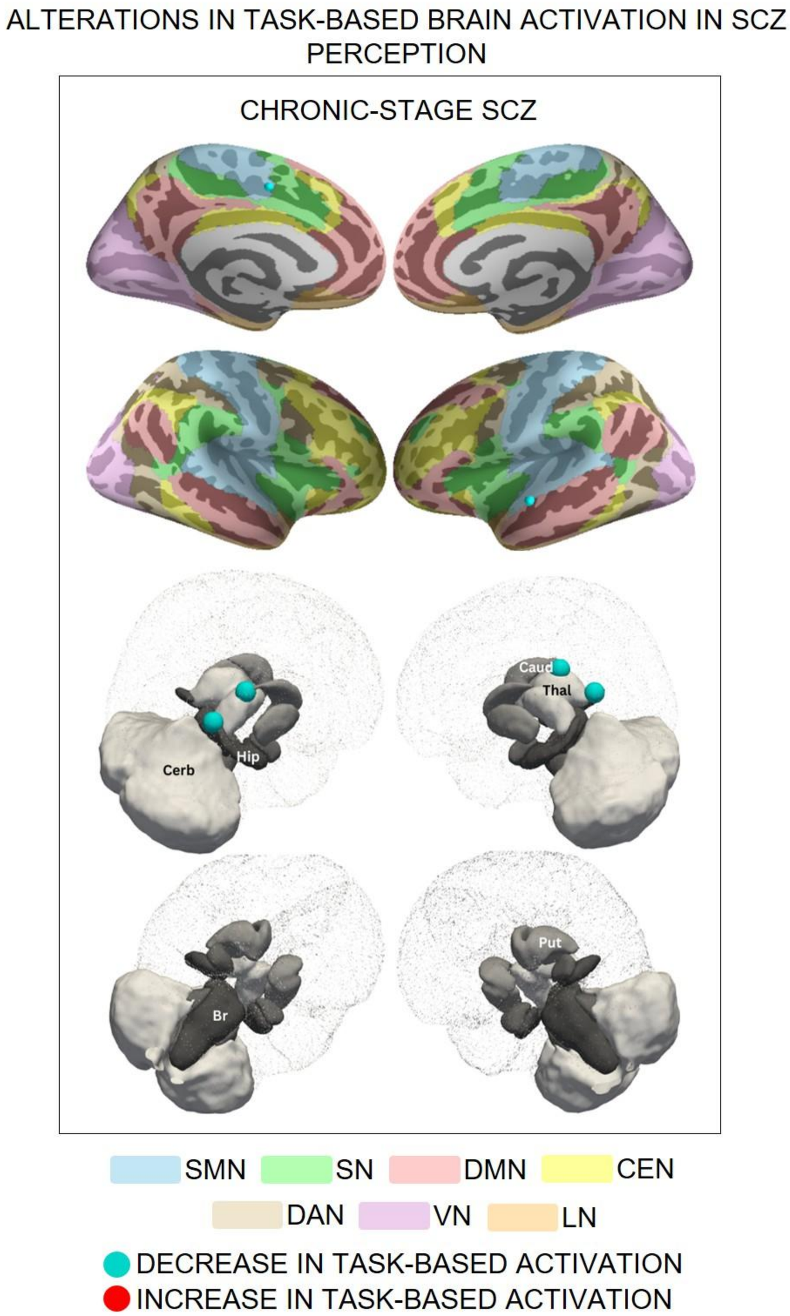

Supplementary Figure 4. Alterations in task-based brain activation in schizophrenia (perception)
Results of the systematic umbrella review of neuroimaging studies investigating task-based brain activation during perception processing in schizophrenia. All peak coordinates of brain activation alterations during perception tasks, as reported in all whole-brain voxelwise meta-analyses on this topic comparing schizophrenia patients and healthy controls, are mapped onto the brain, including both cortical and subcortical structures. Blue spheres indicate decreases in task-based brain activation, and red spheres indicate increases in task-based brain activation in patients relative to controls. Cortical background colors represent the seven large-scale brain networks defined by Yeo *et al*. (2011).
Abbreviations: SCZ, schizophrenia; SMN, somatomotor network; SN, salience network; DMN, default-mode network; CEN, central executive network; DAN, dorsal attention network; VN, visual network; LN, limbic network; Thal, thalamus; Caud, caudate; Put, putamen; Hip, hippocampus; Br, brainstem; Cerb, cerebellum.

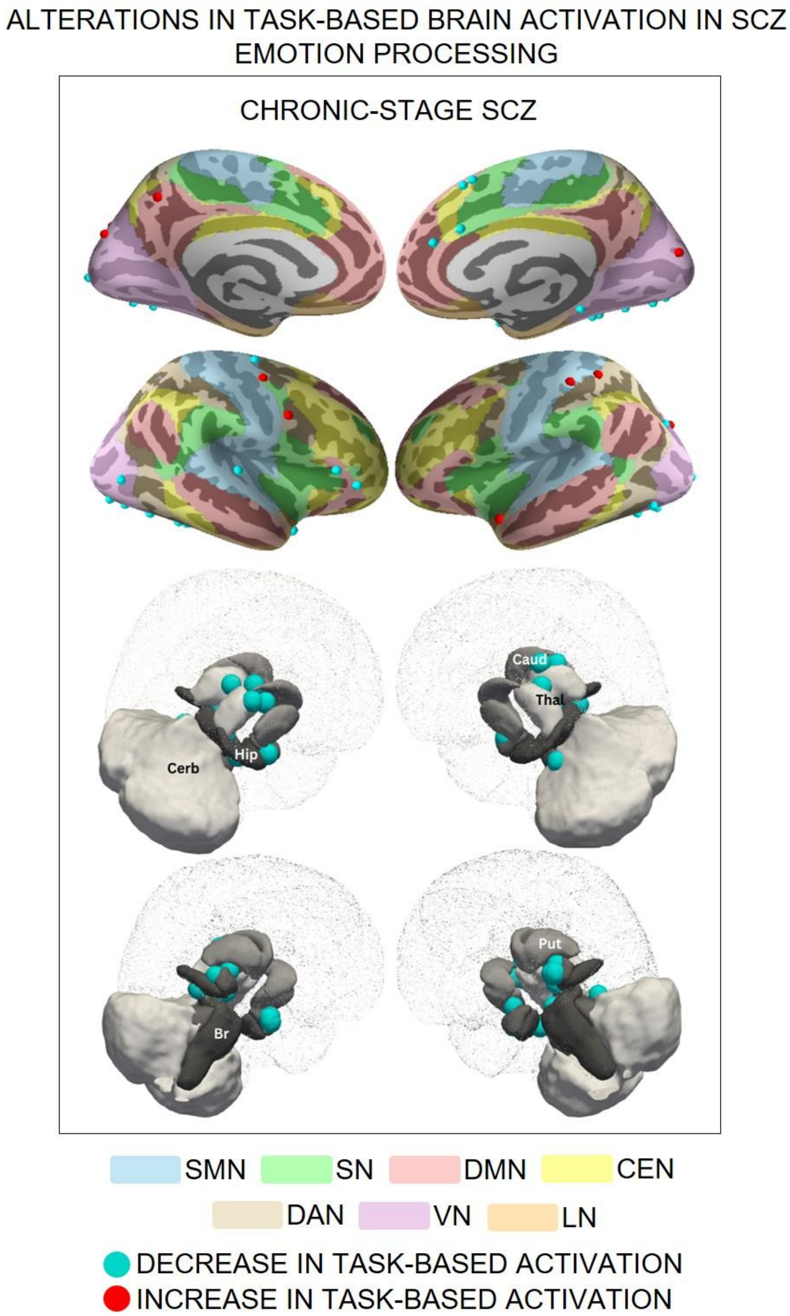

Supplementary Figure 5. Alterations in task-based brain activation in schizophrenia (emotion processing)

Results of the systematic umbrella review of neuroimaging studies investigating task-based brain activation during emotion processing in schizophrenia. All peak coordinates of brain activation alterations during emotion tasks, as reported in all whole-brain voxelwise meta-analyses on this topic comparing schizophrenia patients and healthy controls, are mapped onto the brain, including both cortical and subcortical structures. Blue spheres indicate decreases in task-based brain activation, and red spheres indicate increases in task-based brain activation in patients relative to controls. Cortical background colors represent the seven large-scale brain networks defined by Yeo *et al*. (2011).

Abbreviations: SCZ, schizophrenia; SMN, somatomotor network; SN, salience network; DMN, default-mode network; CEN, central executive network; DAN, dorsal attention network; VN, visual network; LN, limbic network; Thal, thalamus; Caud, caudate; Put, putamen; Hip, hippocampus; Br, brainstem; Cerb, cerebellum.

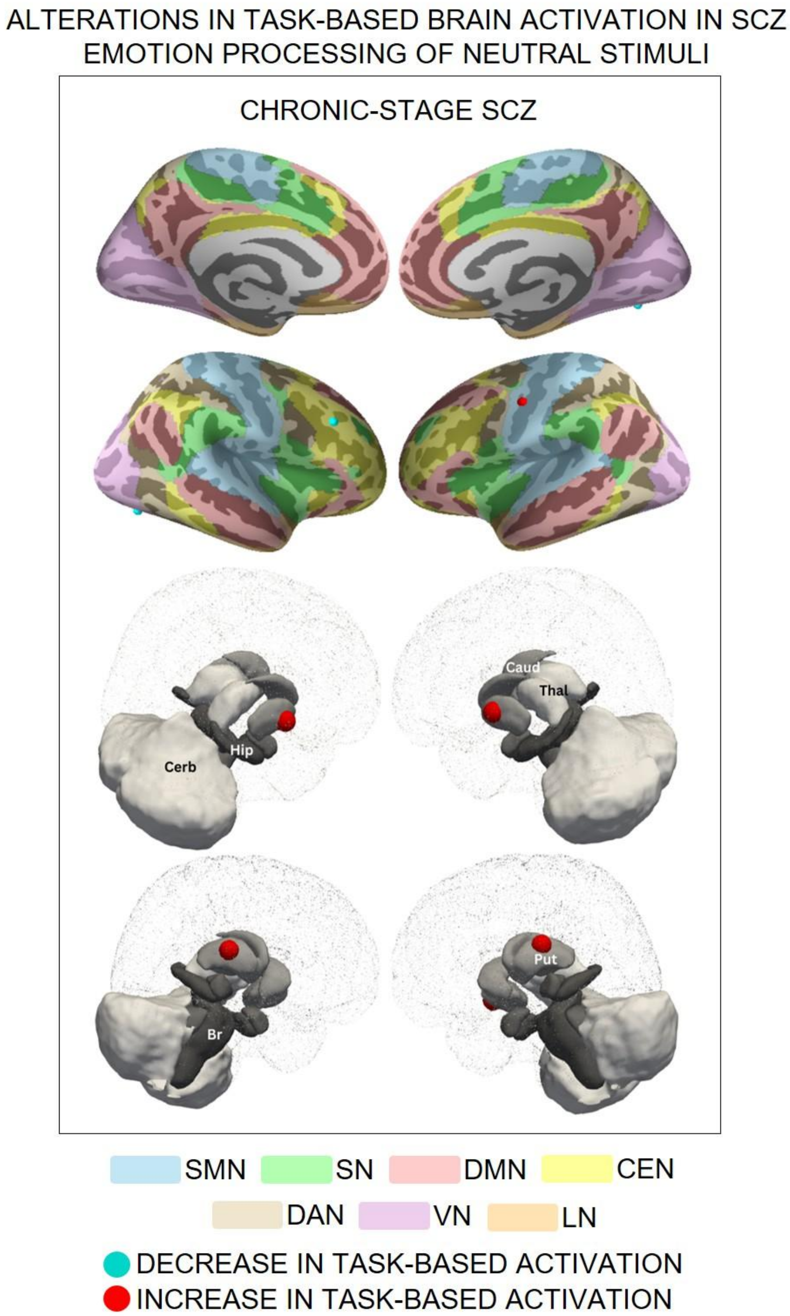

Supplementary Figure 6. Alterations in task-based brain activation in schizophrenia (emotion processing of neutral stimuli)

Results of the systematic umbrella review of neuroimaging studies investigating task-based brain activation during emotion processing of neutral stimuli in schizophrenia. All peak coordinates of brain activation alterations during emotion tasks involving neutral stimuli, as reported in all whole-brain voxelwise meta-analyses on this topic comparing schizophrenia patients and healthy controls, are mapped onto the brain, including both cortical and subcortical structures. Blue spheres indicate decreases in task-based brain activation, and red spheres indicate increases in task-based brain activation in patients relative to controls. Cortical background colors represent the seven large-scale brain networks defined by Yeo *et al*. (2011).

Abbreviations: SCZ, schizophrenia; SMN, somatomotor network; SN, salience network; DMN, default-mode network; CEN, central executive network; DAN, dorsal attention network; VN, visual network; LN, limbic network; Thal, thalamus; Caud, caudate; Put, putamen; Hip, hippocampus; Br, brainstem; Cerb, cerebellum.

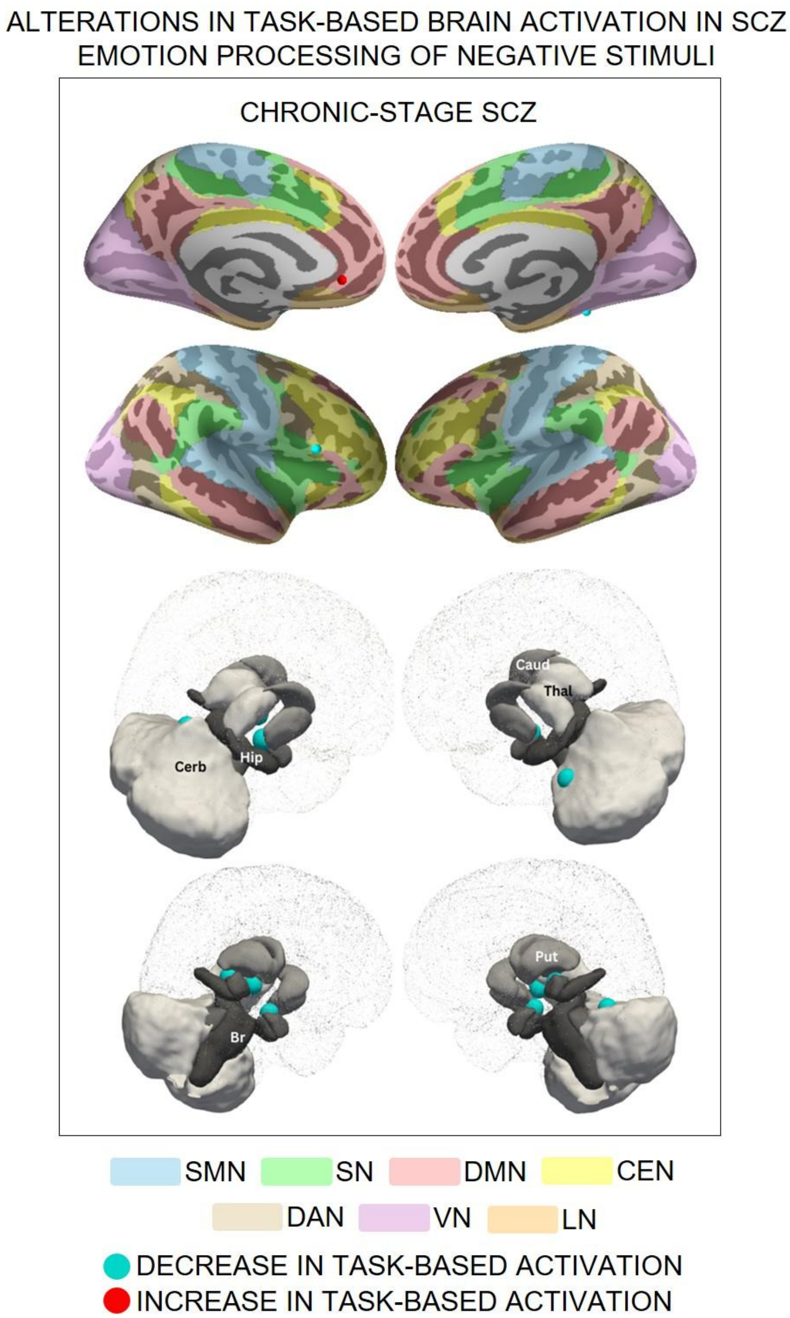

Supplementary Figure 7. Alterations in task-based brain activation in schizophrenia (emotion processing of negative stimuli)

Results of the systematic umbrella review of neuroimaging studies investigating task-based brain activation during emotion processing of negative stimuli in schizophrenia. All peak coordinates of brain activation alterations during emotion tasks involving negative stimuli, as reported in all whole-brain voxelwise meta-analyses on this topic comparing schizophrenia patients and healthy controls, are mapped onto the brain, including both cortical and subcortical structures. Blue spheres indicate decreases in task-based brain activation, and red spheres indicate increases in task-based brain activation in patients relative to controls. Cortical background colors represent the seven large-scale brain networks defined by Yeo *et al*. (2011).

Abbreviations: SCZ, schizophrenia; SMN, somatomotor network; SN, salience network; DMN, default-mode network; CEN, central executive network; DAN, dorsal attention network; VN, visual network; LN, limbic network; Thal, thalamus; Caud, caudate; Put, putamen; Hip, hippocampus; Br, brainstem; Cerb, cerebellum.

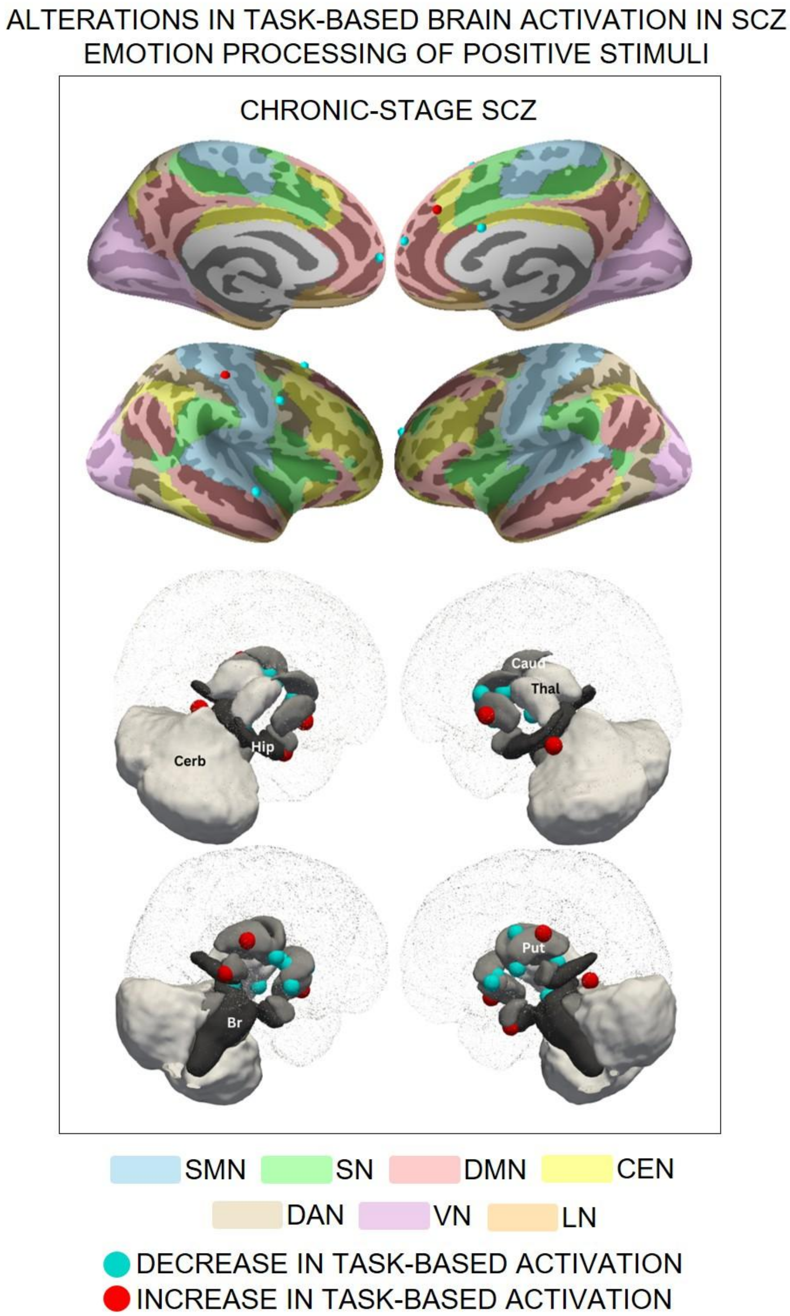

Supplementary Figure 8. Alterations in task-based brain activation in schizophrenia (emotion processing of positive stimuli)

Results of the systematic umbrella review of neuroimaging studies investigating task-based brain activation during emotion processing of positive stimuli in schizophrenia. All peak coordinates of brain activation alterations during emotion tasks involving positive stimuli, as reported in all whole-brain voxelwise meta-analyses on this topic comparing schizophrenia patients and healthy controls, are mapped onto the brain, including both cortical and subcortical structures. Blue spheres indicate decreases in task-based brain activation, and red spheres indicate increases in task-based brain activation in patients relative to controls. Cortical background colors represent the seven large-scale brain networks defined by Yeo *et al*. (2011).

Abbreviations: SCZ, schizophrenia; SMN, somatomotor network; SN, salience network; DMN, default-mode network; CEN, central executive network; DAN, dorsal attention network; VN, visual network; LN, limbic network; Thal, thalamus; Caud, caudate; Put, putamen; Hip, hippocampus; Br, brainstem; Cerb, cerebellum.

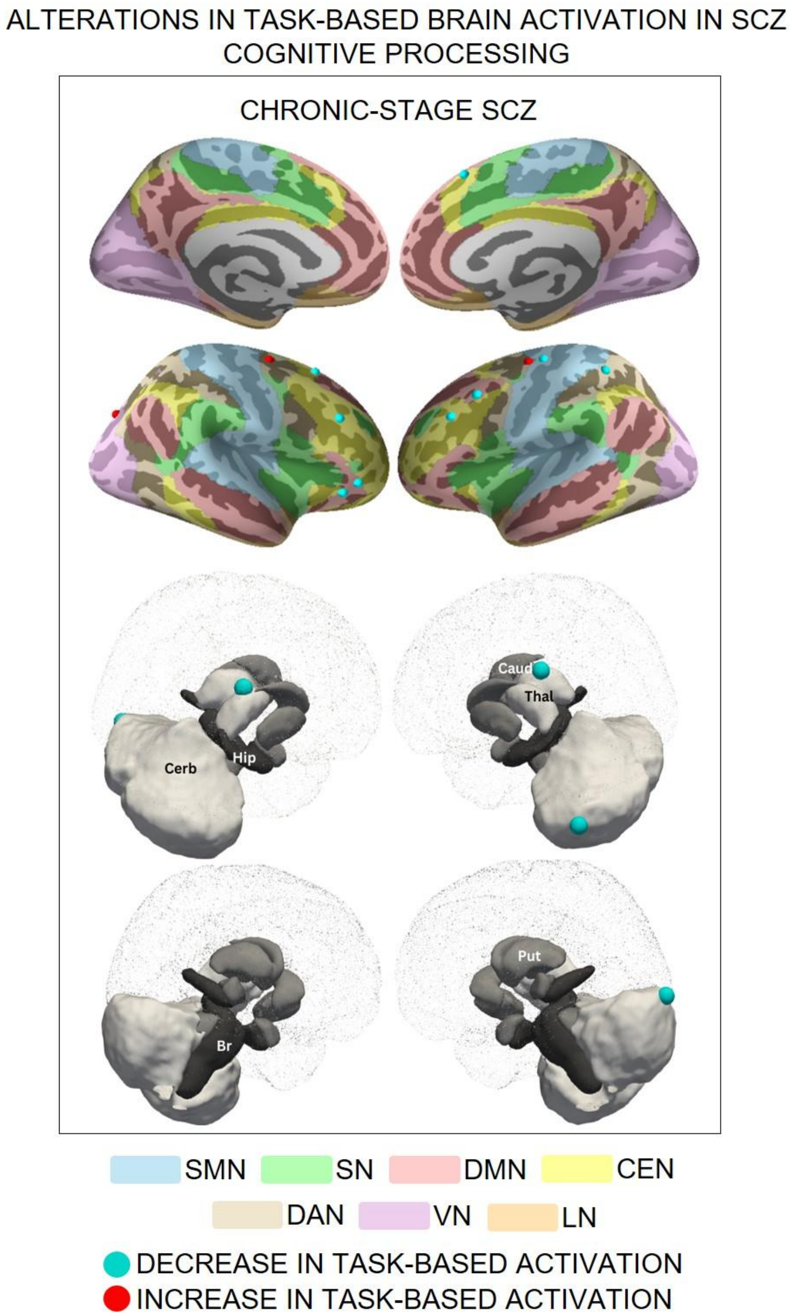

Supplementary Figure 9. Alterations in task-based brain activation in schizophrenia (cognitive processing)

Results of the systematic umbrella review of neuroimaging studies investigating task-based brain activation during cognitive processing in schizophrenia. All peak coordinates of brain activation alterations during cognitive tasks, as reported in all whole-brain voxelwise meta-analyses on this topic comparing schizophrenia patients and healthy controls, are mapped onto the brain, including both cortical and subcortical structures. Blue spheres indicate decreases in task-based brain activation, and red spheres indicate increases in task-based brain activation in patients relative to controls. Cortical background colors represent the seven large-scale brain networks defined by Yeo *et al*. (2011).

Abbreviations: SCZ, schizophrenia; SMN, somatomotor network; SN, salience network; DMN, default-mode network; CEN, central executive network; DAN, dorsal attention network; VN, visual network; LN, limbic network; Thal, thalamus; Caud, caudate; Put, putamen; Hip, hippocampus; Br, brainstem; Cerb, cerebellum.

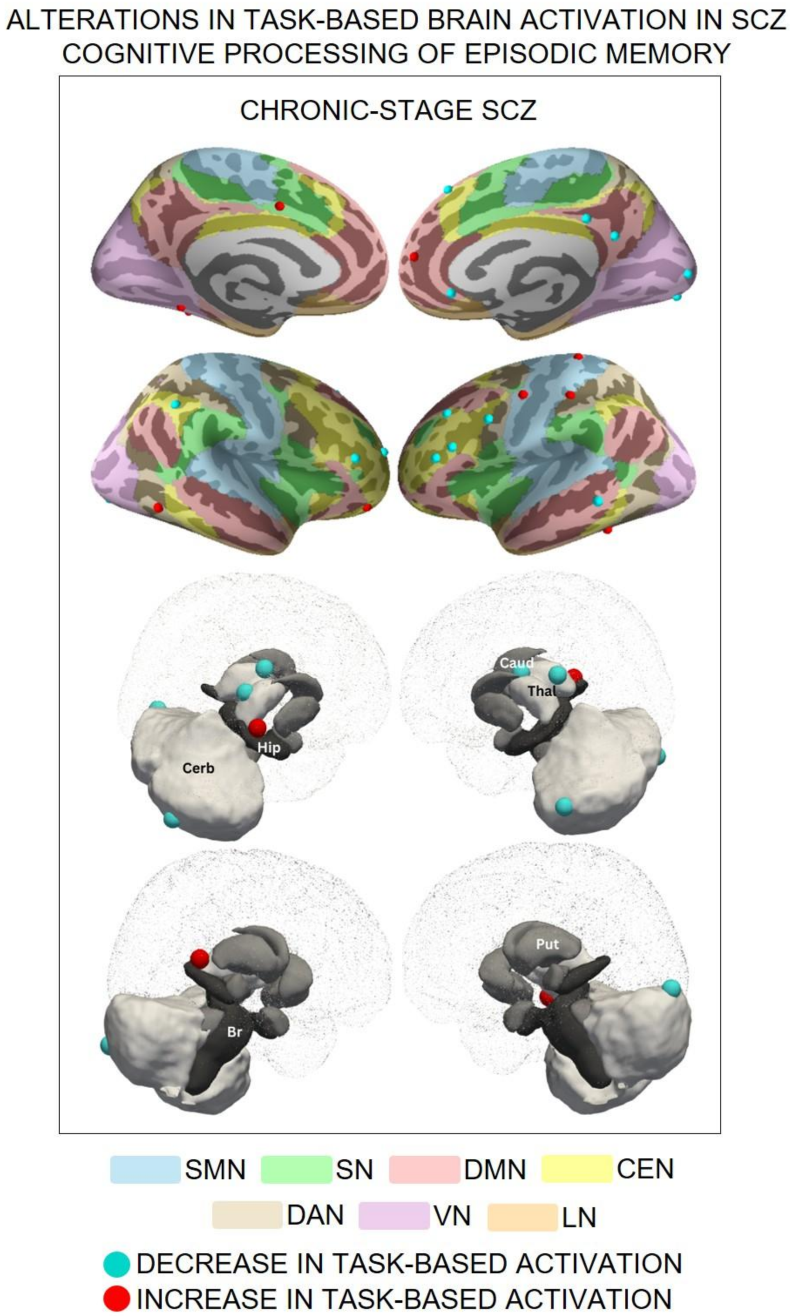

Supplementary Figure 10. Alterations in task-based brain activation in schizophrenia (cognitive processing of episodic memory)

Results of the systematic umbrella review of neuroimaging studies investigating task-based brain activation during cognitive processing of episodic memory in schizophrenia. All peak coordinates of brain activation alterations during cognitive tasks related to episodic memory, as reported in all whole-brain voxelwise meta-analyses on this topic comparing schizophrenia patients and healthy controls, are mapped onto the brain, including both cortical and subcortical structures. Blue spheres indicate decreases in task-based brain activation, and red spheres indicate increases in task-based brain activation in patients relative to controls. Cortical background colors represent the seven large-scale brain networks defined by Yeo *et al*. (2011).

Abbreviations: SCZ, schizophrenia; SMN, somatomotor network; SN, salience network; DMN, default-mode network; CEN, central executive network; DAN, dorsal attention network; VN, visual network; LN, limbic network; Thal, thalamus; Caud, caudate; Put, putamen; Hip, hippocampus; Br, brainstem; Cerb, cerebellum.

Supplementary Figure 11. Alterations in task-based brain activation in schizophrenia (cognitive processing of working memory)

Results of the systematic umbrella review of neuroimaging studies investigating task-based brain activation during cognitive processing of working memory in schizophrenia. All peak coordinates of brain activation alterations during cognitive tasks related to working memory, as reported in all whole-brain voxelwise meta-analyses on this topic comparing schizophrenia patients and healthy controls, are mapped onto the brain, including both cortical and subcortical structures. Blue spheres indicate decreases in task-based brain activation, and red spheres indicate increases in task-based brain activation in patients relative to controls. Cortical background colors represent the seven large-scale brain networks defined by Yeo *et al*. (2011).

Abbreviations: SCZ, schizophrenia; SMN, somatomotor network; SN, salience network; DMN, default-mode network; CEN, central executive network; DAN, dorsal attention network; VN, visual network; LN, limbic network; Thal, thalamus; Caud, caudate; Put, putamen; Hip, hippocampus; Br, brainstem; Cerb, cerebellum.

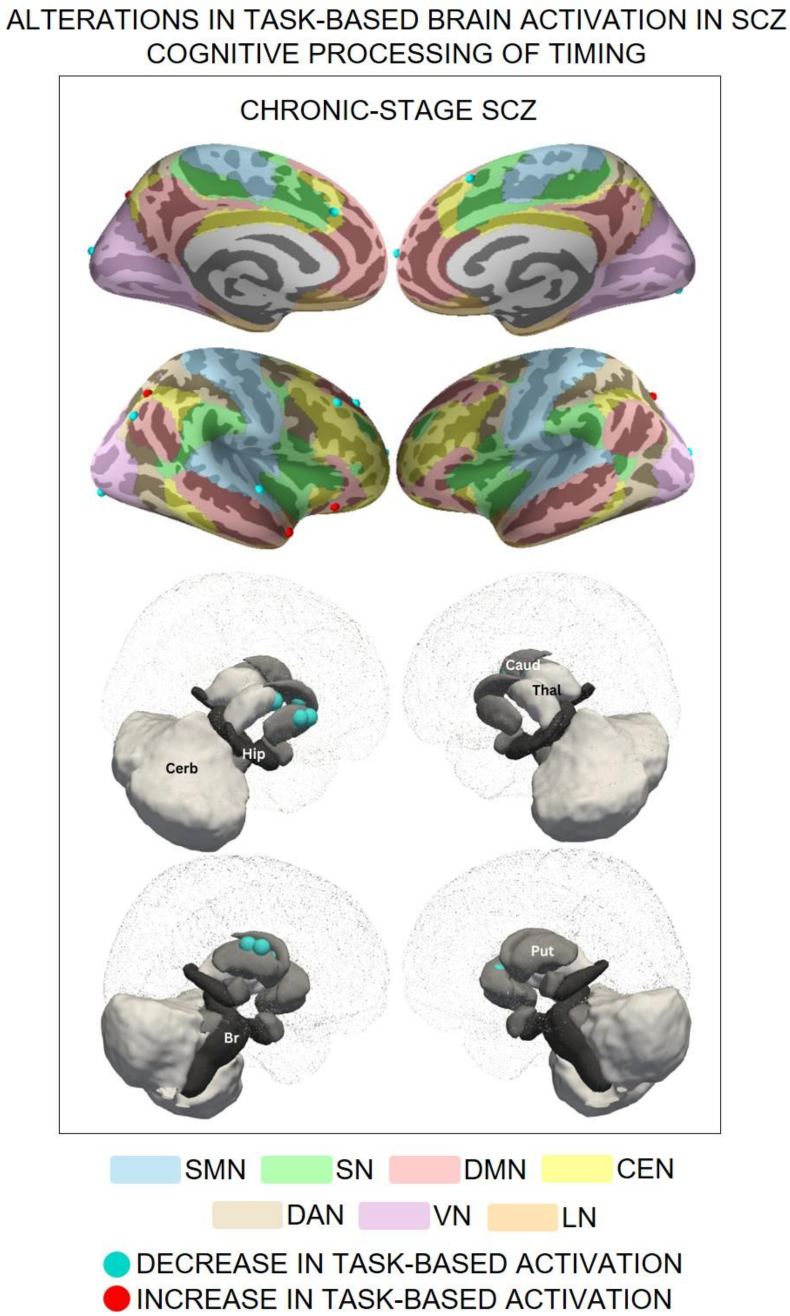

Supplementary Figure 12. Alterations in task-based brain activation in schizophrenia (cognitive processing of timing)

Results of the systematic umbrella review of neuroimaging studies investigating task-based brain activation during cognitive processing of timing in schizophrenia. All peak coordinates of brain activation alterations during cognitive tasks related to timing, as reported in all whole-brain voxelwise meta-analyses on this topic comparing schizophrenia patients and healthy controls, are mapped onto the brain, including both cortical and subcortical structures. Blue spheres indicate decreases in task-based brain activation, and red spheres indicate increases in task-based brain activation in patients relative to controls. Cortical background colors represent the seven large-scale brain networks defined by Yeo *et al*. (2011).

Abbreviations: SCZ, schizophrenia; SMN, somatomotor network; SN, salience network; DMN, default-mode network; CEN, central executive network; DAN, dorsal attention network; VN, visual network; LN, limbic network; Thal, thalamus; Caud, caudate; Put, putamen; Hip, hippocampus; Br, brainstem; Cerb, cerebellum.

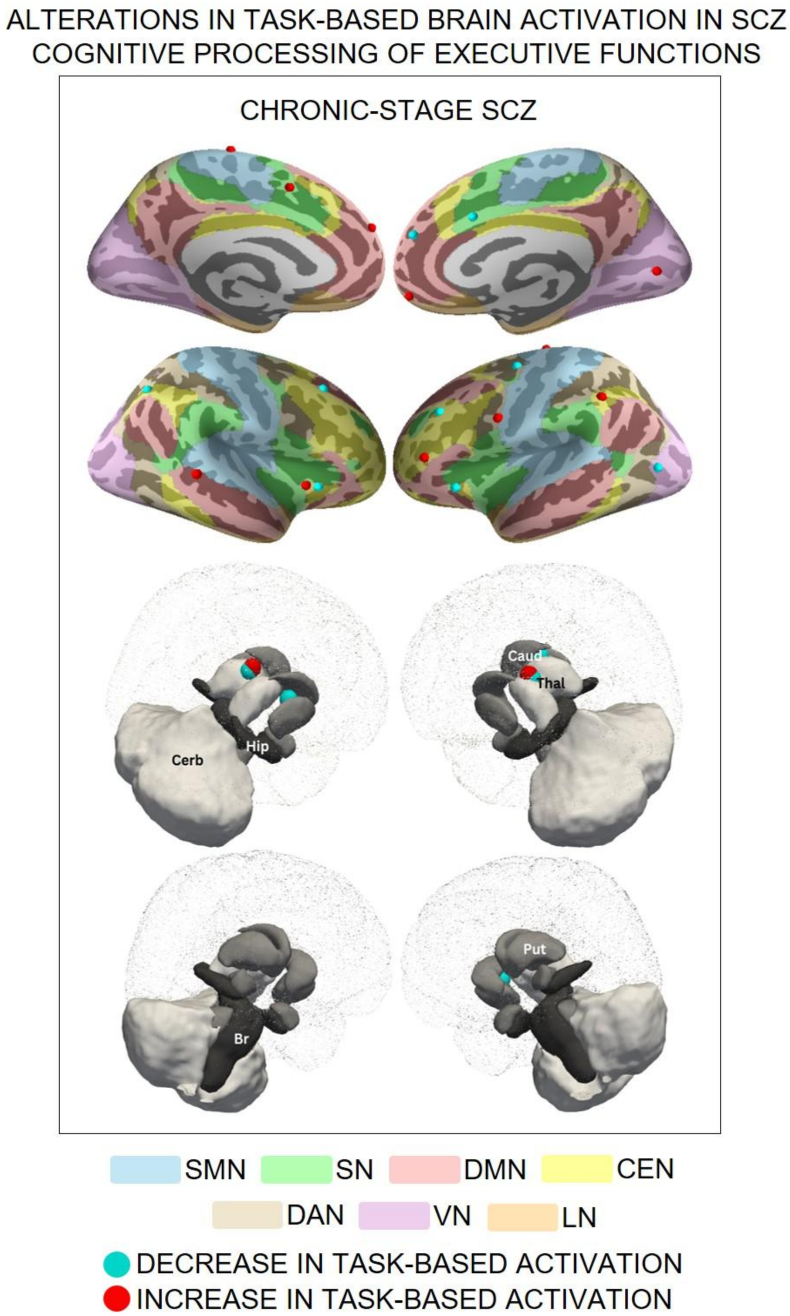

Supplementary Figure 13. Alterations in task-based brain activation in schizophrenia (cognitive processing of executive functions)

Results of the systematic umbrella review of neuroimaging studies investigating task-based brain activation during cognitive processing of executive functions in schizophrenia. All peak coordinates of brain activation alterations during cognitive tasks related to executive functions, as reported in all whole-brain voxelwise meta-analyses on this topic comparing schizophrenia patients and healthy controls, are mapped onto the brain, including both cortical and subcortical structures. Blue spheres indicate decreases in task-based brain activation, and red spheres indicate increases in task-based brain activation in patients relative to controls. Cortical background colors represent the seven large-scale brain networks defined by Yeo *et al*. (2011).

Abbreviations: SCZ, schizophrenia; SMN, somatomotor network; SN, salience network; DMN, default-mode network; CEN, central executive network; DAN, dorsal attention network; VN, visual network; LN, limbic network; Thal, thalamus; Caud, caudate; Put, putamen; Hip, hippocampus; Br, brainstem; Cerb, cerebellum.

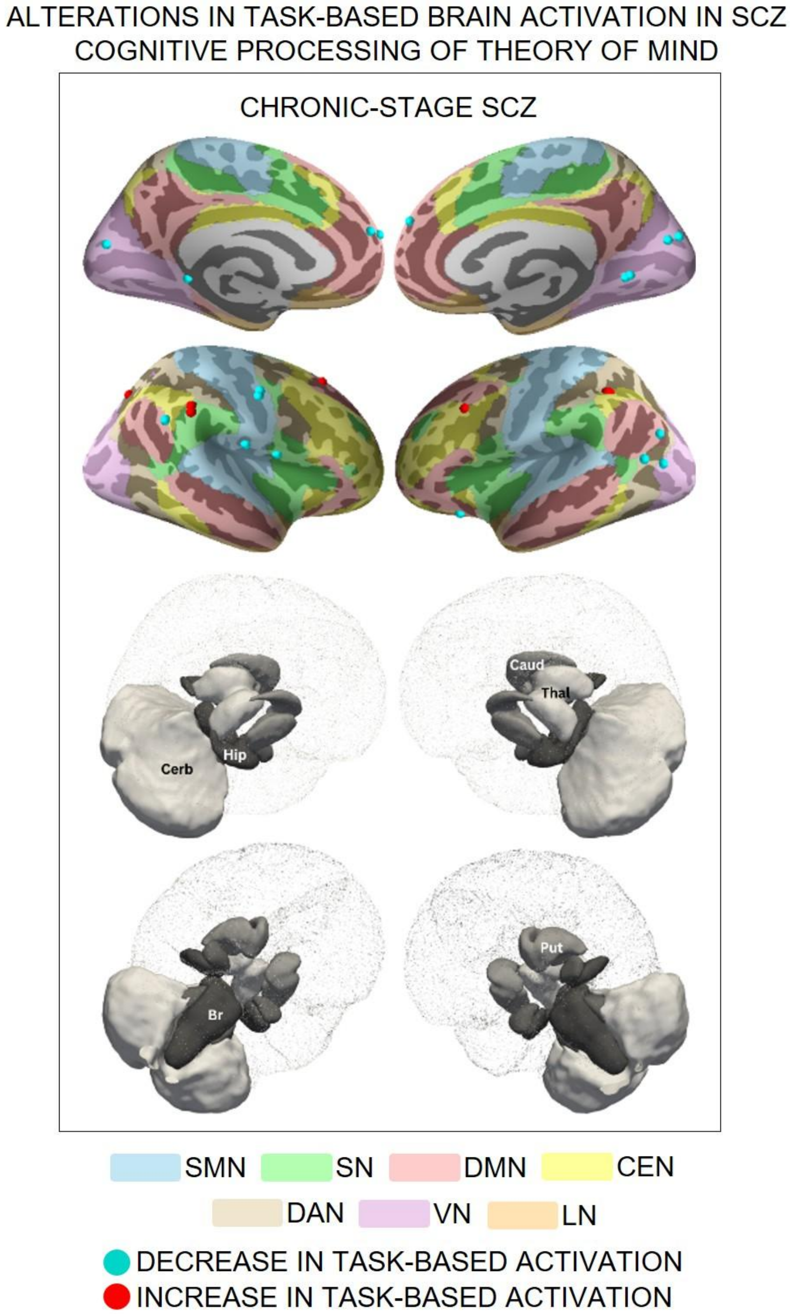

Supplementary Figure 14. Alterations in task-based brain activation in schizophrenia (cognitive processing of theory of mind)

Results of the systematic umbrella review of neuroimaging studies investigating task-based brain activation during cognitive processing of theory of mind in schizophrenia. All peak coordinates of brain activation alterations during cognitive tasks related to theory of mind, as reported in all whole-brain voxelwise meta-analyses on this topic comparing schizophrenia patients and healthy controls, are mapped onto the brain, including both cortical and subcortical structures. Blue spheres indicate decreases in task-based brain activation, and red spheres indicate increases in task-based brain activation in patients relative to controls. Cortical background colors represent the seven large-scale brain networks defined by Yeo *et al*. (2011).

Abbreviations: SCZ, schizophrenia; SMN, somatomotor network; SN, salience network; DMN, default-mode network; CEN, central executive network; DAN, dorsal attention network; VN, visual network; LN, limbic network; Thal, thalamus; Caud, caudate; Put, putamen; Hip, hippocampus; Br, brainstem; Cerb, cerebellum.

Supplementary Figure 15. Brain correlates of symptoms of schizophrenia (visual hallucinations)
Results of the systematic umbrella review of neuroimaging studies investigating brain correlates of visual hallucinations in schizophrenia. All peak coordinates of brain changes related to visual hallucinations, as reported in all whole-brain voxelwise meta-analyses on this topic conducted in schizophrenia patients, are mapped onto the brain, including both cortical and subcortical structures. Red spheres indicate brain activation during the experience of visual hallucinations compared to periods of their absence in the same patients. Cortical background colors represent the seven large-scale brain networks defined by Yeo *et al*. (2011).

Abbreviations: SCZ, schizophrenia; SMN, somatomotor network; SN, salience network; DMN, default-mode network; CEN, central executive network; DAN, dorsal attention network; VN, visual network; LN, limbic network; Thal, thalamus; Caud, caudate; Put, putamen; Hip, hippocampus; Br, brainstem; Cerb, cerebellum.

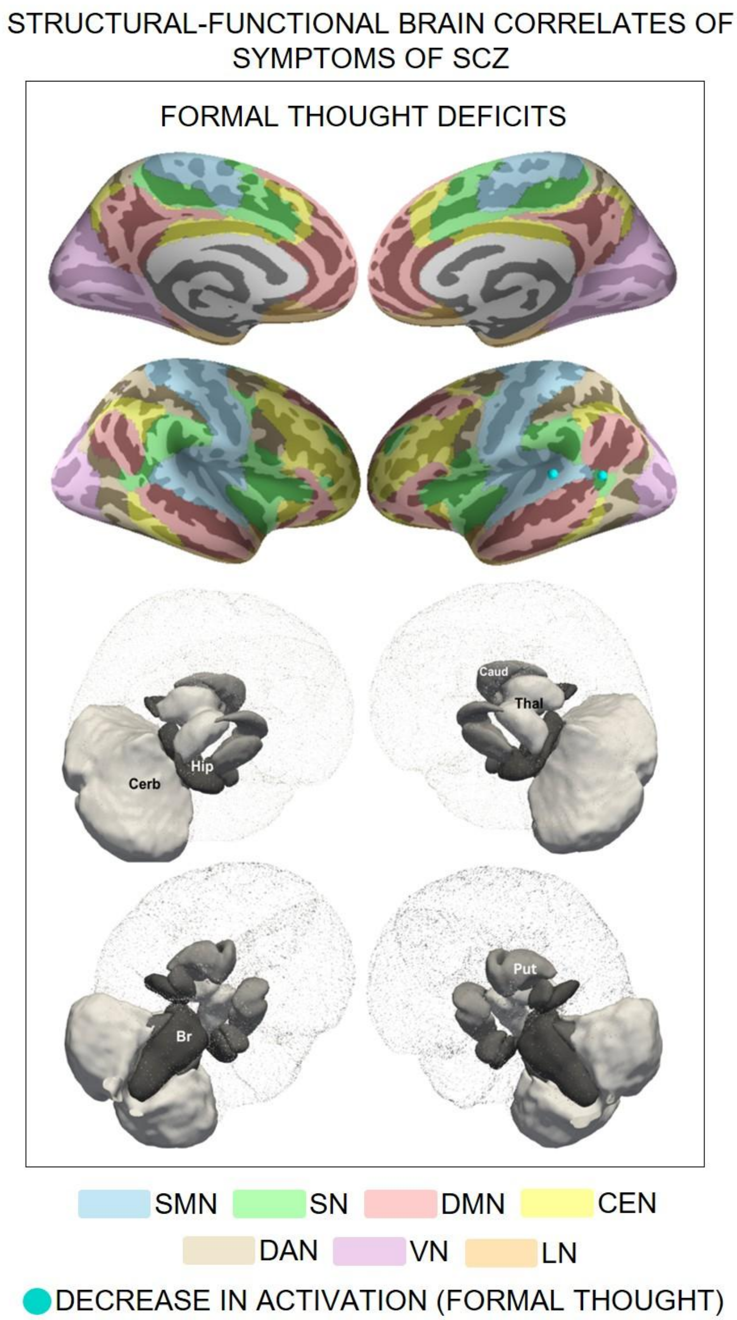

Supplementary Figure 16. Brain correlates of symptoms of schizophrenia (formal thought deficits)
Results of the systematic umbrella review of neuroimaging studies investigating brain correlates of formal thought deficits in schizophrenia. All peak coordinates of brain changes related to formal thought deficits, as reported in all whole-brain voxelwise meta-analyses on this topic conducted in schizophrenia patients, are mapped onto the brain, including both cortical and subcortical structures. Blue spheres indicate decreases in task-based activation during verbal processing correlating with increased severity of formal thought deficits (disorganized speech) in patients. Cortical background colors represent the seven large-scale brain networks defined by Yeo *et al*. (2011).
Abbreviations: SCZ, schizophrenia; SMN, somatomotor network; SN, salience network; DMN, default-mode network; CEN, central executive network; DAN, dorsal attention network; VN, visual network; LN, limbic network; Thal, thalamus; Caud, caudate; Put, putamen; Hip, hippocampus; Br, brainstem; Cerb, cerebellum.

Supplementary Figure 17. Brain correlates of symptoms of schizophrenia (motor deficits)

Results of the systematic umbrella review of neuroimaging studies investigating brain correlates of motor deficits in schizophrenia. All peak coordinates of brain changes related to motor deficits, as reported in all whole-brain voxelwise meta-analyses on this topic conducted in schizophrenia patients, are mapped onto the brain, including both cortical and subcortical structures. Blue spheres indicate decreases in grey matter volume correlating with increased severity of motor deficits in patients. Cortical background colors represent the seven large-scale brain networks defined by Yeo *et al*. (2011).

Abbreviations: SCZ, schizophrenia; SMN, somatomotor network; SN, salience network; DMN, default-mode network; CEN, central executive network; DAN, dorsal attention network; VN, visual network; LN, limbic network; Thal, thalamus; Caud, caudate; Put, putamen; Hip, hippocampus; Br, brainstem; Cerb, cerebellum.

Supplementary Table 1

STRUCTURAL-FUNCTIONAL BRAIN ALTERATIONS IN PRODROME OF SCHIZOPHRENIA										
Study	**Studies/ Subjects**	**Sex (F)**	**Mean Age (years)**	**First-episode / Chronic SCZ**	**Illness Duration**	**Severity**	**Medication-free / Medicated**	**Imaging Modality / Tasks**	**Measure/ Imaging Method**	**Meta-analysis Method**
Ding et al. (2019)	14 datasets 743 CHR 588 HC	321(CHR) 243 (HC) (13/14 datasets)	18.9-25.1 (CHR) 21.0-27.7 (HC)	NA	NA	NS	NS	sMRI	GM/VBM	SDM
Fiorito et al. (2022)	17 datasets 677 C/GHR (392 CHR; 7/17 datasets + 285 GHR; 10/17 datasets) 805 HC	365 (C/GHR) 431 (HC)	14.3-42.3 (C/GHR) 14.3-40.7 (HC)	NA	NA	NS	NS	TB-fMRI (Emotion processing of negative stimuli)	TBA	SDM
Liloia et al. (2021)§	CHR: 16 datasets 580 CHR 621 HC *Early-stage SCZ: 41 datasets 1636 SCZ 1953 HC* *Chronic SCZ: 49 datasets 2120 SCZ 2563 HC*	CHR: 252 (CHR) 227 (HC) (13/16 datasets) *Early-stage SCZ: 625 (SCZ) 735 (HC)* *Chronic SCZ: 711 (SCZ) 968 (HC)*	CHR: 22.4 (CHR) 11-27.7 (HC) (15/16 datasets) *Early-stage SCZ: 22.8 (SCZ) 15.3-31.5 (HC)* *Chronic SCZ: 38.6 (SCZ) 27.2-62.2 (HC)*	CHR: NA *SCZ 1636/2120*	CHR: NA *Early-stage SCZ: 0.8 years* *Chronic SCZ: 15 years*	NS	CHR: 67/580 (14/16 datasets) *Early-stage SCZ: 720/851 (39/41 datasets)* *Chronic SCZ: 105/1825 (44/49 datasets)*	sMRI	GM/VBM	ALE

Luna et al. (2022)	sMRI 19 datasets 599 CHR 620 HC TB-fMRI 22 datasets 519 CHR 503 HC	sMRI 269 (CHR) 267 (HC) (18/19 datasets) TB-fMRI 198 (CHR) 209 (HC) (20/22 datasets)	sMRI 15.8-25 (CHR) 15.7-35.9 (HC) TB-fMRI 13.7-27.1 (CHR) 14.7-29 (HC) (21/22 datasets)	NA	NA	NA	NA	sMRI TB-fMRI (Cognitive and emotion processing)	GM/VBM TBA	SDM
STRUCTURAL-FUNCTIONAL BRAIN ALTERATIONS IN SCHIZOPHRENIA										
Study	**Studies/ Subjects**	**Sex (F)**	**Mean Age (years)**	**First- episode / Chronic SCZ**	**Illness Duration**	**Severity**	**Medication-free / Medicated**	**Imaging Modality / Tasks**	**Measure/ Imaging Method**	**Meta- analysis Method**
Alústiza et al. (2017)	TB-fMRI (Cognitive processing): 37 datasets 1086 SCZ 1182 HC TB-fMRI (Cognitive processing of timing): 10 datasets 200 SCZ 195 HC	NS	NS	NS	NS	NS	NS	TB-fMRI (Cognitive processing / Cognitive processing of timing)	TBA	SDM
Arioli et al. (2021)	19 datasets 292 SCZ 305 HC	NS	NS	NS	NS	NS	NS	TB-fMRI (Cognitive processing of theory of mind)	TBA	ALE
Arsalidou et al. (2020)	8 datasets 118 SCZ 99 HC	32 (SCZ)	15.8 (SCZ)	NS	NS	NS	NS	TB-fMRI (Cognitive processing)	TBA	SDM

Bora et al. (2011)	sMRI/GM: 49 datasets 1999 SCZ 2180 HC sMRI/WM: 24 datasets 903 SCZ 934 HC dMRI/FA: 24 datasets 699 SCZ 681 HC	sMRI/GM: 615 (SCZ) 858 (HC) (48/49 datasets) sMRI/WM: 265 (SCZ) 340 (HC) (24/24 datasets) dMRI/FA: 246 (SCZ) 252 (HC) (24/24 datasets)	sMRI/GM: 19.8-50.9 (44/49 datasets) sMRI/WM: 19.9-40.5 (21/24 datasets) dMRI/FA: 23.7-41.7 (23/24 datasets)	sMRI/GM: 431/1568 (14/35 datasets) sMRI/WM: 217/686 (7/17 datasets) dMRI/FA: 127/527 (4/20 datasets)	sMRI/GM: 0.8-23.1 years (19/49 datasets) sMRI/WM: 5.2-16.5 years (12/24 datasets) dMRI/FA: 1.7-18.2 years (13/24 datasets)	NS	sMRI/GM: 238/1401 (36/49 datasets) sMRI/WM: 56/611 (16/24 datasets) dMRI/FA: 55/421 (18/24 datasets)	sMRI dMRI	GM/VBM WM/VBM FA	SDM
Brandl et al. (2018)	127 datasets 6311 SCZ 6745 HC	NS	11-59.9 (SCZ) 11.8-62.2 (HC) (126/127 datasets)	NS	NS	NS	NS	sMRI	GM/VBM	MKDA
Casale et al. (2016)	11 datasets 290 SCZ 316 HC	102 (SCZ) 112 (HC)	24.5 (SCZ) 25.1 (HC) (10/11 datasets)	290/0	19.2-139 weeks (10/11 datasets)	NS	90/197	TB-fMRI (Cognitive processing of attention / Cognitive processing of working memory)	TBA	ALE
Chase et al. (2018)	20 datasets 471 SCZ 482 HC	NS	NS	NS	NS	NS	45/426[a]	TB-fMRI (Emotion processing of positive stimuli)	TBA	ALE
Di et al. (2009)	17 datasets 712 SCZ 639 HC	231 (SCZ) 235 (HC)	15.7-40.5 (SCZ)	119/577 (16/17 datasets)	<0.1-16.9 years (16/17 datasets)	NS	72/613 (16/17 datasets)	sMRI	WM/VBM	ALE

Dong et al. (2017)	24 datasets 754 SCZ 775 HC	286 (SCZ) 305 (HC)	30.8 (SCZ) 31 (HC)	237/517	0.5-19 years (22/24 datasets)	PANSS (Positive): 10.5-26.3 (11/24 datasets) PANSS (Negative): 6.3-22.9 (11/24 datasets) BPRS: 10.1-46 (2/24 datasets)	204/510 (23/24 datasets)	dMRI	FA	SDM
Dong et al. (2018)	21 datasets 354 SCZ 374 HC	105 (SCZ) (19/21 datasets) 126 (HC) (18/21 datasets)	17.8-44.7 (SCZ) 17.9-41(HC)	25/329	0.5-19.9 years (17/21 datasets)	PANSS (Total): 40.4-85.4 (13/21 datasets) PANSS (Positive): 8.9-24.7 (14/21 datasets) PANSS (Negative): 9.4-22.1 (14/21 datasets) PANSS (General): 12.9-40.7 (12/21 datasets) SAPS: 1.4-25.1 (6/21 datasets)	7/320 (20/21 datasets)	TB-fMRI (Emotion processing of negative stimuli)	TBA	SDM

						SANS: 1.3-27.9 (6/21 datasets)				
Dugré et al. (2019)	14 datasets 304 SCZ 290 HC	30.2% (13/14 datasets)	34.7	NS	NS	PANSS (Positive): 8-19.4 (8/14 datasets)	NS	TB-fMRI (Emotion processing of neutral stimuli)	TBA	SDM
Ellision-Wright and Bullmore (2009)	15 datasets 407 SCZ 383 HC	NS	NS	NS	0.5-18.2 years (10/15 datasets)	NS	NS	dMRI	FA	ALE
Fornara et al. (2017)	31 datasets 1207 SCZ 1328 HC	NS	NS	0/1207	NS	NS	NS	sMRI	GM/VBM	ALE
Gao et al. (2018)	sMRI: 15 datasets 486 SCZ 485 HC RS-fMRI: 16 datasets 403 SCZ 428 HC	sMRI: 221 (SCZ) 232 (HC) (14/15 datasets) RS-fMRI: 145 (SCZ) 188 (HC) (15/16 datasets)	sMRI: 26 (SCZ) 25.8 (HC) (14/15 datasets) RS-fMRI: 24.9 (SCZ) 24.8 (HC)	sMRI: 422/64 RS-fMRI: 358/45	sMRI: 18.9 months (11/15 datasets) RS-fMRI: 17.8 months (13/16 datasets)	sMRI: PANSS (Total): 53.2-97.8 (10/15 datasets) PANSS (Positive): 19-30.4 (11/15 datasets) PANSS: (Negative): 13.8-29.1 (11/15 datasets) RS-fMRI: PANSS (Total):	sMRI: 486/0 RS-fMRI: 403/0	sMRI RS-fMRI	GM/VBM CP: ALFF CBF	SDM

						40-106.2 (12/16 datasets) PANSS (Positive): 19.5-32.2 (12/16 datasets) PANSS (Negative): 17-28.1 (12/16 datasets)				
Gong et al. (2019)	28 datasets 1249 SCZ 1179 HC	528 (SCZ) 543 (HC)	28.9 (SCZ) 29.8 (HC)	583/666	70.2 months	PANSS (Total): 52.9-107.2 (23/28 datasets) PANSS (Positive): 11.4-79.5 (25/28 datasets) PANSS (Negative): 13.4-79.5 (25/28 datasets) PANSS (General): 26.2-51.3 (20/28 datasets)	402/181 (First-episode SCZ)	RS-fMRI	ALFF	SDM
Goodkind et al. (2015)	94 datasets 3795 SCZ 4315 HC	0-97.8 % (SCZ) 0-60% (HC)	15.4-59.9 (SCZ) 15.4-62.2 (HC)	684/3111	NS	NS	NS	sMRI	GM/VBM	ALE

Huang et al. (2021)	80 datasets 3517 SCZ 3676 HC	35.1% (SCZ) 37.6% (HC) (79/80 datasets)	37.3 (SCZ) 32.4 (HC)	NS	NS	NS	NS	sMRI	GM/VBM	ALE
Jáni et al. (2018)	TB-fMRI/PET (Emotion processing): 12 datasets 199 SCZ 215 HC TB-fMRI/PET (Cognitive processing of theory of mind): 16 datasets 262 SCZ 279 HC	NS	NS	NS	TB-fMRI/PET (Emotion processing): 0.4-15.2 (6/12 datasets) TB-fMRI/PET (Cognitive processing of theory of mind): 3.0-17.1 (10/16 datasets)	TB-fMRI/PET (Emotion processing): PANSS (Positive): 8-24.7 (10/12 datasets) PANSS (Negative): 7.5-19.9 (10/12 datasets) TB-fMRI/PET (Cognitive processing of theory of mind): PANSS (Positive): 10.1-18.2 (14/16 datasets) PANSS (Negative): 7.8-21.2 (14/16 datasets)	TB-fMRI/PET (Emotion processing): 21 (1/12 datasets) / 89 (5/12 datasets) TB-fMRI/PET (Cognitive processing of theory of mind): 18 (1/16 datasets) / 189 (11/16 datasets)	TB-fMRI/PET (Emotion processing / Cognitive processing of theory of mind)	TBA	SDM

Kompus et al. (2011)§	TB-fMRI/PET (Auditory perception): 11 datasets 204 SCZ 170 HC *fMRI/PET (Auditory hallucinations): 12 datasets 88 SCZ (15 subclinical hallucinations)*	NS	NS	NS	NS	NS	TB-fMRI/PET (Auditory perception): 23/181 *fMRI/PET (Auditory hallucinations): 15/88*	TB-fMRI/PET (Auditory perception) *fMRI/PET (Symptom capture)*	TBA *Activation (Hallucination experience)*	ALE
Kronbichler et al. (2017)	21 datasets 308 SCZ 315 HC	112 (SCZ) 111 (HC)	6.8-42.4 (SCZ) 8.8-42.9 (HC)	NS	3-17.1 years (15/21 datasets)	PANSS (Positive): 10.1-18.2 (9/21 datasets) PANSS (Negative): 14.9-21.6 (9/21 datasets) SAPS: 1.5-6.9 (5/21 datasets) SANS: 1.7-27.1 (6/21 datasets)	18 (1/21 datasets) / 244 (15/21 datasets)	TB-fMRI (Cognitive processing of theory of mind)	TBA	SDM
Kuhn and Gallinat (2013)	11 datasets 285 SCZ 282 HC	NS	NS	109/176	NS	NS	94/175 (10/11 datasets)	RS-fMRI/ PET/SPECT	CP: ALFF ReHo FC	ALE

									CM CBF	
Li et al. (2010)	17 datasets 268 SCZ 243 HC	NS	20.4-47.7 (SCZ) 24.4-48.2 (HC)	NS	NS	NS	5/263	TB-fMRI (Emotion processing)	TBA	ALE
Liloia et al. (2021)§	*CHR:* *16 datasets* *580 CHR* *621 HC* Early-stage SCZ: 41 datasets 1636 SCZ 1953 HC Chronic SCZ: 49 datasets 2120 SCZ 2563 HC	*CHR:* *252 (CHR)* *227 (HC)* *(13/16 datasets)* Early-stage SCZ: 625 (SCZ) 735 (HC) Chronic SCZ: 711 (SCZ) 968 (HC)	*CHR:* *22.4 (CHR)* *11-27.7 (HC)* *(15/16 datasets)* Early-stage SCZ: 22.8 (SCZ) 15.3-31.5 (HC) Chronic SCZ: 38.6 (SCZ) 27.2-62.2 (HC)	*CHR:* *NA* SCZ: 1636/2120	*CHR:* *NA* Early-stage SCZ: 0.8 years Chronic SCZ: 15 years	NS	*CHR:* *67/580* *(14/16 datasets)* Early-stage SCZ: 720/851 (39/41 datasets) Chronic SCZ: 105/1825 (44/49 datasets)	sMRI	GM/VBM	ALE
McTeague et al. (2017)	139 datasets 2906 SCZ 2622 HC	NS	NS	NS	NS	NS	NS	TB-fMRI/PET (Cognitive processing)	TBA	ALE
McTeague et al. (2020)	59 datasets 906 SCZ 888 HC	NS	NS	NS	NS	NS	NS	TB-fMRI/PET (Emotion processing)	TBA	ALE
Minzenberg et al. (2009)	41 datasets 594 SCZ 623 HC	169 (SCZ) (40/41 datasets)	24.9-46.6 (SCZ)	NS	0.2-25 years (22/41 datasets)	PANSS (Total): 8-64.6 (5/41 datasets) PANSS (Positive): 7.1-23.8 (18/41	78/431 (37/41 datasets)	TB-fMRI (Cognitive processing of executive functions)	TBA	ALE

						datasets) PANSS (Negative): 10.7-21.6 (18/41 datasets) PANSS (General): 7.9-35.2 (14/41 datasets) SAPS: 2.5-27.2 (5/41 datasets) SANS: 2.5-63.9 (8/41 datasets) BPRS: 16-56.6 (8/41 datasets) SSPI (Total): 8.3-19.8 (4/41 datasets) SSPI (Positive): 2.0-2.8 (2/41 datasets) SSPI (Negative): 1-4 (2/41				

						datasets) SSPI (Disorganize): 0.9-1.6 (2/41 datasets) PSAS 15.4 (1/41 datasets)				
Olabi et al. (2012)	18 datasets 555 SCZ 621 HC	NS	24.4 (SCZ) 24.5 (HC)	555/0	NS	NA	NS	sMRI	GM/VBM	ALE
Ortuño et al. (2011)	3 datasets 29 SCZ 35 HC	NS	NS	NS	NS	NS	NS	TB-fMRI/PET (Cognitive processing of timing)	TBA	ALE
Picó-Pérez et al. (2022)	sMRI: 114 datasets 4789 SCZ 5216 HC TB-fMRI (Cognitive processing): 143 datasets 3446 SCZ 3723 HC TB-fMRI (Cognitive processing of social cognition): 86 datasets 1755 SCZ 1819 HC	sMRI: 36.4% (SCZ) 43.3% (HC) TB-fMRI (Cognitive processing): 29.7% (SCZ) 37.2% (HC) TB-fMRI (Cognitive processing of social cognition):	sMRI: 33.5 (SCZ) 32.5 (HC) TB-fMRI (Cognitive processing): 33.2 (SCZ) 32.3 (HC) TB-fMRI (Cognitive processing of social cognition): 33.7 (SCZ) 33 (HC)	NS	sMRI: 0.3-29.2 years (90/114 datasets) TB-fMRI (Cognitive processing): 0.2-29.2 years (100/143 datasets) TB-fMRI (Cognitive processing of social cognition): 0.6-26.1 years (60/86 datasets)	sMRI: PANSS (Total): 48.7-106.6 (75/114 datasets) PANSS (Positive): 6.6-31.11 (71/114 datasets) PANSS: (Negative): 10.4-29.1 (71/114 datasets) PANSS: (General): 7.5-58.7	sMRI: 565/3306 (102/114 datasets) TB-fMRI (Cognitive processing): 196/2852 (129/143 datasets) TB-fMRI (Cognitive processing of social cognition): 53/1531 (76/86 datasets)	sMRI TB-fMRI (Cognitive processing / Cognitive processing of social cognition)	GM/VBM TBA	SDM

		35.8% (SCZ) 41.5% (HC)				(67/114 datasets) TB-fMRI (Cognitive processing): PANSS (Total): 42.6-101 (67/143 datasets) PANSS (Positive): 4.3-22.9 (60/143 datasets) PANSS: (Negative): 10-58.4 (59/143 datasets) PANSS: (General): 13.2-67.2 (51/143 datasets) TB-fMRI (Cognitive processing of social cognition): PANSS (Total): 24.4-105.8 (46/86 datasets) PANSS (Positive):				

						2.2-23.4 (50/86 datasets) PANSS (Negative): 9.4-28.1 (48/86 datasets) PANSS (General): 2.1-54.2 (44/86 datasets)				
Ragland et al. (2009)	18 datasets 248 SCZ 231 HC	NS	NS	NS	NS	NS	0/248	TB-fMRI/PET (Cognitive processing of episodic memory)	TBA	ALE
Taylor et al. (2012)	26 datasets 450 SCZ 422 HC	124 (SCZ) 119 (HC)	32.5 (SCZ) 31.2 (HC)	42/390 (25/26 datasets)	NS	NS	12/438[a]	TB-fMRI/PET (Emotion processing)	TBA	MKDA
Townsend et al. (2022)	8 datasets 234 SCZ 120 HC	NS	NS	NS	NS	NS	NS	PET	CM	SDM
Vitolo et al. (2018)	sMRI: 25 datasets 978 SCZ 934 HC dMRI: 34 datasets 1220 SCZ 1237 HC	sMRI: 305 (SCZ) 340 (HC) (24/25 datasets) dMRI: 442 (SCZ) 461 (HC) (33/34 datasets)	sMRI: 15.8-40.4 (SCZ) 15.8-38.6 (HC) dMRI: 15.2-46.9 (SCZ) 15.3-47.4 (HC)	sMRI: 333 (10/25 datasets) / 28 (1/25 datasets) dMRI: 361 (12/34 datasets) / 90 (4/34 datasets)	sMRI: 0.3-16.8 years (18/25 datasets) dMRI: 0.5-19 years (20/34 datasets)	NS	NS	sMRI dMRI	WM/VBM FA	ALE
Vucurovic et al. (2020)	TB-fMRI/PET (Cognitive processing	NS	TB-fMRI/PET (Cognitive processing	NS	TB-fMRI/PET (Cognitive processing	TB-fMRI/PET (Cognitive processing of	NS	TB-fMRI/PET (Cognitive processing of theory of mind /	TBA	ALE

	of theory of mind): 17 datasets 274 SCZ 286 HC TB-fMRI (Emotion processing): 13 datasets 240 SCZ 242 HC		of theory of mind): 25.5-38.8 (SCZ) 24.7-42.5 (HC) TB-fMRI (Emotion processing): 25.5-46.5 (SCZ) 24.7-46.7 (HC)		of theory of mind): 2.4-13 years (13/17 datasets) TB-fMRI (Emotion processing): 2.4-26.9 years (10/13 datasets)	theory of mind): PANSS (Positive): 3.1-17.8 (12/17 datasets) PANSS (Negative): 1.7-21.6 (12/17 datasets) TB-fMRI (Emotion processing): PANSS (Positive): 12.3-16 (6/13 datasets) PANSS (Negative): 12-21.6 (6/13 datasets) SAPS: 1.5-10 (3/13 datasets) SANS: 7.9-27.1 (5/13 datasets) BPRS (Total): 33.7-40.1 (2/13		Emotion processing)		

						datasets) BPRS (Positive): 1.5-2.3 (2/13 datasets) BPRS (Negative): -1.7-1.9 (2/13 datasets)				
Wang et al. (2021)	38 datasets 1126 SCZ 1139 HC	325 (SCZ) 402 (HC) (33/38 datasets)	33.3 (SCZ) 32.1 (HC) (37/38 datasets)	NS	0.9-21.8 years (22/38 datasets)	PANSS: 2.9-84.2 (17/38 datasets) BPRS: 20.8-25.1 (3/38 datasets)	71/897 (34/38 datasets)	TBA-fMRI (Cognitive processing of working memory)	TBA	SDM
Weng et al. (2022)	25 datasets 427 SCZ 405 HC	159 (SCZ) 157 (HC) (24/25 datasets)	33.1 (SCZ) 32 (HC)	NS	8.9 years (17/25 datasets)	PANSS (Total): 82 (1/25 datasets) PANSS (Positive): 3.1-18.2 (13/25 datasets) PANSS (Negative): 1.7-21.6 (13/25 datasets) SAPS: 1.5-12.3 (5/25	18 (1/25 datasets) / 372[a] (21/25 datasets)	TBA-fMRI/PET (Cognitive processing of theory of mind)	TBA	SDM

						datasets) SANS: 2.1-27.1 (7/25 datasets)				
Wu et al. (2019)	52 datasets 971 SCZ 1028 HC	NS	NS	101/870	NS	NS	153/818[a]	TB-fMRI (Cognitive processing of working memory)	TBA	ALE
Yao et al. (2013)	8 datasets 271 SCZ 297 HC	123 (SCZ) (8/8 datasets) 103 (HC) (7/8 datasets)	NS	271/0	3.8-10.3 months (6/8 datasets)	NS	64 (2/8 datasets) / 197[a] (5/8 datasets)	dMRI	FA	ALE
Zeng et al. (2022)	17 datasets 368 SCZ 428 HC	103 (SCZ) 149 (HC)	32.1 (SCZ) 32.3 (HC)	68/300	NS	NS	83/285	TB-fMRI (Emotion processing of positive stimuli)	TBA	SDM
Zhang et al. (2016)	24 datasets 436 SCZ 412 HC	36.3% (SCZ) 28.6% (HC)	30.7 (SCZ) 31.8 (HC)	NS	NS	NS	120/316	TB-fMRI (Emotion processing of positive stimuli)	TBA	ALE
Zhao et al. (2021)	dMRI: 48 datasets 1543 SCZ 1612 HC sMRI: 24 datasets 1068 SCZ 1073 HC	dMRI: 580 (SCZ) 673 (HC) sMRI: 413 (SCZ) 416 (HC)	dMRI: 30.3 (SCZ) 30.6 (HC) sMRI: 30.2 (SCZ) 29.5 (HC)	dMRI: 478/944 (45/48 datasets) sMRI: 324/510 (20/24 datasets)	dMRI: 0.4-20.2 years (40/48 datasets) sMRI: 0.6-17.4 years (15/24 datasets)	dMRI: PANSS (Total): 50-100.9 (19/48 datasets) PANSS (Positive): 9-27.2 (30/48 datasets) PANSS (Negative):	dMRI: 239/1165 (44/48 datasets) sMRI 155/664 (21/24 datasets)	dMRI sMRI	FA WM	SDM

						13-30.3 (29/48 datasets) PANSS (General): 25-50.9 (16/48 datasets) SAPS: 26.9 (1/48 datasets) SANS: 19.8-52.1 (3/48 datasets) BPRS (Total): 36-42.2 (2/48 datasets) BPRS (Positive): 10.1 (1/48 datasets) BPRS (Negative): 6.3 (1/48 datasets) SSPI: 11.5 (1/48 datasets) sMRI: PANSS (Total):				

						41.4-69 (2/24 datasets) PANSS (Positive): 12.9-26.6 (12/24 datasets) PANSS (Negative): 18-27.1 (12/24 datasets) SAPS: 1.2-31.3 (4/24 datasets) SANS: 1.7-40.3 (4/24 datasets)				
STRUCTURAL-FUNCTIONAL BRAIN CORRELATES OF SYMPTOMS OF SCHIZOPHRENIA										
Study	**Studies/ Subjects**	**Sex (F)**	**Mean Age (years)**	**First-episode / Chronic SCZ**	**Illness Duration**	**Severity**	**Medication-free / Medicated**	**Imaging Modality / Tasks**	**Measure/ Imaging Method**	**Meta-analysis Method**
Jardri et al. (2011)	10 datasets 68 SCZ	NS	NS	15/53	NS	NS	NS	fMRI/PET (Symptom capture)	Activation (Hallucination experience)	ALE
Kompus et al. (2011)§	*TB-fMRI/PET (Auditory perception): 11 datasets 204 SCZ 170 HC*	NS	NS	NS	NS	NS	*TB-fMRI/PET (Auditory perception): 23/181* fMRI/PET (Auditory	*TB-fMRI/PET (Auditory perception)* fMRI/PET (Symptom capture)	*TBA* Activation (Hallucination experience)	ALE

	fMRI/PET (Auditory hallucinatio ns): 12 datasets 88 SCZ (15 subclinical hallucinatio ns)						hallucinations): 15/88			
Kuhn and Gallinat (2012)	fMRI/PET (Auditory hallucinatio ns): 10 datasets 85 SCZ *TB-fMRI/PET (Auditory perception/i magery):* *8 datasets* *120 SCZ* *(81 SCZ with hallucinatio ns* *39 SCZ without hallucinatio ns)* *69 HC*	NS	NS	NS	NS	NS	NS	fMRI/PET (Symptom capture) *TB-fMRI/PET (Auditory perception/imager y)*	Activation (Hallucinati on experience) *TBA*	ALE
Palaniyappan et al. (2012)	7 datasets 350 SCZ	90 (6/7 datasets)	33-36.2 (6/7 datasets)	NS	8-13.6 years (4/7 datasets)	NS	0/350	sMRI	GM/VBM	SDM
Wensing et al. (2017)	17 datasets 165 SCZ	NS	13.3-40	NS	NS	NS	NS	TB-fMRI (Verbal processing)	TBA	ALE

Zhao et al. (2014)	6 datasets 303 SCZ	NS	NS	303/0	NS	NS	107/196	sMRI	GM WM	ALE
Zmigrod et al. (2016)	fMRI/PET (Auditory hallucinations): 16 datasets 161 SCZ (29 non-SCZ with hallucinations) fMRI/PET (Visual hallucinations): 7 datasets 16 SCZ (5 non-SCZ with hallucinations)	NS	NS	NS	NS	NS	NS	fMRI/PET (Symptom capture)	Activation (Hallucination experience)	ALE

Notes:
§ Study reported in multiple sections of the table (data/results in italics are not considered in the current section of the table).
[a] Most medicated/not specified
Abbreviations: CHR, clinical high risk for schizophrenia; GHR, genetic high risk for schizophrenia; SCZ, schizophrenia; HC, healthy controls; MRI, magnetic resonance imaging; sMRI, structural MRI; dMRI, diffusion MRI; RS-fMRI, resting state-functional MRI; TB-fMRI, task based-functional MRI; PET, positron emission tomography; GM, grey matter; WM, white matter; VBM, voxel based morphometry; FA, fractional anisotropy; ALFF, amplitude of low-frequency fluctuations; ReHo, regional homogeneity; FC, functional connectivity; CM, cerebral metabolism; CBF, cerebral blood flow; CP, combined parameters; TBA, task-based activation; PANSS, positive and negative syndrome scale; BPRS, brief psychiatric rating scale; SAPS, scales for the assessment of positive symptoms; SANS, scale for the assessment of negative symptoms; SSPI, signs and symptoms of psychotic illness; PSAS, psychiatric symptom assessment scale; ALE, activation likelihood estimation; SDM, seed-based d-mapping; MKDA, multi-level kernel density analysis; NS, not specified.

Supplementary Table 2

STRUCTURAL-FUNCTIONAL BRAIN ALTERATIONS IN PRODROME OF SCHIZOPHRENIA		
Study	**Main Results**	**Specific Results**
Ding et al. (2019)	Decreased GM in medial prefrontal cortex in CHR. Increased GM in median cingulate, temporal pole, fusiform gyrus, and thalamus in CHR.	Decreased GM in CHR vs. HC: 1) Gyrus rectus R (BA 11); Coordinates: MNI [4, 38, -18]; Cluster size: 480 voxels; #(13/14)/*/† 2) Superior frontal gyrus, medial part R (BA 10); MNI [10, 56, 14]; Cluster size: 287 voxels; #(12/14)/* 3) Superior frontal gyrus, orbital part L (BA 11); MNI [-20, 52, -14]; Cluster size: 136 voxels; #(14/14)/* Increased GM in CHR vs. HC: 1) Median cingulate R; MNI [6, -14, 30]; Cluster size: 234 voxels; #(12/14)/† 2) Fusiform gyrus R (BA 20); MNI [22, 0, -50]; Cluster size: 202 voxels; #(13/14)/† 3) Temporal pole, superior temporal gyrus L (BA 28); MNI [-18, 6, -34]; Cluster size: 164 voxels; #(13/14)/† 4) Thalamus R; MNI [8, -18, 20]; Cluster size: 60 voxels; #(13/14)/†
Fiorito et al. (2022)	No alterations in TBA in CHR during emotion processing of negative stimuli	No significant differences of TBA in C/GHR vs. HC during emotion processing of negative stimuli*/†
Liloia et al. (2021)§	Decreased GM in medial prefrontal cortex in CHR *Decreased GM in insula, superior temporal gyrus/primary auditory cortex pre/postcentral gyrus, and anterior cingulate cortex/medial prefrontal cortex (left-side) in early-stage SCZ* *Decreased GM in insula/superior temporal gyrus, inferior frontal gyrus, anterior cingulate cortex/medial prefrontal cortex, thalamus (associative nuclei), caudate, and amygdala (bilateral) in chronic SCZ* *Progression of GM loss from medial prefrontal cortex (CHR) to left*	Decreased GM in CHR vs. HC: 1) Anterior cingulate cortex R (BA 32); Coordinates: Tal [4, 36, -6] → MNI [5, 41, -7]; Cluster size: 800 mm^3 *Decreased GM in early stage SCZ vs. HC:* *1) Precentral gyrus L (BA 6);* *Coordinates: Tal [-48, -10, 24] → MNI [-50, -10, 24]; Cluster size: 1776 mm3* *2) Transverse temporal gyrus R (BA 41);* *Coordinates: Tal [48, -24, 16] → MNI [50, -24, 14]; Cluster size: 1624* mm^3 *3) Middle temporal gyrus R (BA 22);* *Coordinates: Tal [50, -8, -8] → MNI [53, -5, -15]; Cluster size: 1296* mm^3 *4) Insula L (BA 13);* *Coordinates: Tal [-32, 22, 4] → MNI [-33, 25, 2]; Cluster size: 1096* mm^3 *5) Transverse temporal gyrus L (BA 41);* *Coordinates: Tal [-46, -18, 10] → MNI [-49, -17, 8]; Cluster size: 1032* mm^3 *6) Anterior cingulate cortex L (BA 32);* *Coordinates: Tal [-2, 34, -4] → MNI [-2, 38, -5]; Cluster size: 784* mm^3 *7) Amygdala L;*

	insula/superior temporal gyrus and pre/postcentral gyrus (early-stage SCZ) to bilateral anterior insula/inferior frontal gyrus, basal ganglia, and thalamus (chronic SCZ)	*Coordinates: Tal [-20, -4, -18] → MNI [-20, -1, -25]; Cluster size: 752 mm^3* *Decreased GM in chronic SCZ vs. HC:* *1) Insula L (BA 13);* *Coordinates: Tal [-34, 18, 6] → MNI [-35, 21, 4]; Cluster size: 4928 mm^3* *2) Insula R (BA 13);* *Coordinates: Tal [40, 14, 2] → MNI [42, 17, -2]; Cluster size: 3056 mm^3* *3) Thalamus (medial dorsal nucleus) L;* *Coordinates: Tal [-2, -16, 6] → MNI [-3, -15, 3]; Cluster size: 2312 mm^3* *4) Medial frontal gyrus R (BA 11);* *Coordinates: Tal [4, 36, -14] → MNI [5, 41, -15]; Cluster size: 1656 mm^3* *5) Caudate (nucleus head) L;* *Coordinates: Tal [-4, 6, -4] → MNI [-4, 9, -8]; Cluster size: 1224 mm^3* *6) Amygdala L;* *Coordinates: Tal [-20 -6 -12] → MNI [-20, -4, -18]; Cluster size: 1056 mm^3* *7) Amygdala R;* *Coordinates: Tal [16, -4, -16] → MNI [17, -1, -23]; Cluster size: 680 mm^3* *Subgroup meta-analysis:* *Studies comparing CHR, early-stage and chronic SCZ:* *Decreased GM in CHR and early-stage SCZ vs. HC:* *1) Anterior cingulate cortex R (BA 32);* *Coordinates: Tal [2, 36, -6] → MNI [3, 41, -7]; Cluster size: 144 mm^3* *Decreased GM in early-stage SCZ vs. CHR:* *1) Superior temporal gyrus L (BA 22);* *Coordinates: Tal [-50, -13, 8] → MNI [-53, -12, 6]; Cluster size: 1032 mm^3* *2) Postcentral gyrus L (BA 43);* *Coordinates: Tal [-50, -10, 16] → MNI [-53, -9, 15]; Cluster size: 768 mm^3* *3) Insula L (BA 13);* *Coordinates: Tal [-32, 12, 8] → MNI [-33, 15, 6]; Cluster size: 576 mm^3* *4) Insula L (BA 13);* *Coordinates: Tal [-46, 4, 14] → MNI [-48, 6, 13]; Cluster size: 224 mm^3* *Decreased GM in early-stage and chronic SCZ vs. HC:* *1) Insula L (BA 13);* *Coordinates: Tal [-32, 20, 4] → MNI [-33, 23, 2]; Cluster size: 680 mm^3* *2) Amygdala L;* *Coordinates: Tal [-20, -4, -16] → MNI [-20, -1, -23]; Cluster size: 304 mm^3* *3) Anterior cingulate cortex L (BA 32);* *Coordinates: Tal [0, 34, -4] → MNI [0, 38, -5]; Cluster size: 120 mm^3* *4) Precentral gyrus L (BA 6);* *Coordinates: Tal [-52, -6, 6] → MNI [-55, -4, 3]; Cluster size: 56 mm^3* *5) Inferior frontal gyrus L (BA 47);* *Coordinates: Tal [-48, 6, 14] → MNI [-51, 8, 13]; Cluster size: 24 mm^3* *Decreased GM in early-stage SCZ vs. chronic SCZ:*

		1) Precentral gyrus L (BA 6); *Coordinates: Tal [-49, -5, 24] → MNI [-51, -5, 24]; Cluster size: 520 mm^3* *2) Postcentral gyrus L (BA 43);* *Coordinates: Tal [-47, -17, 14] → MNI [-50, -17, 13]; Cluster size: 136 mm^3* *3) Middle temporal gyrus R (BA 21);* *Coordinates: Tal [44, -8, -12] → MNI [47, -5, -19]; Cluster size: 16 mm^3* *Decreased GM in chronic SCZ vs. early-stage SCZ:* *1) Parahippocampal gyrus R (BA 34);* *Coordinates: Tal [12, -3, -16] → MNI [-13, 0, -23]; Cluster size: 672 mm^3* *2) Thalamus (medial dorsal nucleus/Pulvinar) L;* *Coordinates: Tal [-7, -20, 11] → MNI [-8, -20, 9]; Cluster size: 480 mm^3* *3) Inferior frontal gyrus L (BA 44);* *Coordinates: Tal [-46, 12, 8] → MNI [-48, 15, 6]; Cluster size: 256 mm^3* *4) Insula R (BA 13);* *Coordinates: Tal [36, 20, 2] → MNI [38, 33, -1]; Cluster size: 40 mm^3* *5) Superior temporal gyrus L (BA 22);* *Coordinates: Tal [-51, 8, 4] → MNI [-54, 11, 1]; Cluster size: 16 mm^3* <u>*Meta-regression analysis:*</u> *Effects of clinical variables on GM reduction in SCZ:* *Negative correlation between male percentage in SCZ and GM in:* *1) Thalamus L/R;* *Coordinates: Tal [-1, -9, 7] → MNI [-2, -8, 5]; Cluster size: 94 voxels* *2) Superior temporal gyrus L;* *Coordinates: Tal [-51, -30, 13] → MNI [-54, -30, 11]; Cluster size: 52 voxels* *3) Insula R;* *Coordinates: Tal [32, 14, 8] → MNI [34, 17, 5]; Cluster size: 50 voxels* *4) Inferior temporal gyrus L;* *Coordinates: Tal [-30, -9, -35] → MNI [-31, -6, -44]; Cluster size: 46 voxels* *Negative correlation between percentage of medicated SCZ and GM in:* *1) Superior temporal gyrus R;* *Coordinates: Tal [43, 14, -8] → MNI [46, 18, -15]; Cluster size: 127 voxels* *2) Medial frontal gyrus L;* *Coordinates: Tal [-3, -19, 51] → MNI [-4, -22, 56]; Cluster size: 39 voxels*
Luna et al. (2022)	Decreased GM in medial prefrontal cortex in CHR Decreased TBA in medial/lateral prefrontal cortex and occipital cortex in CHR during cognitive or emotion processing	Decreased GM in CHR vs. HC: 1) Medial frontal gyrus L; MNI [-10, 34, -12]; Cluster size: 11 voxels; * Decreased TBA in CHR vs. HC during cognitive or emotion processing: 1) Precuneus R; MNI [14, -80, 30]; Cluster size: 114 voxels; * 2) Superior frontal gyrus L/R; MNI [0, 32, 26]; Cluster size: 102 voxels; *

		3) Superior frontal gyrus L/R; MNI [0, 32, 46]; Cluster size: 16 voxels; * 4) Inferior frontal gyrus R; MNI [50, 26, 30]; Cluster size: 34 voxels; *
STRUCTURAL-FUNCTIONAL BRAIN ALTERATIONS IN SCHIZOPHRENIA		
Study	**Main Results**	**Specific Results**
Alústiza et al. (2017)	Decreased TBA in anterior cingulate cortex/supplementary motor area, middle frontal gyrus, inferior parietal lobule, thalamus, and cerebellum as well as increased TBA in occipital cortex and precentral gyrus, in SCZ during cognitive processing Decreased TBA in anterior cingulate cortex/supplementary motor area, occipital cortex, and striatum, as well as increased TBA in superior parietal gyrus, inferior frontal gyrus, and temporal pole in SCZ during cognitive processing of timing	Decreased TBA in SCZ vs. HC during cognitive processing: 1) Anterior cingulate/Paracingulate gyri L (BA 32); Coordinates: MNI [-4, 30, 30]; Cluster size: 2004 voxels; #(29/29)/† 2) Inferior parietal gyrus (excluding supramarginal gyrus and angular gyrus) L (BA 40); Coordinates: MNI [-44, -46, 52]; Cluster size: 598 voxels; #(29/29)/† 3) Middle frontal gyrus R; Coordinates: MNI [52, 26, 34]; Cluster size: 443 voxels; #(29/29)/† 4) Thalamus R; Coordinates: MNI [8, -18, 6]; Cluster size: 263 voxels; #(29/29)/† 5) Cerebellum L; Coordinates: MNI [-28, -68, -34]; Cluster size: 280 voxels; #(26/29)/† 6) Middle frontal gyrus L (BA 44); Coordinates: MNI [-44, 14, 40]; Cluster size: 121 voxels; #(27/29)/† 7) Middle frontal gyrus R (BA 8); Coordinates: MNI [26, 18, 52]; Cluster size: 22 voxels; #(26/29)/† Increased TBA in SCZ vs. HC during cognitive processing: 1) Middle occipital gyrus R (BA 19); Coordinates: MNI [30, -80, 28]; Cluster size: 171 voxels; #(28/29) 2) Precentral gyrus L (BA 6); Coordinates: MNI [-30, -8, 54]; Cluster size: 106 voxels; #(27/29) 3) Undefined (BA 6); Coordinates: MNI [26, -8, 50]; Cluster size: 18 voxels; #(25/29) Decreased TBA in SCZ vs. HC during cognitive processing of timing: 1) Anterior thalamic projections R; Coordinates: MNI [12, 10, 6]; Cluster size: 1366 voxels; #(8/8)/† 2) Superior occipital gyrus L (BA 17); Coordinates: MNI [-14, -98, 12]; Cluster size: 636 voxels; #(7/8) 3) Inferior occipital gyrus R (BA 18); Coordinates: MNI [28, -92, -12]; Cluster size: 567 voxels; #(7/8) 4) Supplementary motor area R (BA 6); Coordinates: MNI [4, 16, 52]; Cluster size: 296 voxels; #(6/8)/† 5) Striatum R; Coordinates: MNI [20, 6, 6]; Cluster size: 60 voxels; #(8/8)/†

		Increased TBA in SCZ vs. HC during cognitive processing of timing: 1) Superior parietal gyrus L (BA 7); Coordinates: MNI [-22, -72, 44]; Cluster size: 593 voxels; #(7/8) 2) Inferior frontal gyrus R (BA 38); Coordinates: MNI [36, 26, -18]; Cluster size: 75 voxels; #(7/8) 3) Superior parietal gyrus R (BA 7); Coordinates: MNI [30, -68, 54]; Cluster size: 36 voxels; #(7/8) 4) Temporal pole/Middle temporal gyrus R (BA 38); Coordinates: MNI [48, 14, -28]; Cluster size: 31 voxels; #(7/8)
Arioli et al. (2021)	Decreased TBA in middle temporal gyrus/temporoparietal junction in SCZ during cognitive processing of theory of mind	Decreased TBA in SCZ vs. HC during cognitive processing of theory of mind: 1) Middle temporal gyrus L: Coordinates: MNI [-46, -66, 12]; Cluster size: 1080 mm^3
Arsalidou et al. (2020)	Decreased TBA in fusiform gyrus, increased TBA in inferior frontal gyrus, and altered TBA in precuneus and cerebellum in early-onset SCZ during cognitive processing	Decreased TBA in early-onset SCZ vs. HC during cognitive processing: 1) Fusiform gyrus/Cerebellum L (BA 19); Coordinates: MNI [-38, -68, -12]; Cluster size: 709 voxels; #(77%) 2) Precuneus R (BA 5); Coordinates: MNI [4, -50, 46]; Cluster size: 164 voxels; #(77%) Increased TBA in early-onset SCZ vs. HC during cognitive processing: 1) Precuneus L (BA 23); Coordinates: MNI [-4, -60, 28]; Cluster size: 433 voxels; #(100%) 2) Inferior frontal gyrus L (BA 45); Coordinates: MNI [-52, 38, 12]; Cluster size: 290 voxels; #(57%) 3) Cerebellum R; Coordinates: MNI [10, -80, -22]; Cluster size: 147 voxels; #(86%)
Bora et al. (2011)	Decreased GM in fronto-insular cortex/superior temporal gyrus, anterior cingulate cortex, and thalamus, as well as decreased WM/FA in corpus callosum, anterior thalamic radiation, inferior frontal occipital fasciculus, inferior longitudinal fasciculus, cingulum, and fornix, in SCZ Decreased GM in posterior insula/superior temporal gyrus and anterior cingulate cortex, as well as decreased WM/FA in fornix, inferior longitudinal fasciculus, and inferior frontal occipital fasciculus, in first-episode SCZ	Decreased GM in SCZ vs. HC: 1) Insula/Inferior frontal cortex L; Coordinates: Tal [-42, 8, 6] → MNI [-44, 11, 4]; Cluster size: 1339 voxels; † 2) Insula/Inferior frontal cortex R; Coordinates: Tal [46, 2, 6] → MNI [49, 5, 2]; Cluster size: 1047 voxels; † 3) Thalamus R/L; Coordinates: Tal [-2, -16, 4] → MNI [-3, -15, 1]; Cluster size: 544 voxels; † 4) Dorsal medial frontal cortex/Anterior cingulate cortex R/L; Coordinates: Tal [4, 26, 40] → MNI [4, 25, 44]; Cluster size: 493 voxels; † 5) Rostral medial frontal cortex/Anterior cingulate cortex L; Coordinates: Tal [-4, 46, -2] → MNI [-4, 51, -1]; Cluster size: 467 voxels; † Decreased WM in SCZ vs. HC: 1) Anterior limb of internal capsule R/L (anterior thalamic radiation); Coordinates: Tal [12, 0, 10] → MNI [13, 2, 8]; Cluster size: 409 voxels; † 2) Temporal WM R (inferior frontal occipital fasciculus, inferior longitudinal fasciculus);

	Additional decreased GM in thalamus and fronto-insular cortex, as well as decreased WM in fronto-parietal areas, in chronic SCZ Correlation of negative symptomatology in chronic SCZ with decreased GM in insula and medial prefrontal cortex	Coordinates: Tal [36, -34, 2] → MNI [37, -34, -2]; Cluster size: 93 voxels; † Decreased FA in SCZ vs. HC: 1) Genu of corpus callosum R/L and anterior cingulate/medial frontal area (forceps minor, cingulum, inferior frontal occipital fasciculus R); Coordinates: Tal [18, 24, 10] → MNI [19, 26, 9]; Cluster size: 2501 voxels; † 2) Temporal WM and retrolenticular internal capsule/external capsule L (inferior frontal occipital fasciculus, inferior longitudinal fasciculus, cingulum, fornix); Coordinates: Tal [-32, -26, -2] → MNI [-34, -25, -7]; Cluster size: 349 voxels; † 3) Temporal WM R (inferior frontal occipital fasciculus, inferior longitudinal fasciculus, fornix); Coordinates: Tal [38, -32, -4] → MNI [40, -31, -10]; Cluster size: 154 voxels; † <u>Subgroup meta-analysis:</u> *Studies on first-episode SCZ:* Decreased GM in first-episode SCZ vs. HC: 1) Posterior insula/superior temporal gyrus R; Coordinates: Tal [40, -20, 2] → MNI [42, -19, -2]; Cluster size: 652 voxels 2) Dorsal anterior cingulate R; Coordinates: Tal [14, 18, 30] → MNI [15, 18, 32]; Cluster size: 106 voxels Decreased WM in first-episode SCZ vs. HC: 1) Temporal WM R (inferior frontal occipital fasciculus, inferior longitudinal fasciculus, fornix); Coordinates: Tal [36, -34, 2] → MNI [37, -34, -2]; Cluster size: 1029 voxels 2) Temporal WM L; Coordinates: Tal [-34, -58, 2] → MNI [-36, -59, -3]; Cluster size: 159 voxels Decreased FA in first-episode SCZ vs. HC: 1) Temporal WM and retrolenticular internal capsule/external capsule L (inferior frontal occipital fasciculus, inferior longitudinal fasciculus, cingulum/hippocampus, fornix); Coordinates: Tal [-28, -48, 12] → MNI [-29, -49, 9]; Cluster size: 900 voxels 2) Posterior limb of internal capsule R; Coordinates: Tal [14, -8, 2] → MNI [15, -7, -1]; Cluster size: 45 voxels Decreased GM in chronic SCZ vs. first-episode SCZ: 1) Fronto-insular cortex/superior temporal gyrus L; Coordinates: Tal [-38, 10, 8] → MNI [-40, 13, 6]; Cluster size: 397 voxels 2) Fronto-insular cortex/superior temporal gyrus R; Coordinates: Tal [44, 16, 8] → MNI [46, 18, 5]; Cluster size: 51 voxels 3) Thalamus R; Coordinates: Tal [6, -16, 2] → MNI [7, -15, -2]; Cluster size: 127 voxels Decreased WM in first-episode SCZ vs. chronic SCZ: 1) Genu of Corpus callosum R/L extending to anterior cingulate/medial frontal R/L and anterior limb of internal capsule R; Coordinates: Tal [16, 20, 10] → MNI [17, 22, 9]; Cluster size: 2009 voxels 2) Temporal WM R; Coordinates: Tal [38, -32, 0] → MNI [40, -31, -6]; Cluster size: 45 voxels Decreased WM in chronic SCZ vs. first-episode SCZ:

		1) Anterior limb of internal capsule L; Coordinates: Tal [-8, 2, 4] → MNI [-8, 5, 2]; Cluster size: 417 voxels 2) Fronto-parietal WM R; Coordinates: Tal [22, -16, 28] → MNI [23, -17, 29]; Cluster size: 991 voxels <u>Meta-regression analysis:</u> *Effects of clinical variables on GM reduction:* Negative correlation between male percentage of SCZ and GM in: 1) Insula and Claustrum R; Coordinates: Tal [34, -2, 6] → MNI [36, 0, 3]; Cluster size: 673 voxels 2) Inferior frontal cortex and Insula L; Coordinates: Tal [-40, 4, -8] → MNI [-42, 8, -14]; Cluster size: 50 voxels 3) Thalamus (extending to red nucleus) L; Coordinates: Tal [4, -22, -4] → MNI [4, -21, -10]; Cluster size: 298 voxels 4) Medial frontal cortex L; Coordinates: Tal [-4, 32, -16] → MNI [-4, 37, -17]; Cluster size: 22 voxels Negative correlation between illness duration in chronic SCZ and GM in: 1) Fronto-insular cortex R; Coordinates: Tal [38, -4, 4] → MNI [40, -2, 0]; Cluster size: 88 voxels Negative correlation between negative symptoms in chronic SCZ and GM in: 1) Medial frontal gyrus/Orbitofrontal cortex R/L; Coordinates: Tal [-2, 32, -16] → MNI [-2, 37, -17]; Cluster size: 79 voxels 2) Insula L; Coordinates: Tal [-42, 2, 2] → MNI [-44, 6, -1]; Cluster size: 271 voxels Negative correlation between duration of illness in chronic SCZ and FA in: 1) Medial frontal area R; Coordinates: Tal [14, 50, 6] → MNI [15, 54, 8]; Cluster size: 52 voxels
Brandl et al. (2018)	Decreased GM in superior temporal gyrus, insula, anterior cingulate cortex, ventromedial prefrontal cortex, thalamus, and basal ganglia, as well as increased GM in cerebellum, in SCZ	Decreased GM in SCZ vs. HC: 1) Amygdala L; Coordinates: MNI [-22 -2 -24]; Cluster size: 470 voxels 2) Ventromedial Prefrontal cortex L; Coordinates: MNI [-2, 48, -6]; Cluster size: 1330 voxels 3) Insula and Superior temporal gyrus R; Coordinates: MNI [42, 14, -2]; Cluster size: 2465 voxels 4) Central operculum and Superior temporal gyrus L; Coordinates: MNI [-44, 8, 0]; Cluster size: 4409 voxels 5) Thalamus L; Coordinates: MNI [0, -14, 4]; Cluster size: 740 voxels 6) Dorsal anterior cingulate cortex R/L; Coordinates: MNI [0, 36, 32]; Cluster size: 114 voxels 7) Insula and Superior temporal gyrus L; Coordinates: MNI [-36 -2 -2]; Cluster size: 6415 voxels 8) Pregenual anterior cingulate cortex L;

		Coordinates: MNI [-2, 44, 6]; Cluster size: 3115 voxels 9) Central operculum and Superior temporal gyrus R; Coordinates: MNI [48, -2, 6]; Cluster size: 2580 voxels 10) Caudate L; Coordinates: MNI [-6,10, 2]; Cluster size: 9946 voxels 11) Insula R; Coordinates: MNI [36 -4 4]; Cluster size: 41 voxels 12) Heschl's gyrus R; Coordinates: MNI [46, -20, 4]; Cluster size: 32 voxels 13) Insula L; Coordinates: MNI [-28, 18, 8]; Cluster size: 21 voxels 14) Pallidum L; Coordinates: MNI [-12, -2, 0]; Cluster size: 14083 voxels Increased GM in SCZ vs. HC: 1) Pons R; Coordinates: MNI [14, -42, -34]; Cluster size: 1249 voxels 2) Pons R; Coordinates: MNI [20, -42, -38]; Cluster size: 523 voxels 3) Cerebellum L; Coordinates: MNI [-4, -48, -32]; Cluster size:79 voxels 4) Cerebellum R; Coordinates: MNI [4, -44, -20]; Cluster size: 39 voxels 5) Cerebellum R; Coordinates: MNI [6, -66, -32]; Cluster size: 4530 voxels 6) Cerebellum R; Coordinates: MNI [18, -36, -20]; Cluster size: 32 voxels
Casale et al. (2016)	Decreased TBA in insula, middle frontal gyrus, and inferior parietal lobule in first-episode SCZ during cognitive processing of attention Decreased TBA in insula in first-episode SCZ during cognitive processing of working memory	Decreased TBA in first-episode SCZ vs. HC during cognitive processing of attention: 1) Middle frontal gyrus R (BA 9); Coordinates: MNI [48, 30, 28]; Cluster size: 80 mm^3 2) Inferior parietal lobule R (BA 40); Coordinates: MNI [52, -46, 48]; Cluster size: 56 mm^3 3) Insula R (BA 13); Coordinates: MNI [41, 10, 16]; Cluster size: 16 mm^3 Decreased TBA in first-episode SCZ vs. HC during cognitive processing of working memory: 1) Insula L (BA 13); Coordinates: MNI [-28, 22, -10]; Cluster size: 72 mm^3
Chase et al. (2018)	Decreased TBA in ventral striatum in SCZ during emotion processing of positive stimuli (reward)	Decreased TBA in SCZ vs. HC during emotion processing of positive stimuli (reward): 1) Ventral striatum R; Coordinates: MNI [10, 12, -2]; Cluster size: 181 voxels

Di et al. (2009)	Decreased WM in frontal areas and internal capsule in SCZ	Decreased WM in SCZ vs. HC: 1) Frontal WM R; Coordinates: Tal [20, 46, 26] → MNI [21, 47, 28]; Cluster size: 544 mm^3 2) Internal capsule R; Coordinates: Tal [16, 4, 8] → MNI [17, 7, 6]; Cluster size: 352 mm^3 3) Frontal WM L; Coordinates: Tal [-8, 48, -2] → MNI [-8, 53, -1]; Cluster size: 336 mm^3 4) Internal capsule L; Coordinates: Tal [-16, 2, 2] → MNI [-17, 5, -2]; Cluster size: 248 mm^3
Dong et al. (2017)	Decreased FA in genu of corpus callosum, anterior thalamic radiation, uncinate fasciculus, inferior fronto-occipital fasciculus, superior longitudinal fasciculus, and cingulum in SCZ	Decreased FA in SCZ vs. HC: 1) Frontal WM/Genu of corpus callosum (forceps minor)/Anterior thalamic radiation/Inferior fronto-occipital fasciculus/Uncinate fasciculus L; Coordinates: MNI [-20, 34, 8]; Cluster size: 356 voxels; */† 2) Cingulum R; Coordinates: MNI [10, -38, 20]; Cluster size: 156 voxels; † 3) Anterior thalamic radiation/Caudate nucleus L; Coordinates: MNI [-4, -20, 18]; Cluster size: 92 voxels; */† 4) Corpus callosum L; Coordinates: MNI [-26, -60, 14]; Cluster size: 56 voxels 5) Superior longitudinal fasciculus L; Coordinates: MNI [-34, -52, 30]; Cluster size: 43 voxels; */† 6) Superior longitudinal fasciculus R; Coordinates: MNI [26, -10, 44]; Cluster size: 24 voxels 7) Corpus callosum R; Coordinates: MNI [22, -14, 36]; Cluster size: 21 voxels 8) Anterior thalamic radiation R; Coordinates: MNI [12, 0, 4]; Cluster size: 19 voxels <u>Meta-regression analysis:</u> *Effects of clinical variables on FA reduction:* Negative correlation between age and FA in: 1) Cingulum R; Coordinates: MNI [22, -50, 18] Negative correlation between illness duration and FA in: 1) Cingulum R; Coordinates: MNI [24, -55, 20]

Dong et al. (2018)	Decreased TBA in amygdala-hippocampal complex, fusiform gyrus, inferior frontal gyrus, and thalamus, as well as increased TBA in medial prefrontal cortex, in chronic SCZ during emotion processing of negative stimuli (threatening faces) Correlation of positive symptomatology in chronic SCZ with decreased TBA in amygdala and fusiform gyrus during emotion processing of negative stimuli; Correlation of negative symptomatology in chronic SCZ with decreased TBA in fusiform gyrus with during emotion processing of negative stimuli	Decreased TBA in SCZ vs. HC during emotion processing of negative stimuli (threatening faces): 1) Amygdala/Putamen/Hippocampus/Parahippocampal gyrus L: Coordinates: MNI [-14, -8, -12]; Cluster size: 1615 voxels; #(21/21)/† 2) Fusiform gyrus/Cerebellum L: Coordinates: MNI [-32, -38, -28]; Cluster size: 1811 voxels; #(21/21)/† 3) Amygdala/Putamen/Hippocampus/Parahippocampal gyrus R: Coordinates: MNI [22, -14, -8]; Cluster size: 1408 voxels; #(21/21)/† 4) Inferior frontal gyrus (triangular part) R: Coordinates: MNI [54, 18, 16]; Cluster size: 699 voxels; #(18/21)/† 5) Fusiform gyrus/Cerebellum R: Coordinates: MNI [30, -40, -24]; Cluster size: 514 voxels; #(18/21)/† 6) Thalamus R: Coordinates: MNI [4, -8, -2]; Cluster size: 393 voxels; #(19/21)/† Increased TBA in SCZ vs. HC during emotion processing of negative stimuli (threatening faces): 1) Ventral anterior cingulate cortex and Medial/superior prefrontal gyrus L: Coordinates: MNI [-2, 36, -6]; Cluster size: 2573 voxels; #(20/21)/† <u>Subgroup meta-analysis:</u> *Studies on explicit/implicit emotion processing of threatening faces:* Decreased TBA in SCZ vs. HC during explicit emotion processing of threatening faces: 1) Inferior frontal gyrus R: Coordinates: MNI [56, 16, 14]; Cluster size: 964 voxels 2) Cerebellum R: Coordinates: MNI [32, -74, -22]; Cluster size: 200 voxels 3) Fusiform gyrus L: Coordinates: MNI [-36, -52, -20]; Cluster size: 276 voxels 4) Thalamus L: Coordinates: MNI [-4, -6, 2]; Cluster size: 819 voxels Increased TBA in SCZ vs. HC during explicit emotion processing of threatening faces: 1) Medial/superior prefrontal gyrus L: Coordinates: MNI [-8, 58, 12]; Cluster size: 990 voxels Decreased TBA in SCZ vs. HC during implicit emotion processing of threatening faces: 1) Amygdala/Putamen/Hippocampus/Parahippocampal gyrus/Fusiform gyrus/Cerebellum L: Coordinates: MNI [-30, -6, -8]; Cluster size: 3953 voxels 2) Amygdala/Putamen/Hippocampus/Parahippocampal gyrus/Fusiform gyrus/Cerebellum R: Coordinates: MNI [26, 4, -8]; Cluster size: 2137 voxels <u>Meta-regression analysis:</u> *Effects of clinical variables on TBA during emotion processing of threatening faces:* Negative correlation between positive symptoms and TBA during explicit processing in: 1) Amygdala R; Coordinates: MNI [20, -2, -18]; Cluster size: 125 voxels

		Negative correlation between age and TBA during implicit processing in: 1) Hippocampus L; Coordinates: MNI [-26, -12, -14]; Cluster size: 149 voxels Positive correlation between female percentage and TBA during implicit processing in: 1) Hippocampus R; Coordinates: MNI [18, -12, -18]; Cluster size: 211 voxels Positive correlation between illness duration and TBA during implicit processing in: 1) Hippocampus L; Coordinates: MNI [-26, -14, -12]; Cluster size: 59 voxels Positive correlation between chlorpromazine dosage and TBA during implicit processing in: 1) Amygdala L; Coordinates: MNI [-22, -8, -16]; Cluster size: 194 voxels Negative correlation between negative symptoms and TBA during implicit processing in: 1) Fusiform gyrus L; Coordinates: MNI [-30, -36, -24]; Cluster size: 579 voxels Negative correlation between positive symptoms and TBA during implicit processing in: 1) Fusiform gyrus L; Coordinates: MNI [-32, -40, -22]; Cluster size: 270 voxels
Dugré et al. (2019)	Increased TBA in putamen, hippocampus-amygdala, and insula, as well as decreased TBA in dorsolateral prefrontal cortex, in SCZ during emotion processing of neutral stimuli	Increased TBA in SCZ vs. HC during emotion processing of neutral stimuli: 1) Putamen/Insula/Hippocampus/Amygdala L; Coordinates: MNI [-30, 2, -2]; Cluster size: 1338 voxels 2) Putamen/Insula R; Coordinates: MNI [32, 2, 2]; Cluster size: 924 voxels 3) Postcentral gyrus L; Coordinates: MNI [-46, -12, 34]; Cluster size: 212 voxels Decreased TBA in SCZ vs. HC during emotion processing of neutral stimuli: 1) Middle/inferior frontal gyrus R; Coordinates: MNI [48, 20, 38]; Cluster size: 360 voxels 2) Fusiform gyrus R; Coordinates: MNI [36, -70, -10]; Cluster size: 300 voxels
Ellison-Wright and Bullmore (2009)	Decreased FA in frontal and temporal WM (left-side), involving fornix, cingulum, inferior fronto-occipital fasciculus, inferior longitudinal fasciculus, anterior thalamic radiation, corticospinal tract, and corpus callosum, in SCZ	Decreased FA in SCZ vs. HC: 1) Frontal WM L (genu of corpus callosum, cingulum, anterior thalamic radiation, corticobulbar tract, inferior fronto-occipital fasciculus); Coordinates: Tal [-12, 34, 10] →MNI [-12, 37, 10]; Cluster size: 2368 mm^3 2) Temporal WM L (splenium of corpus callosum, fornix/stria terminalis, inferior longitudinal fasciculus, inferior fronto-occipital fasciculus); Coordinates: Tal [-30, -32, -2] →MNI [-32, -31, -8]; Cluster size: 2264 mm^3

Fornara et al. (2017)	Decreased GM in insula, frontal cortex, temporal cortex, occipital cortex, hippocampal complex, and thalamus in chronic SCZ	Decreased GM in SCZ vs. HC: 1) Inferior frontal gyrus (pars orbitalis) L; Coordinates: MNI [-50, 30, -6]; Cluster size: 128 mm^3 2) Inferior frontal gyrus (pars orbitalis) L; Coordinates: MNI [-36, 38, -14]; Volume: 40 mm^3 3) Inferior frontal gyrus (pars triangularis) L; Coordinates: MNI [-40, 24, 16]; Cluster size: 80 mm^3 4) Inferior frontal gyrus (pars opercularis) L; Coordinates: MNI [-50, 10, 10]; Cluster size: 688 mm^3 5) Middle frontal gyrus L; Coordinates: MNI [-32, 54, 22]; Cluster size: 192 mm^3 6) Superior frontal gyrus L; Coordinates: MNI [-22, 4, 66]; Cluster size: 160 mm^3 7) Superior frontal gyrus L; Coordinates: MNI [-14, 32, 50]; Cluster size: 64 mm^3 8) Superior frontal gyrus L; Coordinates: MNI [-30, 54, 2]; Cluster size: 8 mm^3 9) Precentral gyrus L; Coordinates: MNI [-46, 12, 34]; Cluster size: 1096 mm^3 10) Rectus gyrus L; Coordinates: MNI [-10, 52, -14]; Cluster size: 10 mm^3 11) Middle frontal gyrus (pars orbitalis) L; Coordinates: MNI [-6, 46, -8); Cluster size: 608 mm^3 12) Superior frontal gyrus (pars medialis) L; Coordinates: MNI [-4, 58, 6); Cluster size: 760 mm^3 13) Superior frontal gyrus (pars medialis) L; Coordinates: MNI [-2 , 44, 38]; Cluster size: 48 mm^3 14) Insular cortex L; Coordinates: MNI [-42, 16, -8]; Cluster size: 1768 mm^3 15) Insular cortex L; Coordinates: MNI [-38, 8, 14]; Cluster size: 8 mm^3 16) Rolandic opercular gyrus L; Coordinates: MNI [-44, -22, 12]; Cluster size: 648 mm^3 17) Middle temporal pole L; Coordinates: MNI [-48, 12, -26]; Cluster size: 152 mm^3 18) Inferior temporal gyrus L; Coordinates: MNI [-48, -18, -34]; Cluster size: 480 mm^3 19) Middle temporal gyrus L; Coordinates: MNI [-54, -40, 2]; Cluster size: 16 mm^3 20) Superior temporal gyrus L; Coordinates: MNI [-54, -4, 2]; Cluster size: 832 mm^3 21) Hippocampus L; Coordinates: MNI [-20, -6, -18]; Cluster size: 640 mm^3 22) Fusiform gyrus L; Coordinates: MNI [-36, -12, -38]; Cluster size: 216 mm^3

		23) Fusiform gyrus L; Coordinates: MNI [-30, -2, -32]; Cluster size: 40 mm^3 24) Lingual gyrus L; Coordinates: MNI [-16, -40, -4]; Cluster size: 208 mm^3 25) Calcarine cortex L; Coordinates: MNI [-4, -64, 14]; Cluster size: 96 mm^3 26) Cuneus L; Coordinates: MNI [-4, -72, 20]; Cluster size: 96 mm^3 27) Inferior frontal gyrus (pars triangularis) R; Coordinates: MNI [54, 20, 24]; Cluster size: 88 mm^3 28) Superior frontal gyrus R; Coordinates: MNI [26, 60, 2]; Cluster size: 112 mm^3 29) Precentral gyrus R; Coordinates: MNI [46, 8, 32]; Cluster size: 152 mm^3 30) Rectus gyrus R; Coordinates: MNI [4, 38, -24]; Cluster size: 1200 mm^3 31) Superior frontal gyrus (pars orbitalis) R; Coordinates: MNI [32, 62, -2]; Cluster size: 8 mm^3 32) Supplementary motor area R; Coordinates: MNI [0, 14, 46]; Cluster size: 256 mm^3 33) Insular cortex R; Coordinates: MNI [44, 18, -8]; Cluster size: 840 mm^3 34) Insular cortex R; Coordinates: MNI [36, 20, 4]; Cluster size: 464 mm^3 35) Rolandic opercular gyrus R; Coordinates: MNI [50, -20, 16]; Cluster size: 216 mm^3 36) Middle temporal pole R; Coordinates: MNI [42, 14, -28]; Cluster size: 304 mm^3 37) Superior temporal pole R; Coordinates: MNI [40, 6, -20]; Cluster size: 72 mm^3 38) Superior temporal pole R; Coordinates: MNI [56, 4, 0]; Cluster size: 72 mm^3 39) Inferior temporal gyrus R; Coordinates: MNI [46, -14, -30]; Cluster size: 46 mm^3 40) Middle temporal gyrus R; Coordinates: MNI [64, -28, -2]; Cluster size: 168 mm^3 41) Middle temporal gyrus R; Coordinates: MNI [54, -64, 2]; Cluster size: 160 mm^3 42) Middle temporal gyrus R; Coordinates: MNI [54, -4, -20]; Cluster size: 136 mm^3 43) Superior temporal gyrus R; Coordinates: MNI [62, -20, 12]; Cluster size: 272 mm^3 44) Superior temporal gyrus R; Coordinates: MNI [50, -4, 2]; Cluster size: 224 mm^3 45) Parahippocampal gyrus R;

		Coordinates: MNI [20 -2 -22]; Cluster size: 280 mm^3 46) Fusiform gyrus R; Coordinates: MNI [42, -14, -38]; Cluster size: 608 mm^3 47) Lingual gyrus R; Coordinates: MNI [16, -38, -2]; Cluster size: 112 mm^3 48) Lingual gyrus R; Coordinates: MNI [14, -50, 4]; Cluster size: 592 mm^3 49) Thalamus R; Coordinates: MNI [2, -12, 4]; Cluster size: 960 mm^3
Gao et al. (2018)	Decreased GM in superior temporal gyrus, inferior frontal gyrus, insula, supramarginal gyrus, and fusiform gyrus, as well as increased GM in frontal pole and brainstem, in drug-free (mainly first-episode) SCZ Decreased CP in inferior frontal gyrus, angular gyrus, and insula, as well as increased CP in striatum and occipital cortex, in drug-free (mainly first-episode) SCZ	Decreased GM in SCZ vs. HC: 1) Fusiform gyrus L; Coordinates: MNI [-26, -54, -16]; Cluster size: 771 voxels; #(15/15)/† 2) Inferior frontal gyrus L; Coordinates: MNI [-46, 16, 0]; Cluster size: 649 voxels; #(15/15) 3) Superior temporal gyrus R; Coordinates: MNI [52, -6, -6]; Cluster size: 330 voxels; #(15/15)/† 4) Supramarginal gyrus L; Coordinates: MNI [-56, -40, 36]; Cluster size: 293 voxels; #(15/15) Increased GM in SCZ vs. HC: 1) Lingual gyrus R; Coordinates: MNI [6, -34, -6]; Cluster size: 466 voxels; #(15/15) 2) Superior frontal gyrus (orbital part) R; Coordinates: MNI [6, 60, -22]; Cluster size: 155 voxels; #(15/15) Decreased CP (ALFF/CBF) in SCZ vs. HC: 1) Inferior frontal gyrus (opercular part) R; Coordinates: MNI [46, 10, 30]; Cluster size: 893; #(16/16)/† 2) Angular gyrus R; Coordinates: MNI [40, -60, 52]; Cluster size: 331; #(15/16) 3) Insula R; Coordinates: MNI [38, 14, -14]; Cluster size: 339; #(16/16)/† Increased CP (ALFF/CBF) in SCZ vs. HC: 1) Striatum L; Coordinates: MNI [-28, -2, 4]; Cluster size: 2761; #(16/16) 2) Striatum R; Coordinates: MNI [26, -2, 8]; Cluster size: 212; #(15/16) 3) Inferior occipital gyrus L; Coordinates: MNI [-34, -76, -12]; Cluster size: 168; #(15/16)

Gong et al. (2019)	Decreased ALFF in postcentral gyrus, occipital cortex, precuneus, and inferior parietal lobule, as well as increased ALFF in anterior cingulate cortex, inferior frontal gyrus, inferior temporal gyrus, and putamen, in SCZ Decreased ALFF in medial prefrontal cortex, precuneus, and inferior parietal lobule, as well as increased ALFF in putamen, in first-episode medication-naïve SCZ Decreased ALFF in postcentral gyrus, occipital cortex, and precuneus, as well as increased ALFF in anterior cingulate cortex, insula, inferior frontal gyrus, superior frontal gyrus, inferior temporal gyrus, and amygdala, in chronic SCZ Correlation of positive and negative symptomatology in SCZ with altered ALFF in precuneus; Correlation of general symptomatology in SCZ with decreased ALFF in inferior frontal gyrus, inferior temporal gyrus, and anterior cingulate cortex, as well as increased ALFF in putamen Correlation of positive symptomatology in first-episode SCZ with increased ALFF in medial prefrontal cortex, precuneus, and inferior parietal lobule; Correlation of negative symptomatology in first-episode SCZ with decreased ALFF in putamen Correlation of positive symptomatology in chronic SCZ with increased ALFF in superior frontal gyrus, as well as decreased ALFF in precuneus; Correlation of negative symptomatology in chronic SCZ with decreased ALFF in precuneus; Correlation of general symptomatology	Decreased ALFF in SCZ vs. HC: 1) Postcentral gyrus R (BA 4); Coordinates: MNI [46, -20, 44]; Cluster size: 2615 voxels; #(28/28)/† 2) Precuneus L (BA 5); Coordinates: MNI [-2, -44, 60]; Cluster size: 641 voxels; #(28/28)/† 3) Postcentral gyrus L (BA 4); Coordinates: MNI [-50, -18, 44]; Cluster size: 296 voxels; #(27/28)/† 4) Inferior parietal gyrus L (BA 40); Coordinates: MNI [-48, -54, 42]; Cluster size: 214 voxels; #(27/28)/† 5) Precuneus R (BA 30); Coordinates: MNI [4, -54, 16]; Cluster size: 185 voxels; #(26/28)/† 6) Superior occipital gyrus R (BA 19); Coordinates: MNI [26, -86, 34]; Cluster size: 37 voxels; #(27/28) 7) Calcarine gyrus R (BA 17); Coordinates: MNI [18, -68, 12]; Cluster size: 12 voxels; #(26/28) Increased ALFF in SCZ vs. HC 1) Putamen R; Coordinates: MNI [26, 4, 2]; Cluster size: 4830 voxels; #(28/28)/† 2) Inferior frontal gyrus R (BA 45); Coordinates: MNI [50, 36, -4]; Cluster size: 841 voxels; #(28/28)/† 3) Inferior temporal gyrus L (BA 20); Coordinates: MNI [-50, 0, -36]; Cluster size: 233 voxels; #(28/28) 4) Anterior cingulate cortex R (BA 32); Coordinates: MNI [8, 40, 26]; Cluster size: 145 voxels; #(26/28)/† 5) Inferior frontal gyrus R (BA 48); Coordinates: MNI [48, 20, 14]; Cluster size: 41 voxels; #(26/28)/† <u>Subgroup meta-analysis:</u> *Studies on first-episode SCZ:* Decreased ALFF in first-episode SCZ vs. HC: 1) Medial prefrontal cortex L; Coordinates: MNI [-2, 54, -12]; Cluster size: 1609 voxels; #(13/13)/† 2) Inferior parietal gyrus R (BA 40); Coordinates: MNI [50, -48, 46]; Cluster size: 1294 voxels; #(13/13) 3) Precuneus R; Coordinates: MNI [2, -52, 18]; Cluster size: 628 voxels; #(13/13) 4) Inferior parietal gyrus L (BA 40); Coordinates: MNI [-42, -52, 46]; Cluster size: 21 voxels; #(11/13)/† Increased ALFF in first-episode SCZ vs. HC: 1) Putamen R; Coordinates: MNI [28, 6, 0]; Cluster size: 2223 voxels; #(13/13)/† 2) Putamen L; Coordinates: MNI [-22, 4, 0]; Cluster size: 1837 voxels; #(13/13)/†

	in chronic SCZ with decreased ALFF in inferior frontal gyrus, inferior temporal gyrus, and anterior cingulate cortex	3) Middle occipital gyrus R (BA 19); Coordinates: MNI [36, -82, 8]; Cluster size: 46 voxels; #(12/13)/† 4) Middle occipital gyrus L (BA 19); Coordinates: MNI [-34, -72, -8]; Cluster size: 20 voxels; #(12/13)/† *Studies on first-episode medication-naïve SCZ:* Decreased ALFF in first-episode medication-naïve SCZ vs. HC: 1) Medial prefrontal cortex L (BA 11); Coordinates: MNI [-2, 48, -12]; Cluster size: 1551 voxels 2) Inferior parietal gyrus/Angular gyrus R (BA 39); Coordinates: MNI [48, -60, 26]; Cluster size: 853 voxels 3) Precuneus R; Coordinates: MNI [4, -54, 16]; Cluster size: 281 voxels Increased ALFF in first-episode medication-naïve SCZ vs. HC: 1) Putamen R; Coordinates: MNI [26, 6, -4]; Cluster size: 2749 voxels 2) Putamen L; Coordinates: MNI [-22, 8, 2]; Cluster size: 1870 voxels *Studies on chronic SCZ:* Decreased ALFF in chronic SCZ vs. HC: 1) Postcentral gyrus R (BA 4); Coordinates: MNI [46, -20, 44]; Cluster size: 2517 voxels; #(15/15)/† 2) Postcentral gyrus L (BA 4); Coordinates: MNI [-50, -22, 44]; Cluster size: 747 voxels; #(15/15)/† 3) Precuneus L (BA 5); Coordinates: MNI [-4, -48, 60]; Cluster size: 766 voxels; #(15/15)/† 4) Cuneus R (BA 19); Coordinates: MNI [18, -80, 40]; Cluster size: 175 voxels; #(15/15)/† 5) Calcarine gyrus R (BA 18); Coordinates: MNI [22, -70, 12]; Cluster size: 40 voxels; #(14/15) Increased ALFF in chronic SCZ vs. HC: 1) Amygdala L; Coordinates: MNI [-28, -6, -16]; Cluster size: 1558 voxels; #(15/15)/† 2) Inferior frontal gyrus R (BA 47); Coordinates: MNI [50, 36, -10]; Cluster size: 1255 voxels; #(15/15)/† 3) Inferior temporal gyrus L (BA 20); Coordinates: MNI [-50, -28, -24]; Cluster size: 742 voxels; #(15/15)/† 4) Anterior cingulate cortex R (BA 32); Coordinates: MNI [8, 44, 28]; Cluster size: 384 voxels; #(14/15)/† 5) Inferior frontal gyrus L (BA 47); Coordinates: MNI [-42, 38, -2]; Cluster size: 97 voxels; #(14/15) 6) Insula L (BA 48); Coordinates: MNI [-40, 10, -10]; Cluster size: 20 voxels; #(12/15) 7) Superior frontal gyrus R (BA 11);

		Coordinates: MNI [26, 68, 0]; Cluster size: 16 voxels; #(14/15) 8) Superior frontal gyrus L; Coordinates: MNI [-16, 70, 12]; Cluster size: 10 voxels; #(11/15)/† <u>Meta-regression analysis:</u> *Effects of clinical variables on ALFF in SCZ:* Positive correlation between PANSS total score and ALFF in: 1) Putamen R; Coordinates: MNI [32, -2, 4]; Cluster size: 235 voxels 2) Superior occipital gyrus R (BA 19); Coordinates: MNI [18, -86, 36]; Cluster size: 55 voxels Negative correlation between PANSS total score and ALFF in: 1) Inferior frontal gyrus R (BA 45); Coordinates: MNI [48, 40, -4]; Cluster size: 471 voxels 2) Anterior cingulate cortex R (BA 32); Coordinates: MNI [8, 42, 26]; Cluster size: 90 voxels 3) Inferior frontal gyrus R (BA 48); Coordinates: MNI [52, 16, 20]; Cluster size: 31 voxels 4) Inferior temporal gyrus L (BA 20); Coordinates: MNI [-50, -24, -24]; Cluster size: 29 voxels Positive correlation between PANSS positive score and ALFF in: 1) Precuneus R (BA 29); Coordinates: MNI [4, -42, 6]; Cluster size: 86 voxels Negative correlation between PANSS positive score and ALFF in: 1) Precuneus L (BA 7); Coordinates: MNI [-10, -64, 68]; Cluster size: 18 voxels Positive correlation between PANSS negative score and ALFF in: 1) Precuneus R (BA 29); Coordinates: MNI [4, -42, 6]; Cluster size: 59 voxels Negative correlation between PANSS negative score and ALFF in: 1) Precuneus L (BA 7); Coordinates: MNI [-10, -64, 68]; Cluster size: 18 voxels Positive correlation between PANSS general score and ALFF in: 1) Putamen R; Coordinates: MNI [32, 0, 4]; Cluster size: 364 voxels Negative correlation between PANSS general score and ALFF in: 1) Inferior frontal gyrus R (BA 45); Coordinates: MNI [48, 40, -4]; Cluster size: 380 voxels 2) Inferior frontal gyrus R (BA 48); Coordinates: MNI [52, 16, 20]; Cluster size: 73 voxels 3) Anterior cingulate cortex R (BA 32); Coordinates: MNI [8, 42, 26]; Cluster size: 46 voxels 4) Inferior temporal gyrus L (BA 20); Coordinates: MNI [-50, -24, -24]; Cluster size: 38 voxels

		Effects of clinical variables on ALFF in first-episode SCZ: Positive correlation between PANSS positive score and ALFF in: 1) Inferior parietal gyrus R (BA 40); Coordinates: MNI [44, -54, 50]; Cluster size: 218 voxels 2) Precuneus R; Coordinates: MNI [6, -54, 14]; Cluster size: 116 voxels 3) Medial prefrontal cortex L; Coordinates: MNI [-24, 10, 58]; Cluster size: 29 voxels Negative correlation between PANSS negative score and ALFF in: 1) Putamen R; Coordinates: MNI [22, 14, -10]; Cluster size: 13 voxels *Effects of clinical variables on ALFF in chronic SCZ:* Negative correlation between PANSS total score and ALFF in: 1) Inferior frontal gyrus R (BA 45); Coordinates: MNI [46, 38, -2]; Cluster size: 289 voxels 2) Anterior cingulate cortex R (BA 32); Coordinates: MNI [8, 42, 26]; Cluster size: 119 voxels 3) Inferior temporal gyrus L (BA 20); Coordinates: MNI [-50, -24, -24]; Cluster size: 54 voxels Positive correlation between PANSS positive score and ALFF in: 1) Superior frontal gyrus L (BA 10); Coordinates: MNI [-18, 64, 4]; Cluster size: 29 voxels Negative correlation between PANSS positive score and ALFF in: 1) Precuneus L (BA 7); Coordinates: MNI [-10, -64, 68]; Cluster size: 19 voxels Negative correlation between PANSS negative score and ALFF in: 1) Precuneus L (BA 7); Coordinates: MNI [-10, -64, 68]; Cluster size: 18 voxels Negative correlation between PANSS general score and ALFF in: 1) Anterior cingulate cortex R (BA 32); Coordinates: MNI [8, 42, 26]; Cluster size: 181 voxels 2) Inferior temporal gyrus L (BA 20); Coordinates: MNI [-50, -26, -24]; Cluster size: 172 voxels 3) Inferior frontal gyrus R (BA 47); Coordinates: MNI [44, 36, -6]; Cluster size: 73 voxels
Goodkind et al. (2015)	Decreased GM in insula, parietal operculum, dorsal anterior cingulate cortex, medial prefrontal cortex, and thalamus, as well as increased GM in striatum, in SCZ	Decreased GM in SCZ vs. HC: 1) Thalamus R; Coordinates: MNI [2, -14, 4]; Cluster size: 486 voxels 2) Insula R; Coordinates: MNI [44, 12, 1]; Cluster size: 1053 voxels 3) Insula L; Coordinates: MNI [-42, 22, -14]; Cluster size: 1629 voxels

		4) Subgenual anterior cingulate cortex L; Coordinates: MNI [-4, 10, -10]; Cluster size: 282 voxels 5) Ventromedial prefrontal cortex R; Coordinates: MNI [4, 40, -24]; Cluster size: 506 voxels 6) Parietal operculum R; Coordinates: MNI [52, -22, 16]; Cluster size: 256 voxels 7) Dorsal anterior cingulate cortex R; Coordinates: MNI [6, 38, 24]; Cortex size: 430 voxels 8) Anterior medial prefrontal cortex L; Coordinates: MNI [-6, 48, -8]; Cluster size: 476 voxels Increased GM in SCZ vs. HC: 1) Striatum R; Coordinates: MNI [12, 4, -4]; Cluster size: 176 voxels 2) Striatum L; Coordinates: MNI [-20, 10, 2]; Cluster size: 223 voxels
Huang et al. (2021)	Decreased GM in insula, superior temporal gyrus, claustrum, anterior cingulate cortex, and thalamus in SCZ	Decreased GM in SCZ vs. HC: 1) Claustrum L; Coordinates: MNI [-36, 16, -2]; Cluster size: 41240 voxels; #(70%) 2) Transverse temporal gyrus R (BA 41); Coordinates: MNI [52, -18, 12]; Cluster size: 27240 voxels; #(54%) 3) Anterior cingulate cortex L (BA 32); Coordinates: MNI [-6, 48, -8]; Cluster size: 25600 voxels; #(51%) 4) Thalamus R; Coordinates: MNI [4, -16, 2]; Cluster size: 14496 voxels; #(40%) 5) Posterior cingulate cortex L (BA 30); Coordinates: MNI [-6, -60, 18]; Cluster size: 4360 voxels; #(16%) 6) Parahippocampal gyrus R (BA 34); Coordinates: MNI [18, -4, -22]; Cluster size: 2920 voxels; #(14%) 7) Superior frontal gyrus L (BA 10); Coordinates: MNI [-28, 58, 8]; Cluster size: 1984 voxels; #(12%) 8) Superior frontal gyrus R (BA 10); Coordinates: MNI [30, 60, -2]; Cluster size: 1600 voxels; #(11%) 9) Middle occipital gyrus L (BA 19); Coordinates: MNI [-56, -62, -2]; Cluster size: 1448 voxels; #(12%) 10) Middle frontal gyrus L (BA 11); Coordinates: MNI [-30, 32, 26]; Cluster size: 1160 voxels; #(11%) 11) Uncus L (BA 20); Coordinates: MNI [-36, -14, -38]; Cluster size: 1032 voxels; #(9%) 12) Middle frontal gyrus R (BA 6); Coordinates: MNI [48, 8, 38]; Cluster size: 864 voxels; #(8%) 13) Uncus R (BA 20); Coordinates: MNI [40, -14, -38]; Cluster size: 760 voxels; #(8%) 14) Parahippocampal gyrus R;

		Coordinates: MNI [30, -20, -14]; Cluster size: 664 voxels; #(7%) 15) Cingulate cortex L (BA 24); Coordinates: MNI [-10, -14, 42]; Cluster size: 648 voxels; #(7%) 16) Middle temporal gyrus L (BA 21); Coordinates: MNI [-56, -2, -30]; Cluster size: 624 voxels; #(7%) 17) Inferior temporal gyrus R (BA 19); Coordinates: MNI [52, -64, -4]; Cluster size: 552 voxels; #(5%)
Jáni et al. (2018)	Decreased TBA in inferior frontal gyrus/insula and anterior cingulate cortex, as well as increased TBA in posterior parietal cortex, occipital cortex, and middle frontal gyrus, in SCZ during emotion processing (emotion recognition) Decreased TBA in insula, superior frontal gyrus/anterior cingulate cortex, and occipital cortex, as well as increased TBA in inferior/superior frontal gyrus and posterior parietal cortex, in SCZ during cognitive processing of theory of mind Decreased TBA in insula/superior temporal gyrus and anterior cingulate cortex, as well as increased TBA in inferior parietal lobule, in SCZ during emotion processing (emption recognition) and cognitive processing of theory of mind Correlation of positive symptomatology in SCZ with increased TBA in inferior frontal gyrus during cognitive processing of theory of mind; Correlation of negative symptomatology in SCZ with decreased TBA in supramarginal gyrus during cognitive processing of theory of mind	Decreased TBA in SCZ vs. HC during emotion processing (emotion recognition): 1) Inferior frontal gyrus R (BA 25, 34, 45, 47); Coordinates: MNI [48, 34, -6]; Cluster size: 5611 voxels; #(12/12)/† 2) Cingulate cortex/Paracingulate gyrus R (BA 24, 32); Coordinates: MNI [2, 26, 30]; Cluster size: 560 voxels; #(10/12)/*/† Increased TBA in SCZ vs. HC during emotion processing (emotion recognition): 1) Postcentral gyrus L (BA 2, 4); Coordinates: MNI [-46, -32, 48]; Cluster size: 1243 voxels; #(12/12)/† 2) Middle frontal gyrus R (BA 3, 6); Coordinates: MNI [44, -4, 56]; Cluster size: 65 voxels; #(10/12)/*/† 3) Cingulum L; Coordinates: MNI [-10, -58, 40]; Cluster size: 11 voxels; #(8/12)/*/† 4) Middle occipital gyrus L (BA 18, 19); Coordinates: MNI [-28, -88, 22]; Cluster size: 12 voxels; #(9/12)/*/† Decreased TBA in SCZ vs. HC during cognitive processing of theory of mind: 1) Insula R (BA 48); Coordinates: MNI [50, -2, 0]; Cluster size: 1340 voxels; #(16/16)/† 2) Superior frontal gyrus R (BA 9, 32); Coordinates: MNI [8, 52, 28]; Cluster size: 580 voxels; #(14/16)/*/† 3) Cuneus L (BA 7, 18); Coordinates: MNI [0, -84, 22]; Cluster size: 569 voxels; #(16/16)/*/† 4) Posterior cingulate cortex/Lingual gyrus R; Coordinates: MNI [12, -60, 4]; Cluster size: 71 voxels; #(14/16)/*/† 5) Precentral gyrus R (BA 4); Coordinates: MNI [46, -12, 34]; Cluster size: 14 voxels; #(13/16)/*/† Increased TBA in SCZ vs. HC during cognitive processing of theory of mind: 1) Superior frontal gyrus R (BA 8); Coordinates: MNI [18, 24, 46]; Cluster size: 375 voxels; #(15/16)/† 2) Inferior parietal lobule R (BA 40, 48); Coordinates: MNI [64, -40, 38]; Cluster size: 258 voxels; #(15/16)/*/† 3) Inferior frontal gyrus L (BA 44); Coordinates: MNI [-44, 16, 34]; Cluster size: 203 voxels; #(15/16)/*/† 4) Precuneus R (BA 7); Coordinates: MNI [16, -60, 38]; Cluster size: 183 voxels; #(15/16)/†

		5) Supramarginal gyrus R (BA 40); Coordinates: MNI [-44, -46, 36]; Cluster size: 143 voxels; #(15/16)/*/† <u>Subgroup meta-analysis:</u> *Studies on TBA during emotion processing (emotion recognition) and cognitive processing of theory of mind:* Decreased TBA in SCZ vs. HC: 1) Insula/Superior temporal gyrus R (BA 38, 47, 48); Coordinates: MNI [50, 16, -6]; Cluster size: 1036 voxels 2) Anterior cingulate cortex/Paracingulate gyrus R (BA 24, 32); Coordinates: MNI [4, 40, 26]; Cluster size: 823 voxels Increased TBA in SCZ vs. HC: 1) Inferior parietal lobule R (BA 40); Coordinates: MNI [56, -42, 40]; Cluster size: 505 voxels 2) Inferior parietal lobule L (BA 40); Coordinates: MNI [-44, -42, 42]; Cluster size: 136 voxels <u>Meta-regression analysis:</u> *Effect of clinical variables on TBA during emotion processing (emotion recognition):* Positive correlation behavioral performance in SCZ and TBA in: 1) Precentral gyrus R (BA 6); Coordinates: MNI [54, 2, 38]; Cluster size: 395 voxels *Effect of clinical variables on TBA during cognitive processing of theory of mind:* Positive correlation between behavioral performance in SCZ and TBA in: 1) Inferior frontal gyrus (opercular part) and Insula R (BA 48); Coordinates: MNI [51, 16, 4]; Cluster size: 424 voxels Negative correlation between illness duration in SCZ and TBA in: 1) Cuneus L (BA 18); Coordinates: MNI [2, -80, 22]; Cluster size: 72 voxels Positive correlation between positive symptoms in SCZ and TBA in: 1) Inferior frontal gyrus (triangular part) L (BA 45); Coordinates: MNI [-52, 26, 10]; Cluster size: 297 voxels Negative correlation between negative symptoms in SCZ and TBA in: 2) Supramarginal gyrus R (BA 40); Coordinates: MNI [60, -36, 38]; Cluster size: 314 voxels
Kompus et al. (2011)§	Decreased TBA in superior temporal gyrus, anterior cingulate cortex, superior frontal gyrus, hippocampus, and thalamus in SCZ during auditory perception	Decreased TBA in SCZ vs. HC during auditory perception: 1) Superior temporal gyrus L (BA 22, 41); Coordinates: Tal [-54, -8, 0] → MNI [-57, -6, -4]; Cluster size: 1824 mm^3 2) Anterior cingulate cortex L (BA 24); Coordinates: Tal [-10, 0, 40] → MNI [-11, -2, 43]; Cluster size: 520 mm^3 3) Thalamus R;

	Activation in superior temporal gyrus, insula, postcentral gyrus, middle temporal gyrus, inferior parietal lobule, inferior frontal gyrus, superior frontal gyrus, hippocampus, and cerebellum in SCZ during auditory verbal hallucinations *Decreased TBA during auditory perception and activation during auditory verbal hallucinations in superior temporal gyrus/primary auditory cortex (left-side) in SCZ*	Coordinates: Tal [12, -22, 18] → MNI [12, -22, 16]; Cluster size: 520 mm^3 4) Superior frontal gyrus R (BA 10); Coordinates: Tal [24, 50, 14] → MNI [25, 52, 15]; Cluster size: 456 mm^3 5) Retrosplenial cortex/Hippocampus L; Coordinates: Tal [-12, -38, 10] → MNI [-13, -39, 7]; Cluster size: 200 mm^3 *Activation in SCZ during auditory (verbal) hallucinatory experience:* *1) Insula L (BA 13);* *Coordinates: Tal [-44, -2, 6] → MNI [-46, 0, 3]; Cluster size: 2656* mm^3 *2) Hippocampus L;* *Coordinates: Tal [-24, -32, -4] → MNI [-26, -31, -10]; Cluster size: 1064* mm^3 *3) Postcentral gyrus L (BA 2);* *Coordinates: Tal [-50, -24, 40] → MNI [-51, -26, 43]; Cluster size: 1016* mm^3 *4) Inferior parietal lobule R (BA 40);* *Coordinates: Tal [32, -40, 48] → MNI [31, -44, 53]; Cluster size: 960* mm^3 *5) Superior temporal gyrus L (BA 42);* *Coordinates: Tal [-52, -22, 16] → MNI [-55, -22, 15]; Cluster size: 952* mm^3 *6) Inferior frontal gyrus R (BA 44);* *Coordinates: Tal [40, 12, 16] → MNI [42, 14, 13]; Cluster size: 408* mm^3 *7) Middle temporal gyrus R (BA 21);* *Coordinates: Tal [54, -32, -4] → MNI [57, -31, -11]; Cluster size: 368* mm^3 *8) Cerebellum R;* *Coordinates: Tal [20, -46, -16] → MNI [21, -45, -24]; Cluster size: 248* mm^3 *9) Superior frontal gyrus R (BA 10);* *Coordinates: Tal [26, 42, 26] → MNI [27, 42, 28]; Cluster size: 240* mm^3 *10) Middle temporal gyrus R (BA 22);* *Coordinates: Tal [58, -44, 14] → MNI [59, -45, 11]; Cluster size: 200* mm^3 *Subgroup meta-analysis:* *Studies on combination between auditory perception and auditory hallucinations in SCZ:* *Decreased TBA during auditory perception and activation during auditory (verbal) hallucinatory experience in SCZ:* *1) Superior temporal gyrus L;* *Coordinates: Tal [-52, -22, 13] → MNI [-55, -22, 11]; Cluster size: 184* mm^3
Kronbichler et al. (2017)	Decreased TBA in medial prefrontal cortex, temporoparietal junction, premotor cortex, and occipital cortex, as well as increased TBA in posterior parietal cortex, in SCZ during cognitive processing of theory of mind	Decreased TBA during cognitive processing of theory of mind: 2) Medial prefrontal cortex L; Coordinates: MNI [-2, 52, 18]; Cluster size: 1573 voxels; #(20/21)/† 3) Premotor cortex R; Coordinates: MNI [54, -14, 18]; Cluster size: 1101 voxels; #(21/21)/† 4) Medial occipitoparietal cortex L; Coordinates: MNI [-4, -76, 14]; Cluster size: 128 voxels; #(19/21)/† 5) Lingual gyrus R; Coordinates: MNI [12, -58, 2]; Cluster size: 99 voxels; #(19/21)/†

		6) Orbitofrontal cortex L; Coordinates: MNI [-30, 22, -24]; Cluster size: 30 voxels; #(14/21)/† 7) Lateral occipitotemporal cortex L; Coordinates: MNI [-48, -72, 22]; Cluster size: 27 voxels; #(18/21)/† 8) Cingulate gyrus L; Coordinates: MNI [-18, -44, -2]; Cluster size: 24 voxels; #(18/21)/† Increased TBA during cognitive processing of theory of mind: 1) Inferior parietal cortex L; Coordinates: MNI [-42, -48, 38]; Cluster size: 486 voxels; #(21/21)/† 2) Inferior parietal cortex R; Coordinates: MNI [58, -40, 40]; Cluster size: 405 voxels; #(19/21)/†
Kuhn and Gallinat (2013)	Decreased CP in medial prefrontal cortex, precuneus/posterior cingulate cortex and hippocampus, as well as increased CP in occipital cortex, in SCZ	Decreased CP (ALFF/ReHo/FC/CM/CBF) in SCZ vs. HC: 1) Precuneus R (BA 7); Coordinates: MNI [3, -44, 69]; Cluster size: 528 mm^3 2) Precuneus L (BA 7); Coordinates: MNI [-6, -70, 35]; Cluster size: 488 mm^3 3) Posterior cingulate cortex L (BA 23); Coordinates: MNI [-1, -29, 26]; Cluster size: 384 mm^3 4) Ventromedial prefrontal cortex L (BA 32, 10, 11); Coordinates: MNI [-10, 48, -20]; Cluster size: 312 mm^3 5) Ventromedial prefrontal cortex L (BA 24, 32); Coordinates: MNI [-4, 40, -9]; Cluster size: 272 mm^3 6) Hippocampus L; Coordinates: MNI [-21, -10, -24]; Cluster size: 264 mm^3 7) Precuneus R (BA 23); Coordinates: MNI [10, -48, 28]; Cluster size: 248 mm^3 Increased CP (ALFF/ReHo/FC/CM/CBF) in SCZ vs. HC: 1) Lingual gyrus L (BA 19); Coordinates: MNI [-11, -57, 2]; Cluster size: 1296 mm^3 2) Lingual gyrus R (BA 19); Coordinates: MNI [11, -55, 2]; Cluster size: 1200 mm^3
Li et al. (2010)	Decreased TBA in parahippocampal gyrus/amygdala, occipital cortex/fusiform gyrus, and superior frontal gyrus in SCZ during emotion processing (faces)	Decreased TBA in SCZ vs. HC during emotion processing (faces): 1) Parahippocampal gyrus/Amygdala R; Coordinates: Tal [26, -8, -12] → MNI [27, -6, -19]; Cluster size: 368 mm^3 2) Superior frontal gyrus R (BA 6); Coordinates: Tal [9, 22, 51] → MNI [9, 19, 56]; Cluster size: 288 mm^3 3) Parahippocampal gyrus/Amygdala L; Coordinates: Tal [-26, -10, -13] → MNI [-27, -8, -20]; Cluster size: 272 mm^3 4) Middle occipital gyrus L (BA 19); Coordinates: Tal [48, -72, 4] → MNI [47, -73, -1]; Cluster size: 208 mm^3 5) Fusiform gyrus L (BA 19);

		Coordinates: Tal [-38, -66, -13] → MNI [-39, -65, -21]; Cluster size: 1768 mm^3 6) Parahippocampal gyrus/Amygdala L; Coordinates: Tal [-22, -5, -9] → MNI [-23, -3, -15]; Cluster size: 464 mm^3 7) Lentiform nucleus R; Coordinates: Tal [23, -4, -7] → MNI [24, -2, -13]; Cluster size: 424 mm^3 8) Fusiform gyrus R (BA 19); Coordinates: Tal [38, -64, -10] → MNI [38, -64, -18]; Cluster size: 408 mm^3 9) Fusiform gyrus R (BA 37); Coordinates: Tal [40, -50, -15] → MNI [41, -49, -23]; Cluster size: 408 mm^3 <u>Subgroup meta-analysis:</u> *Studies on explicit/implicit emotion processing of faces:* Decreased TBA in SCZ vs. HC during explicit emotion processing of faces: 1) Fusiform gyrus L (BA 19/37); Coordinates: Tal [-39, -65, -13] → MNI [-41, -64, -21]; Cluster size: 1840 mm^3 2) Fusiform gyrus R (BA 37); Coordinates: Tal [40, -52, -14] → MNI [41, -51, -22]; Cluster size: 472 mm^3 3) Fusiform gyrus R (BA 19); Coordinates: Tal [38, -64, -10] → MNI [38, -64, -18]; Cluster size: 432 mm^3 4) Amygdala L; Coordinates: Tal [-21, -7, -8] → MNI [-22, -5, -14]; Cluster size: 368 mm^3 5) Lentiform nucleus R; Coordinates: Tal [22, -3, -5] → MNI [23, -1, -11]; Cluster size: 256 mm^3 Decreased TBA in SCZ vs. HC during explicit emotion processing of faces: 1) Superior frontal gyrus R (BA 6); Coordinates: Tal [10, 22, 50] → MNI [10, 19, 55]; Cluster size: 312 mm^3 2) Parahippocampal gyrus/Amygdala L; Coordinates: Tal [-26, -10, -14] → MNI [-27, -8, -21]; Cluster size: 280 mm^3 3) Parahippocampal gyrus/Amygdala R; Coordinates: Tal [24, -8, -12] → MNI [25, -6, -19]; Cluster size: 280 mm^3 4) Middle occipital gyrus L (BA 19); Coordinates: Tal [48, -72, 4] → MNI [47, -73, -1]; Cluster size: 216 mm^3
Liloia et al. (2021)§	*Decreased GM in medial prefrontal cortex in CHR* Decreased GM in insula, superior temporal gyrus/primary auditory cortex pre/postcentral gyrus, and anterior cingulate cortex/medial prefrontal cortex (left-side) in early-stage SCZ Decreased GM in insula/superior temporal gyrus, inferior frontal gyrus,	*Decreased GM in CHR vs. HC:* *2) Anterior cingulate cortex R (BA 32);* *Coordinates: Tal [4, 36, -6] → MNI [5, 41, -7]; Cluster size: 800* mm^3 Decreased GM in early stage SCZ vs. HC: 1) Precentral gyrus L (BA 6); Coordinates: Tal [-48, -10, 24] → MNI [-50, -10, 24]; Cluster size: 1776 mm^3 2) Transverse temporal gyrus R (BA 41); Coordinates: Tal [48, -24, 16] → MNI [50, -24, 14]; Cluster size: 1624 mm^3 3) Middle temporal gyrus R (BA 22); Coordinates: Tal [50, -8, -8] → MNI [53, -5, -15]; Cluster size: 1296 mm^3

	anterior cingulate cortex/medial prefrontal cortex, thalamus (associative nuclei), caudate, and amygdala (bilateral) in chronic SCZ Progression of GM loss from medial prefrontal cortex (CHR) to left insula/superior temporal gyrus and pre/postcentral gyrus (early-stage SCZ) to bilateral anterior insula/inferior frontal gyrus, basal ganglia, and thalamus (chronic SCZ)	4) Insula L (BA 13); Coordinates: Tal [-32, 22, 4] → MNI [-33, 25, 2]; Cluster size: 1096 mm^3 5) Transverse temporal gyrus L (BA 41); Coordinates: Tal [-46, -18, 10] → MNI [-49, -17, 8]; Cluster size: 1032 mm^3 6) Anterior cingulate cortex L (BA 32); Coordinates: Tal [-2, 34, -4] → MNI [-2, 38, -5]; Cluster size: 784 mm^3 7) Amygdala L; Coordinates: Tal [-20, -4, -18] → MNI [-20, -1, -25]; Cluster size: 752 mm^3 Decreased GM in chronic SCZ vs. HC: 8) Insula L (BA 13); Coordinates: Tal [-34, 18, 6] → MNI [-35, 21, 4]; Cluster size: 4928 mm^3 9) Insula R (BA 13); Coordinates: Tal [40, 14, 2] → MNI [42, 17, -2]; Cluster size: 3056 mm^3 10) Thalamus (medial dorsal nucleus) L; Coordinates: Tal [-2, -16, 6] → MNI [-3, -15, 3]; Cluster size: 2312 mm^3 11) Medial frontal gyrus R (BA 11); Coordinates: Tal [4, 36, -14] → MNI [5, 41, -15]; Cluster size: 1656 mm^3 12) Caudate (nucleus head) L; Coordinates: Tal [-4, 6, -4] → MNI [-4, 9, -8]; Cluster size: 1224 mm^3 13) Amygdala L; Coordinates: Tal [-20 -6 -12] → MNI [-20, -4, -18]; Cluster size: 1056 mm^3 14) Amygdala R; Coordinates: Tal [16, -4, -16] → MNI [17, -1, -23]; Cluster size: 680 mm^3 Subgroup meta-analysis: *Studies comparing CHR, early-stage and chronic SCZ:* Decreased GM in CHR and early-stage SCZ vs. HC: 2) Anterior cingulate cortex R (BA 32); Coordinates: Tal [2, 36, -6] → MNI [3, 41, -7]; Cluster size: 144 mm^3 Decreased GM in early-stage SCZ vs. CHR: 5) Superior temporal gyrus L (BA 22); Coordinates: Tal [-50, -13, 8] → MNI [-53, -12, 6]; Cluster size: 1032 mm^3 6) Postcentral gyrus L (BA 43); Coordinates: Tal [-50, -10, 16] → MNI [-53, -9, 15]; Cluster size: 768 mm^3 7) Insula L (BA 13); Coordinates: Tal [-32, 12, 8] → MNI [-33, 15, 6]; Cluster size: 576 mm^3 8) Insula L (BA 13); Coordinates: Tal [-46, 4, 14] → MNI [-48, 6, 13]; Cluster size: 224 mm^3 Decreased GM in early-stage and chronic SCZ vs. HC: 6) Insula L (BA 13); Coordinates: Tal [-32, 20, 4] → MNI [-33, 23, 2]; Cluster size: 680 mm^3 7) Amygdala L; Coordinates: Tal [-20, -4, -16] → MNI [-20, -1, -23]; Cluster size: 304 mm^3

		8) Anterior cingulate cortex L (BA 32); Coordinates: Tal [0, 34, -4] → MNI [0, 38, -5]; Cluster size: 120 mm^3 9) Precentral gyrus L (BA 6); Coordinates: Tal [-52, -6, 6] → MNI [-55, -4, 3]; Cluster size: 56 mm^3 10) Inferior frontal gyrus L (BA 47); Coordinates: Tal [-48, 6, 14] → MNI [-51, 8, 13]; Cluster size: 24 mm^3 Decreased GM in early-stage SCZ vs. chronic SCZ: 4) Precentral gyrus L (BA 6); Coordinates: Tal [-49, -5, 24] → MNI [-51, -5, 24]; Cluster size: 520 mm^3 5) Postcentral gyrus L (BA 43); Coordinates: Tal [-47, -17, 14] → MNI [-50, -17, 13]; Cluster size: 136 mm^3 6) Middle temporal gyrus R (BA 21); Coordinates: Tal [44, -8, -12] → MNI [47, -5, -19]; Cluster size: 16 mm^3 Decreased GM in chronic SCZ vs. early-stage SCZ: 6) Parahippocampal gyrus R (BA 34); Coordinates: Tal [12, -3, -16] → MNI [-13, 0, -23]; Cluster size: 672 mm^3 7) Thalamus (medial dorsal nucleus/Pulvinar) L; Coordinates: Tal [-7, -20, 11] → MNI [-8, -20, 9]; Cluster size: 480 mm^3 8) Inferior frontal gyrus L (BA 44); Coordinates: Tal [-46, 12, 8] → MNI [-48, 15, 6]; Cluster size: 256 mm^3 9) Insula R (BA 13); Coordinates: Tal [36, 20, 2] → MNI [38, 33, -1]; Cluster size: 40 mm^3 10) Superior temporal gyrus L (BA 22); Coordinates: Tal [-51, 8, 4] → MNI [-54, 11, 1]; Cluster size: 16 mm^3 <u>Meta-regression analysis:</u> *Effects of clinical variables on GM reduction in SCZ:* Negative correlation between male percentage in SCZ and GM in: 5) Thalamus L/R; Coordinates: Tal [-1, -9, 7] → MNI [-2, -8, 5]; Cluster size: 94 voxels 6) Superior temporal gyrus L; Coordinates: Tal [-51, -30, 13] → MNI [-54, -30, 11]; Cluster size: 52 voxels 7) Insula R; Coordinates: Tal [32, 14, 8] → MNI [34, 17, 5]; Cluster size: 50 voxels 8) Inferior temporal gyrus L; Coordinates: Tal [-30, -9, -35] → MNI [-31, -6, -44]; Cluster size: 46 voxels Negative correlation between percentage of medicated SCZ and GM in: 3) Superior temporal gyrus R; Coordinates: Tal [43, 14, -8] → MNI [46, 18, -15]; Cluster size: 127 voxels 4) Medial frontal gyrus L; Coordinates: Tal [-3, -19, 51] → MNI [-4, -22, 56]; Cluster size: 39 voxels
McTeague et al. (2017)	Decreased TBA in lateral prefrontal cortex and insula in SCZ during	Decreased TBA in SCZ vs. HC during cognitive processing: 1) Insula/Ventrolateral prefrontal cortex R;

	cognitive processing	Coordinates: MNI [44, 28, -12]; Cluster size: 309 voxels 2) Prefrontal cortex L; Coordinates: MNI [-48, 24, 26]; Cluster size: 686 voxels
McTeague et al. (2020)	Decreased TBA in dorsomedial thalamus and fusiform gyrus, as well as increased TBA in cuneus, in SCZ during face emotion processing (faces)	Decreased TBA in SCZ vs. HC during emotion processing (faces): 1) Fusiform gyrus R; Coordinates: MNI [32, -78, -6]; Cluster size: 244 voxels 2) Fusiform gyrus L; Coordinates: MNI [-36, -70, -8]; Cluster size: 343 voxels 3) Thalamus (dorsomedial nucleus) L; Coordinates: MNI [-2, -18, 2]; Cluster size: 416 voxels Increased TBA in SCZ vs. HC during emotion processing (faces): 1) Cuneus/Calcarine fissure R; Coordinates: MNI [8, -82, 16]; Cluster size: 301 voxels
Minzenberg et al. (2009)	Decreased TBA in dorsolateral prefrontal cortex, insula/claustrum, and thalamus, as well as altered TBA in anterior cingulate cortex and inferior parietal lobule, in SCZ during cognitive processing of executive functions	Decreased TBA in SCZ vs. HC during cognitive processing of executive functions: 1) Middle frontal gyrus L (BA 9); Coordinates: Tal [-38, 30, 30] → MNI [-39, 30, 32]; Cluster size: 3096 mm^3 2) Middle frontal gyrus L (BA 6); Coordinates: Tal [-30, -6, 44] → MNI [-30, -9, 48]; Cluster size: 664 mm^3 3) Middle frontal gyrus R (BA 9); Coordinates: Tal [32, 24, 42] → MNI [32, 22, 44]; Cluster size: 712 mm^3 4) Medial frontal gyrus R (BA 9); Coordinates: Tal [6, 42, 18] → MNI [7, 45, 20]; Cluster size: 1480 mm^3 5) Cingulate gyrus R (BA 32); Coordinates: Tal [2, 18, 34] → MNI [2, 17, 37]; Cluster size: 1704 mm^3 6) Claustrum R; Coordinates: Tal [26, 22, 2] → MNI [27, 25, -1]; Cluster size: 1776 mm^3 7) Middle occipital gyrus L (BA 19); Coordinates: Tal [-42, -70, 6] → MNI [-43, -71, 2]; Cluster size: 416 mm^3 8) Inferior parietal lobule R (BA 7); Coordinates: Tal [36, -58, 42] → MNI [35, -62, 46]; Cluster size: 792 mm^3 9) Claustrum L; Coordinates: Tal [-28, 24, 0] → MNI [-29, 28, -3]; Cluster size: 880 mm^3 10) Putamen R; Coordinates: Tal [20, -4, 14] → MNI [21, -3, 13]; Cluster size: 448 mm^3 11) Thalamus (mediodorsal nucleus) L; Coordinates: Tal [-4, -14, 10] → MNI [-5, -13, 8]; Cluster size: 1736 mm^3 Increased TBA in SCZ vs. HC during cognitive processing of executive functions: 1) Superior frontal gyrus L (BA 6); Coordinates: Tal [-8, -14, 68] → MNI [-9, -20, 76]; Cluster size: 440 mm^3 2) Superior frontal gyrus L (BA 9); Coordinates: Tal [-2, 52, 24] → MNI [-2, 54, 28]; Cluster size: 1320 mm^3

		3) Inferior frontal gyrus L (BA 46); Coordinates: Tal [-40, 36, 12] → MNI [-41, 38, 11]; Cluster size: 656 mm^3 4) Medial frontal gyrus R (BA 10); Coordinates: Tal [8, 44, -12] → MNI [9, 50, -12]; Cluster size: 424 mm^3 5) Precentral gyrus L (BA 6); Coordinates: Tal [-54, 4, 30] → MNI [-56, 5, 31]; Cluster size: 752 mm^3 6) Cingulate gyrus L (BA 32); Coordinates: Tal [-2, 10, 40] → MNI [-3, 9, 44]; Cluster size: 2208 mm^3 7) Superior temporal gyrus R (BA 41); Coordinates: Tal [38, -36, 6] → MNI [39, -36, 2]; Cluster size: 584 mm^3 8) Inferior parietal lobule L (BA 40); Coordinates: Tal [-54, -42, 42] → MNI [-54, -46, 44]; Cluster size: 1200 mm^3 9) Lingual gyrus R (BA 18); Coordinates: Tal [14, -74, 6] → MNI [14, -76, 2]; Cluster size: 800 mm^3 10) Insula R (BA 13); Coordinates: Tal [38, 16, 4] → MNI [40, 19, 0]; Cluster size: 1136 mm^3 11) Amygdala R; Coordinates: Tal [18, -4, -12] → MNI [19, -2, -19]; Cluster size: 592 mm^3 Subgroup meta-analysis: *Studies on cognitive processing of executive functions excluding working memory in SCZ:* Decreased TBA in SCZ vs. HC: 1) Medial frontal gyrus R (BA 9); Coordinates: Tal [6, 42, 18] → MNI [7, 45, 20]; Cluster size: 360 mm^3 2) Medial frontal gyrus L (BA 8); Coordinates: Tal [-12, 34, 36] → MNI [-12, 34, 39]; Cluster size: 184 mm^3 3) Middle frontal gyrus L (BA 6); Coordinates: Tal [-30, -6, 42] → MNI [-31, -8, 45]; Cluster size: 240 mm^3 4) Middle frontal gyrus L (BA 9); Coordinates: Tal [-40, 32, 28] → MNI [-41, 32, 29]; Cluster size: 120 mm^3 5) Cingulate gyrus R (BA 32); Coordinates: Tal [2, 18, 34] → MNI [2, 18, 37]; Cluster size: 848 mm^3 6) Inferior parietal lobule L (BA 7); Coordinates: Tal [-28, -70, 46] → MNI [-28, -75, 50]; Cluster size: 224 mm^3 7) Inferior parietal lobule R (BA 7); Coordinates: Tal [36, -60, 42] → MNI [35, -64, 46]; Cluster size: 368 mm^3 *Studies on co-occurring TBA changes during cognitive processing of executive functions in SCZ:* Decreased TBA in SCZ vs. HC: 1) Middle frontal gyrus L (BA 9); Coordinates: Tal [-38, 30, 30] → MNI [-39, 30, 32]; Cluster size: 1456 mm^3 2) Middle frontal gyrus R (BA 9); Coordinates: Tal [6, 42, 18] → MNI [7, 45, 20]; Cluster size: 696 mm^3 3) Anterior cingulate gyrus R (BA 32);

		Coordinates: Tal [2, 18, 34] → MNI [2, 17, 37]; Cluster size: 792 mm^3 4) Claustrum L; Coordinates: Tal [-28, 24, 0] → MNI [-29, -28, -3]; Cluster size: 488 mm^3 5) Claustrum R; Coordinates: Tal [26, 22, 2] → MNI [27, 25, -1]; Cluster size: 936 mm^3 6) Thalamus (mediodorsal nucleus) L; Coordinates: Tal [-4, -14, 10] → MNI [-5, -13, 8]; Cluster size: 760 mm^3 Increased TBA in SCZ vs. HC: 1) Anterior cingulate gyrus L (BA 32); Coordinates: Tal [-2, 10, 40] → MNI [-3, 9, 44]; Cluster size: 1256 mm^3 2) Inferior parietal lobule L (BA 40); Coordinates: Tal [-54, -42, 42] → MNI [-54, -46, 44]; Cluster size: 584 mm^3
Olabi et al. (2012)	Decreased GM in insula, superior/middle temporal gyrus, postcentral gyrus, cingulate gyrus, medial frontal cortex, middle frontal gyrus, caudate, and amygdala/uncus in first-episode SCZ	Decreased GM in first-episode SCZ vs. HC: 1) Caudate R/L; Coordinates: Tal [2, 14, 0] → MNI [3, 17, -3]; Cluster size: 1624 mm^3 2) Uncus L; Coordinates: Tal [-18, -2, -22] → MNI [-18, 1, -30]; Cluster size: 1272 mm^3 3) Superior temporal gyrus R; Coordinates: Tal [48, -24, 10] → MNI [50, -24, 7]; Cluster size: 400 mm^3 4) Insula L; Coordinates: Tal [-36, 20, 6] → MNI [-37, 23, 4]; Cluster size: 376 mm^3 5) Transverse temporal gyrus L; Coordinates: Tal [-46, -18, 10] → MNI [-49, -17, 8]; Cluster size: 288 mm^3 6) Middle temporal gyrus R; Coordinates: Tal [54, -26, -2] → MNI [57, -25, -8]; Cluster size: 272 mm^3 7) Superior temporal gyrus L; Coordinates: Tal [-58, -26, 12] → MNI [-61, -26, 10]; Cluster size: 272 mm^3 8) Superior temporal gyrus L; Coordinates: Tal [-56, 2, -4] → MNI [-59, 6, -9]; Cluster size: 216 mm^3 9) Insula R; Coordinates: Tal [36, 8, 10] → MNI [38, 10, 7]; Cluster size: 216 mm^3 10) Postcentral gyrus R; Coordinates: Tal [54, -20, 44] → MNI [54, -23, 47]; Cluster size: 216 mm^3 11) Middle frontal gyrus L; Coordinates: Tal [-30, 50, 4] → MNI [-30, 53, 4]; Cluster size: 200 mm^3 12) Inferior frontal gyrus L; Coordinates: Tal [-22, 28, -6] → MNI [-22, 32, -9]; Cluster size: 184 mm^3 13) Postcentral gyrus L; Coordinates: Tal [-60, -18, 20] → MNI [-63, -18, 19]; Cluster size: 184 mm^3 14) Amygdala/Uncus R; Coordinates: Tal [20, -4, -22] → MNI [21, -1, -30]; Cluster size: 168 mm^3 15) Superior temporal gyrus L; Coordinates: Tal [-32, 14, -22] → MNI [-32, 20, -28]; Cluster size: 152 mm^3 16) Inferior temporal gyrus L;

		Coordinates: Tal [-46, -14, -18] → MNI [-49, -12, -25]; Cluster size: 152 mm^3 17) Cingulate gyrus L; Coordinates: Tal [-8, -4, 38] → MNI [-9, -6, 41]; Cluster size: 152 mm^3 18) Insula/Claustrum R; Coordinates: Tal [34, -14, 12] → MNI [36, -14, 10]; Cluster size: 136 mm^3 19) Medial frontal gyrus R (BA 8); Coordinates: Tal [14, 34, 36] → MNI [14, 33, 39]; Cluster size: 136 mm^3 20) Cingulate gyrus L; Coordinates: Tal [0, -42, 38] → MNI [-1, -45, 41]; Cluster size: 112 mm^3 21) Medial frontal gyrus R (BA 6); Coordinates: Tal [6, 6, 48] → MNI [6, 3, 53]; Cluster size: 112 mm^3
Ortuño et al. (2011)	Decreased TBA in dorsolateral prefrontal cortex, posterior parietal cortex, anterior cingulate cortex, opercular cortex, putamen, and thalamus in SCZ during cognitive processing of timing (time estimation)	Decreased TBA in SCZ vs. HC during cognitive processing of timing (time estimation): 1) Lentiform nucleus R; Coordinates: Tal [28, -14, 0] → MNI [29, -13, -5]; Cluster size: 1408 mm^3 2) Precentral gyrus R (BA 6); Coordinates: Tal [48, -6, 5] → MNI [51, -4, 1]; Cluster size: 1208 mm^3 3) Superior frontal gyrus R (BA 9); Coordinates: Tal [16, 38, 34] → MNI [17, 38, 37]; Cluster size: 560 mm^3 4) Parietal cortex R (BA 39); Coordinates: Tal [46, -70, 34] → MNI [45, -74, 35]; Cluster size: 504 mm^3 5) Thalamus R; Coordinates: Tal [8, -7, 11] → MNI [9, -6, 9]; Cluster size: 488 mm^3 6) Anterior cingulate gyrus L (BA 32); Coordinates: Tal [-9, 24, 28] → MNI [-10, 25, 30]; Cluster size: 392 mm^3 7) Middle frontal gyrus R (BA 8); Coordinates: Tal [36, 36, 40] → MNI [36, 34, 42]; Cluster size: 224 mm^3 8) Superior frontal gyrus R (BA 10); Coordinates: Tal [14, 66, 8] → MNI [15, 70, 11]; Cluster size: 128 mm^3
Picó-Pérez et al. (2022)	Decreased GM in widespread areas in SCZ Decreased GM in superior temporal gyrus/insula/inferior frontal gyrus in early-stage SCZ Decreased TBA in dorsomedial/lateral prefrontal cortex in SCZ during cognitive processing Decreased TBA in angular gyrus during cognitive processing of social cognition Decreased TBA in superior parietal gyrus	Decreased GM in SCZ vs. HC: Widespread cortical and subcortical areas; Cluster size: 68950 voxels 1) Rolandic operculum L; Coordinates: MNI [-52, -4, 8]; */† 2) Superior temporal gyrus L; Coordinates: MNI [-48, -22, 10]; */† 3) Temporal pole L; Coordinates: MNI [-44, 6, -12]; */† 4) Temporal pole R; Coordinates: MNI [54, 6, -8]; † 5) Rolandic operculum R; Coordinates: MNI [60, -8, 8]; */† 6) Superior temporal gyrus R; Coordinates: MNI [60, -12, 4]; */† 7) Superior frontal gyrus/Dorsomedial prefrontal cortex L;

	in early-stage SCZ during cognitive processing	Coordinates: MNI [-2, 52, 14]; */† 8) Superior frontal gyrus/Ventromedial prefrontal cortex R; Coordinates: MNI [6, 50, -18]; † 9) Superior frontal gyrus/Dorsomedial prefrontal cortex R; Coordinates: MNI [4, 52, 14]; */† 10) Inferior frontal gyrus L (orbital); Coordinates: MNI [-44, 24, -14]; † 11) Inferior frontal gyrus R (opercular); Coordinates: MNI [54, 10, 10]; */† 12) Insula R; Coordinates: MNI [42, 12, -6]; † 13) Superior frontal gyrus/Ventromedial prefrontal cortex L; Coordinates: MNI [-6, 50, -10]; † 14) Anterior cingulate gyrus R; Coordinates: MNI [6, 34, 18]; † 15) Median cingulate gyrus L; Coordinates: MNI [-4, -26, 44]; */† 16) Median cingulate gyrus R; Coordinates: MNI [4, -20, 44]; † 17) Anterior cingulate gyrus L; Coordinates: MNI [-8, 44, -4]; */† 18) Middle temporal gyrus L; Coordinates: MNI [-60, -32, 2]; */† 19) Inferior frontal gyrus R (orbital); Coordinates: MNI [38, 24, -12]; */† 20) Thalamus L; Coordinates: MNI [-2, -12, 4]; */† 21) Inferior frontal gyrus (triangular) R; Coordinates: MNI [52, 14, 24]; */† 22) Inferior frontal gyrus L (triangular); Coordinates: MNI [-52, 14, 30]; */† 23) Insula L: Coordinates: MNI [-32, 24, -4]; † 24) Precentral gyrus R; Coordinates: MNI [50, 8, 30]; */† 25) Middle frontal gyrus (orbital) L; Coordinates: MNI [-38, 50, -8]; */† 26) Middle frontal gyrus R; Coordinates: MNI [46, 46, 8]; */† 27) Supplementary motor area R; Coordinates: MNI [4, 12, 46]; */† 28) Cuneus L; Coordinates: MNI [-2, -86, 0]; */† 29) Middle temporal gyrus R; Coordinates: MNI [64, -30, 0]; */†

		30) Middle frontal gyrus L; Coordinates: MNI [-36, 54, 10]; */† 31) Cuneus R; Coordinates: MNI [8, -88, 14]; */† 32) Inferior temporal gyrus L; Coordinates: MNI [-50, -58, -12]; */† 33) Inferior occipital gyrus L; Coordinates: MNI [-48, -62, -12]; † 34) Supplementary motor area L; Coordinates: MNI [-4, 10, 50]; */† 35) Fusiform gyrus L; Coordinates: MNI [-48, -58, -20]; */† 36) Supramarginal gyrus R; Coordinates: MNI [60, -24, 44]; */† 37) Angular gyrus R; Coordinates: MNI [50, -62, 34]; */† 38) Parahippocampal gyrus R; Coordinates: MNI [24, -6, -28]; */† 39) Supramarginal gyrus L; Coordinates: MNI [-58, -48, 30]; */† 40) Inferior frontal gyrus L; Coordinates: MNI [-52, 16, 12]; † 41) Hippocampus L; Coordinates: MNI [-22, -16, -14]; */† 42) Caudate L; Coordinates: MNI [-6, 10, 4]; */† 43) Superior frontal gyrus (orbital) R; Coordinates: MNI [32, 60, -4]; */† 44) Lingual gyrus L; Coordinates: MNI [-14, -40, -10]; */† 45) Middle frontal gyrus (orbital) R; Coordinates: MNI [44, 52, -4]; */† 46) Middle occipital gyrus R; Coordinates: MNI [38, -72, 38]; */† 47) Postcentral gyrus R; Coordinates: MNI [50, -18, 40]; † 48) Inferior occipital gyrus R; Coordinates: MNI [38, -84, -8]; */† 49) Inferior temporal gyrus R; Coordinates: MNI [50, -60, -16]; */† 50) Subgenual anterior cingulate L; Coordinates: MNI [-8, 18, -14]; */† 51) Angular gyrus L; Coordinates: MNI [-50, -58, 26]; */† 52) Precuneus R;

		Coordinates: MNI [14, -64, 26]; */† 53) Parahippocampal gyrus L; Coordinates: MNI [-28, -18, -22]; */† 54) Precuneus L; Coordinates: MNI [-4, -58, 20]; */† 55) Superior occipital gyrus R; Coordinates: MNI [28, -82, 28]; */† 56) Middle occipital gyrus L; Coordinates: MNI [-44, -70, 0]; */† 57) Inferior parietal gyrus L; Coordinates: MNI [-50, -46, 48]; */† 58) Postcentral gyrus L; Coordinates: MNI [-60, -12, 28]; */† 59) Inferior parietal gyrus R; Coordinates: MNI [42, -40, 50]; † 60) Posterior cingulate gyrus L; Coordinates: MNI [-8, -52, 28]; */† 61) Posterior cingulate gyrus R; Coordinates: MNI [4, -50, 24]; † 62) Caudate R; Coordinates: MNI [8, 16, 2]; */† 63) Thalamus R; Coordinates: MNI [14, -14, 14]; */† 64) Cerebellum L; Coordinates: MNI [-14, -62, -18]; */† Parahippocampal gyrus R; Cluster size: 449 voxels 65) Parahippocampal gyrus R; Coordinates: MNI [26, -34, -14]; */† 66) Cerebellum R; Coordinates: MNI [26, -40, -24]; † Decreased TBA in SCZ vs. HC during cognitive processing: 1) Dorsomedial prefrontal cortex/Supplementary motor area L/R; Coordinates: MNI [0, 24, 52]; Cluster size: 704 voxels; */† 2) Inferior frontal gyrus R; Coordinates: MNI [48, 36, -8]; Cluster size: 157 voxels; */† Decreased TBA in SCZ vs. HC during cognitive processing of social cognition: 1) Angular gyrus R; Coordinates: MNI [54, -52, 26]; Cluster size: 98 voxels; */† <u>Subgroup meta-analysis:</u> *Studies on GM in medication-free and medicated SCZ:* Decreased GM in medication-free SCZ vs. HC:

		1) Rolandic operculum/Insula/Superior temporal gyrus/Inferior frontal gyrus L; Coordinates: MNI [-44, -8, 6]; Cluster size: 4753 voxels 2) Dorsomedial prefrontal cortex/Supplementary motor area/Cingulate gyrus L; Coordinates: MNI [-2, 30, -10]; Cluster size: 1490 voxels 3) Dorsomedial prefrontal cortex/Supplementary motor area/Cingulate gyrus R; Coordinates: MNI [2, -24, 34]; Cluster size: 924 voxels 4) Superior temporal gyrus R; Coordinates: MNI [56, -10, -2]; Cluster size: 126 voxels 5) Postcentral gyrus R; Coordinates: MNI [56, -20, 38]; Cluster size: 116 voxels 6) Middle temporal gyrus R; Coordinates: MNI [54, -56, 18]; Cluster size: 73 voxels 7) Precentral gyrus R; Coordinates: MNI [38, -14, 46]; Cluster size: 35 voxels Decreased GM in medicated SCZ vs. HC: 1) Rolandic operculum/Insula/Superior temporal gyrus/Inferior frontal gyrus L; Coordinates: MNI [-44, 4, -10]; Cluster size: 7492 voxels 2) Superior temporal gyrus/Insula/Inferior frontal gyrus R; Coordinates: MNI [52, 8, -10]; Cluster size: 6427 voxels 3) Dorsomedial prefrontal cortex/Cingulate gyrus R/L; Coordinates: MNI [0, 44, 34]; Cluster size: 5781 voxels *Studies on GM in SCZ with different illness duration:* Decreased GM in early-stage SCZ (illness duration=0-2 years) vs. HC: 1) Superior temporal gyrus/Insula/Inferior frontal gyrus L; Coordinates: MNI [-48, -10, 0]; Cluster size: 1839 voxels Decreased GM in intermediate-stage SCZ (illness duration=3-10 years) vs. HC: 1) Rolandic operculum/Insula/Superior temporal gyrus/Inferior frontal gyrus L; Coordinates: MNI [-50, -4, 6]; Cluster size: 6249 voxels 2) Rolandic operculum/Insula/Superior temporal gyrus/Inferior frontal gyrus R; Coordinates: MNI [50, 2, 0]; Cluster size: 4641 voxels 3) Dorsomedial prefrontal cortex/Cingulate gyrus L; Coordinates: MNI [-8, 52, -4]; Cluster size: 1125 voxels 4) Supplementary motor area R; Coordinates: MNI [4, 16, 48]; Cluster size: 591 voxels 5) Cingulate gyrus R; Coordinates: MNI [10, -24, 40]; Cluster size: 160 voxels 6) Middle frontal gyrus R; Coordinates: MNI [46, 48, 12]; Cluster size: 21 voxels Decreased GM in chronic-stage SCZ (illness duration>10 years) vs. HC: 1) Dorsomedial prefrontal cortex/Supplementary motor area/Cingulate gyrus R/L; Coordinates: MNI [0, 48, 16]; Cluster size: 4913 voxels 2) Inferior frontal gyrus/Insula/Superior temporal gyrus L; Coordinates: MNI [-46, 14, 0]; Cluster size: 2668 voxels 3) Rolandic operculum/Insula/Superior temporal gyrus/Inferior frontal gyrus R;

		Coordinates: MNI [44, 14, -14]; Cluster size: 1748 voxels *Studies on GM in SCZ with different levels of symptomatology:* Decreased GM in SCZ with high symptoms (PANSS total score) vs. HC: 1) Rolandic operculum/Insula/Superior temporal gyrus/Inferior frontal gyrus L; Coordinates: MNI [-48, -22, 12]; Cluster size: 8905 voxels 2) Dorsomedial prefrontal cortex/Supplementary motor area/Cingulate gyrus R/L; Coordinates: MNI [-6, -28, 44]; Cluster size: 8271 voxels 3) Rolandic operculum/Insula/Superior temporal gyrus/Inferior frontal gyrus R; Coordinates: MNI [54, -10, -8]; Cluster size: 2806 voxels 4) Middle frontal gyrus R; Coordinates: MNI [46, 44, 8]; Cluster size: 478 voxels 5) Precentral gyrus/Postcentral gyrus R; Coordinates: MNI [56, -18, 38]; Cluster size: 114 voxels 6) Supramarginal gyrus L; Coordinates: MNI [-58, -46, 34]; Cluster size: 62 voxels 7) Supramarginal gyrus L; Coordinates: MNI [-48, -42, 26]; Cluster size: 30 voxels 8) Superior frontal gyrus (dorsolateral prefrontal cortex) R; Coordinates: MNI [24, 44, 34]; Cluster size: 22 voxels Decreased GM in SCZ with low symptoms (PANSS total score) vs. HC: 1) Inferior frontal gyrus/Insula/Superior temporal gyrus L; Coordinates: MNI [-44, 16, -12]; Cluster size: 9640 voxels 2) Insula/Superior temporal gyrus/Supramarginal gyrus/Inferior frontal gyrus R; Coordinates: MNI [48, 12, -6]; Cluster size: 6113 voxels 3) Dorsomedial prefrontal cortex/Supplementary motor area/Cingulate gyrus R/L; Coordinates: MNI [2, 48, 12]; Cluster size: 5676 voxels Decreased GM in SCZ with high positive symptoms (PANSS positive score) vs. HC: 1) Rolandic operculum/Insula/Superior temporal gyrus/Inferior frontal gyrus L; Coordinates: MNI [-52, -10, 6]; Cluster size: 7896 voxels 2) Dorsomedial prefrontal cortex/Supplementary motor area/Cingulate gyrus R/L; Coordinates: MNI [-8, 52, -4]; Cluster size: 7854 voxels 3) Rolandic operculum/Insula/Superior temporal gyrus/Inferior frontal gyrus R; Coordinates: MNI [52, 16, -6]; Cluster size: 4782 voxels 4) Thalamus R/L; Coordinates: MNI [-4, -12, 4]; Cluster size: 469 voxels 5) Angular gyrus R; Coordinates: MNI [52, -54, 32]; Cluster size: 457 voxels Decreased GM in SCZ with low positive symptoms (PANSS positive score) vs. HC: 1) Insula/Superior temporal gyrus/Supramarginal gyrus/Inferior frontal gyrus R; Coordinates: MNI [50, 6, -10]; Cluster size: 6976 voxels 2) Superior temporal gyrus/Insula/Inferior frontal gyrus/Cerebellum L; Coordinates: MNI [-44, 4, -12]; Cluster size: 6343 voxels 3) Dorsomedial prefrontal cortex/Supplementary motor area/Cingulate gyrus R/L; Coordinates: MNI [2, 36, 20]; Cluster size: 4261 voxels

		4) Middle temporal gyrus L; Coordinates: MNI [-58, -32, 0]; Cluster size: 646 voxels Decreased GM in SCZ with high negative symptoms (PANSS negative score) vs. HC: 1) Rolandic operculum/Insula/Superior temporal gyrus/Inferior frontal gyrus L; Coordinates: MNI [-52, 10, -12]; Cluster size: 6597 voxels 2) Superior temporal gyrus/Postcentral gyrus/Rolandic operculum R; Coordinates: MNI [54, -10, -8]; Cluster size: 5625 voxels 3) Dorsomedial prefrontal cortex/Supplementary motor area/Cingulate gyrus R/L; Coordinates: MNI [4, -20, 44]; Cluster size: 5110 voxels 4) Inferior frontal gyrus R; Coordinates: MNI [50, 12, 30]; Cluster size: 295 voxels Decreased GM in SCZ with low negative symptoms (PANSS negative score) vs. HC: 1) Dorsomedial prefrontal cortex/Supplementary motor area/Cingulate gyrus R/L; Coordinates: MNI [-2, 44, -6]; Cluster size: 6633 voxels 2) Insula/Superior temporal gyrus/Hippocampus/Amygdala L; Coordinates: MNI [-36, 22, -2]; Cluster size: 8126 voxels 3) Rolandic operculum/Insula/Superior temporal gyrus/Inferior frontal gyrus R; Coordinates: MNI [44, 14, -14]; Cluster size: 5346 voxels 4) Fusiform gyrus R; Coordinates: MNI [24, -38, -16]; Cluster size: 30 voxels 5) Middle frontal gyrus L; Coordinates: MNI [-34, 56, -4]; Cluster size: 19 voxels Decreased GM in SCZ with high general symptoms (PANSS general score) vs. HC: 1) Rolandic operculum/Insula/Superior temporal gyrus L; Coordinates: MNI [-48, -20, 12]; Cluster size: 7506 voxels 2) Dorsomedial prefrontal cortex/Supplementary motor area/Cingulate gyrus R/L; Coordinates: MNI [-6, -26, 42]; Cluster size: 5516 voxels 3) Superior temporal gyrus/Postcentral gyrus R; Coordinates: MNI [54, -10, -8]; Cluster size: 1537 voxels 4) Middle frontal gyrus R; Coordinates: MNI [46, 44, 10]; Cluster size: 10 voxels Decreased GM in SCZ with low general symptoms (PANSS general score) vs. HC: 1) Insula/Superior temporal gyrus/Cerebellum/Amygdala L; Coordinates: MNI [-38, 20, -4]; Cluster size: 8810 voxels 2) Dorsomedial prefrontal cortex/Supplementary Motor Area/Cingulate gyrus R/L; Coordinates: MNI [2, 44, -6]; Cluster size: 5642 voxels 3) Rolandic operculum/Insula/Superior temporal gyrus R; Coordinates: MNI [50, 12, -8]; Cluster size: 5344 voxels *Studies on TBA during cognitive processing in medicated SCZ:* Decreased TBA in medicated SCZ vs. HC: 1) Dorsomedial prefrontal cortex/Supplementary motor area R/L; Coordinates: MNI [0, 22, 50]; Cluster size: 153 voxels 2) Inferior frontal gyrus R; Coordinates: MNI [42, 10, 32]; Cluster size: 13 voxels

		3) Inferior frontal gyrus R; Coordinates: MNI [50, 18, 26]; Cluster size: 11 voxels *Studies on TBA during cognitive processing in SCZ with different illness duration:* Decreased TBA in early-stage SCZ (illness duration=0-2 years) vs. HC: 1) Superior parietal gyrus R; Coordinates: MNI [22, -66, 50]; Cluster size: 220 voxels Decreased TBA in chronic-stage SCZ (illness duration>10 years) vs. HC: 1) Dorsomedial prefrontal cortex/Supplementary motor area R/L; Coordinates: MNI [-2, 24, 50]; Cluster size: 408 voxels Increased TBA in chronic-stage SCZ (illness duration>10 years) vs. HC: 1) Ventromedial prefrontal cortex R/L; Coordinates: MNI [4, 48, 0]; Cluster size: 330 voxels *Studies on TBA during cognitive processing in SCZ with different levels of symptomatology:* Decreased TBA in SCZ with high symptoms (PANSS total score) vs. HC: 1) Precentral gyrus L; Coordinates: MNI [-46, -4, 48]; Cluster size: 38 voxels Increased TBA in SCZ with low symptoms (PANSS total score) vs. HC: 1) Median/Posterior cingulate gyrus R/L; Coordinates: MNI [0, -42, 34]; Cluster size: 136 voxels Increased TBA in SCZ with low positive symptoms (PANSS positive score) vs. HC: 1) Rolandic operculum R; Coordinates: MNI [58, -16, 16]; Cluster size: 355 voxels Increased TBA in SCZ with low negative symptoms (PANSS negative score) vs. HC: 1) Rolandic operculum R; Coordinates: MNI [56, -14, 10]; Cluster size: 127 voxels 2) Median/Posterior cingulate gyrus R/L; Coordinates: MNI [0, -36, 36]; Cluster size: 106 voxels *Studies on TBA during cognitive processing of attention/vigilance in SCZ:* Decreased TBA in SCZ vs. HC: 1) Dorsomedial prefrontal cortex/Cingulate gyrus R/L; Coordinates: MNI [-6, 12, 34]; Cluster size: 864 voxels 2) Middle temporal gyrus L; Coordinates: MNI [-60, -34, 4]; Cluster size: 142 voxels 3) Precentral gyrus/Postcentral gyrus; Coordinates: MNI [-58, -2, 28]; Cluster size: 64 voxels 4) Superior temporal gyrus L; Coordinates: MNI [-60, -38, 18]; Cluster size: 20 voxels *Studies on TBA during cognitive processing of social cognition in SCZ with different levels of symptomatology:* Decreased TBA in SCZ with high positive symptoms (PANSS positive score) vs. HC: 1) Inferior frontal gyrus R;

		Coordinates: MNI [50, 34, 10]; Cluster size: 49 voxels Decreased TBA in SCZ with high negative symptoms (PANSS negative score) vs. HC: 1) Angular gyrus R; Coordinates: MNI [54, -52, 34]; Cluster size: 126 voxels 2) Middle occipital gyrus R; Coordinates: MNI [38, -70, 36]; Cluster size: 40 voxels *Studies on TBA during cognitive processing of theory of mind in SCZ:* Decreased TBA in SCZ vs. HC: 1) Middle temporal gyrus R; Coordinates: MNI [48, -58, 16]; Cluster size: 24 voxels
Ragland et al. (2009)	Decreased TBA in lateral prefrontal cortex, posterior parietal cortex, middle temporal gyrus, posterior cingulate cortex, occipital cortex, thalamus, and cerebellum, as well as increased TBA in pre/postcentral gyrus and inferior temporal areas (along with altered TBA in medial prefrontal cortex/anterior cingulate cortex) in SCZ during cognitive processing of episodic memory (encoding/retrieval)	Decreased TBA in SCZ vs. HC during cognitive processing of episodic memory (encoding): 1) Superior frontal gyrus R (BA 10, 32); Coordinates: Tal [22, 48, 14)] → MNI [23, 50, 15]; Cluster size: 4608 mm^3 2) Superior frontal gyrus R (BA 8); Coordinates: Tal [6, 36, 48] → MNI [6, 34, 53]; Cluster size: 1104 mm^3 3) Inferior frontal gyrus R (BA 45, 46); Coordinates: Tal [40, 30, 12] → MNI [41, 31, 10]; Cluster size: 2760 mm^3 4) Inferior frontal gyrus L (BA 45); Coordinates: Tal [-36, 26, 12] → MNI [-37, 28, 11]; Cluster size: 1424 mm^3 5) Inferior parietal gyrus R (BA 40); Coordinates: Tal [50, -48, 36] → MNI [49, -51, 38]; Cluster size: 1056 mm^3 6) Lingual gyrus R (BA 17); Coordinates: Tal [18, -86, 0)] → MNI [18, -88, -6]; Cluster size: 1192 mm^3 7) Posterior cingulate gyrus R (BA 31); Coordinates: Tal [4, -36, 32] → MNI [4, -38, 33]; Cluster size: 896 mm^3 Increased TBA in SCZ vs. HC during cognitive processing of episodic memory (encoding): 1) Precentral gyrus L (BA 6); Coordinates: Tal [-46, -8, 40] → MNI [-47, -10, 43]; Cluster size: 2704 mm^3 2) Middle temporal gyrus L (BA 37); Coordinates: Tal [-44, -42, -8] → MNI [-47, -41, -15]; Cluster size: 352 mm^3 3) Postcentral gyrus L (BA 2); Coordinates: Tal [-44, -28, 36] → MNI [-45, -30, 38]; Cluster size: 344 mm^3 4) Cingulate gyrus L (BA 24); Coordinates: Tal [-2, 6, 38] → MNI [-3, 5, 41]; Cluster size: 1368 mm^3 5) Parahippocampal gyrus L (BA 19); Coordinates: Tal [-28, -50, -4] → MNI [-30, -50, -10]; Cluster size: 304 mm^3 Decreased activity in SCZ vs. HC during cognitive processing of episodic memory (retrieval): 1) Inferior frontal gyrus L (BA 45, 46); Coordinates: Tal [-40, 22, 20] → MNI [-42, 23, 20]; Cluster size: 3048 mm^3 2) Precentral gyrus L (BA 6); Coordinates: Tal [-36, -2, 28] → MNI [-37, -2, 29]; Cluster size: 1064 mm^3

		3) Middle frontal gyrus L (BA 8); Coordinates: Tal [-38, 32, 38] → MNI [-39, 31, 41]; Cluster size: 888 mm^3 4) Anterior cingulate gyrus R (BA 24); Coordinates: Tal [4, 26, -6] → MNI [5, 30, -8]; Cluster size: 888 mm^3 5) Middle temporal gyrus L (BA 21); Coordinates: Tal [-56, -42, 0] → MNI [-60, -42, -6]; Cluster size: 560 mm^3 6) Cuneus R (BA 17); Coordinates: Tal [16, -86, 10] → MNI [16, -89, 6]; Cluster size: 2568 mm^3 7) Thalamus L; Coordinates: Tal [-4, -8, 18] → MNI [-5, -8, 18]; Cluster size: 1496 mm^3 8) Thalamus R; Coordinates: Tal [8, -24, 10] → MNI [8, -24, 8]; Cluster size: 1448 mm^3 9) Posterior cingulate gyrus R (BA 31); Coordinates: Tal [10, -52, 20] → MNI [10, -54, 19]; Cluster size: 520 mm^3 10) Cerebellum L; Coordinates: Tal [-24, -62, -42] → MNI [-25, -59, -53]; Cluster size: 1488 mm^3 11) Cerebellum R; Coordinates: Tal [30, -80, -34] → MNI [29, -79, -45]; Cluster size: 624 mm^3 Increased TBA in SCZ vs. HC during cognitive processing of episodic memory (retrieval): 1) Precentral gyrus L (BA 4); Coordinates: Tal [-28, -26, 66] → MNI [-27, -31, 74]; Cluster size: 1296 mm^3 2) Medial frontal gyrus R (BA 10); Coordinates: Tal [12, 44, 10] → MNI [13, 47, 11]; Cluster size: 1168 mm^3 3) Middle frontal gyrus R (BA 11); Coordinates: Tal [34, 36, -16] → MNI [36, 41, -21]; Cluster size: 600 mm^3 4) Middle temporal gyrus R (BA 21); Coordinates: Tal [60, -58, 0] → MNI [61, -58, -6]; Cluster size: 336 mm^3 5) Thalamus R; Coordinates: Tal [26, -30, 6] → MNI [27, -30, 3]; Cluster size: 792 mm^3 <u>Subgroup meta-analysis:</u> *Studies on TBA during episodic memory encoding with encoding strategies in SCZ:* Decreased TBA in SCZ vs. HC: 1) Superior frontal gyrus R (BA 10, 32); Coordinates: Tal [22, 48, 14] → MNI [23, 50, 15]; Cluster size: 5576 mm^3 2) Superior frontal gyrus R (BA 8); Coordinates: Tal [6, 36, 48] → MNI [6, 34, 53]; Cluster size: 1328 mm^3 3) Inferior frontal gyrus R (BA 46); Coordinates: Tal [40, 30, 12] → MNI [41, 31, 10]; Cluster size: 2112 mm^3 4) Inferior parietal gyrus R (BA 40); Coordinates: Tal [50, -48, 36] → MNI [49, -51, 38]; Cluster size: 1232 mm^3 5) Lingual gyrus R (BA 17); Coordinates: Tal [18, -86, 0] → MNI [18, -88, -6]; Cluster size: 1272 mm^3

		6) Cingulate gyrus R (BA 31); Coordinates: Tal [4, -36, 32] → MNI [4, -38, 33]; Cluster size: 928 mm^3 *Studies on TBA during episodic memory retrieval in SCZ with matched performance between groups:* Decreased TBA in SCZ vs. HC: 1) Cuneus R (BA 17, 18); Coordinates: Tal [16, -86, 10] → MNI [16, -89, 6]; Cluster size: 2784 mm^3 2) Inferior frontal gyrus L (BA 13, 46); Coordinates: Tal [-36, 28, 14] → MNI [-37, 30, 13]; Cluster size: 1920 mm^3 3) Middle frontal gyrus L (BA 8); Coordinates: Tal [-38, 32, 38] → MNI [-39, 31, 48]; Cluster size: 688 mm^3 4) Anterior cingulate gyrus R (BA 24); Coordinates: Tal [4, 26, -6] → MNI [5, 30, -8]; Cluster size: 912 mm^3 5) Thalamus L; Coordinates: Tal [-4, -8, 18] → MNI [-5, -8, 18]; Cluster size: 1406 mm^3 6) Thalamus R; Coordinates: Tal [8, -24, 10] → MNI [8, -24, 8]; Cluster size: 1624 mm^3 7) Cerebellum L; Coordinates: Tal [-24, -62, -42] → MNI [-25, -59, -53]; Cluster size: 1464 mm^3 8) Cerebellum R; Coordinates: Tal [30, -80, -34] → MNI [29, -79, -45]; Cluster size: 712 mm^3 Increased TBA in SCZ vs. HC: 1) Precentral gyrus L (BA 4); Coordinates: Tal [-28, -26, 66] → MNI [-27, -31, 74]; Cluster size: 1144 mm^3 2) Precentral gyrus L (BA 4); Coordinates: Tal [-40, -14, 56] → MNI [-40, -18, 61]; Cluster size: 336 mm^3 3) Medial frontal gyrus R (BA 11); Coordinates: Tal [8, 54, -16] → MNI [9, 60, -15]; Cluster size: 864 mm^3 4) Thalamus R; Coordinates: Tal [26, -30, 6] → MNI [27, -30, 3]; Cluster size: 792 mm^3 5) WM R; Coordinates: Tal [36, -56, 8] → MNI [36, -57, 4]; Cluster size: 328 mm^3
Taylor et al. (2012)	Decreased TBA in medial prefrontal cortex/anterior cingulate cortex and amygdala/hippocampus, along with dorsolateral prefrontal cortex, middle temporal gyrus/temporal pole, basal ganglia, midbrain, thalamus, and cerebellum, as well as altered TBA in precentral/postcentral gyrus, superior temporal gyrus, occipital cortex, and fusiform gyrus, in SCZ during emotion processing (emotion experience and perception)	Decreased TBA in SCZ vs. HC during emotion processing (emotion experience): 1) Occipital pole L: Coordinates: MNI [-34, -70, 16]; Cluster size: 34 voxels Decreased TBA in SCZ vs. HC during emotion processing (emotion perception): 1) Anterior cingulate R (BA 24, 32); Coordinates: MNI [16, 32, 14]; Cluster size: 347 voxels 2) Medial frontal cortex R (BA 8); Coordinates: MNI [4, 22, 52]; Cluster size: 122 voxels 3) Dorsolateral frontal cortex R (BA 44); Coordinates: MNI [48, 12, 12]; Cluster size: 118 voxels 4) Anterior temporal pole R (BA 38);

		Coordinates: MNI [34, 12, -24]; Cluster size: 59 voxels 5) Caudate body R; Coordinates: MNI [16, -4, 12]; Cluster size: 18 voxels 6) Amygdala L; Coordinates: MNI [-22, -6, -20]; Cluster size: 305 voxels 7) Thalamus R; Coordinates: MNI [10, -10, 12]; Cluster size: 21 voxels 8) Amygdala/Hippocampus L; Coordinates: MNI [24, -12, -18]; Cluster size: 515 voxels 9) Superior temporal gyrus R (BA 22); Coordinates: MNI [50, -20, 4]; Cluster size: 89 voxels 10) Midbrain R/L; Coordinates: MNI [0, -22, -6]; Cluster size: 51 voxels 11) Midbrain R; Coordinates: MNI [4, -28, -12)]; Cluster size: 62 voxels 12) Fusiform gyrus R (BA 37); Coordinates: MNI [28, -36, -18]; Cluster size: 32 voxels 13) Fusiform gyrus R (BA 37); Coordinates: MNI [38, -44, -18]; Cluster size: 12 voxels 14) Fusiform gyrus L (BA 19); Coordinates: MNI [-34, -76, -12]; Cluster size: 340 voxels 15) Occipital pole R (BA 19); Coordinates: MNI [32, -86, -10]; Cluster size: 413 voxels 16) Occipital pole L (BA 17); Coordinates: MNI [-10, -100, -6]; Cluster size: 146 voxels 17) Cerebellum L; Coordinates: MNI [-16, -32, -22]; Cluster size: 11 voxels Increased TBA in SCZ vs. HC during emotion processing (emotion perception): 1) Superior temporal gyrus L (BA 21); Coordinates: MNI [-44, 4, -18]; Cluster size: 266 voxels 2) Precentral gyrus R (BA 6); Coordinates: MNI [50, 0, 28]; Cluster size: 215 voxels 3) Parietal lobule L (BA 2); Coordinates: MNI [-36, -44, 54]; Cluster size: 204 voxels 4) Cuneus L (BA 19); Coordinates: MNI [-4, -88, 32]; Cluster size: 439 voxels Subgroup meta-analysis: *Studies on TBA in SCZ vs. HC during emotion processing (experience/perception) with matched effort:* Decreased TBA in SCZ vs. HC: 1) Anterior cingulate cortex R (BA 24); Coordinates: MNI [22, 30, 14]; Cluster size: 149 voxels 2) Dorsomedial frontal cortex R (BA 32);

		Coordinates: MNI [10, 26, 46]; Cluster size: 29 voxels 3) Medial frontal cortex R (BA 6); Coordinates: MNI [8, 20, 52]; Cluster size: 67 voxels 4) Anterior cingulate cortex L (BA 32); Coordinates: MNI [-12, 20, 40]; Cluster size: 22 voxels 5) Amygdala L; Coordinates: MNI [-22, -6, -20]; Cluster size: 304 voxels 6) Amygdala R; Coordinates: MNI [26, -8, -20]; Cluster size: 363 voxels 7) Hippocampus R; Coordinates: MNI [30, -32, -6]; Cluster size: 14 voxels 8) Midbrain R; Coordinates: MNI [2, -30, -10]; Cluster size: 62 voxels 9) Lingual gyrus R (BA 19); Coordinates: MNI [18, -48, -2]; Cluster size: 34 voxels 10) Cerebellum L; Coordinates: MNI [-18, -34, -20]; Cluster size: 76 voxels Increased TBA in SCZ vs. HC: 1) Fusiform gyrus R (BA 37); Coordinates: MNI [34, -54, -20]; Cluster size: 37 voxels *Studies on TBA during implicit emotion processing of faces:* Decreased TBA in SCZ vs. HC: 1) Anterior cingulate cortex (BA 24); Coordinates: MNI [22, 30, 14]; Cluster size: 149 voxels 2) Medial frontal cortex R (BA 6); Coordinates: MNI [8, 20, 52]; Cluster size: 314 voxels 3) Amygdala R; Coordinates: MNI [28, 0, -16]; Cluster size: 309 voxels 4) Amygdala/Hippocampus L; Coordinates: MNI [-26, -10, -24]; Cluster size: 138 voxels 5) Hippocampus L; Coordinates: MNI [-24, -20, -20]; Cluster size: 41 voxels 6) Cerebellum L; Coordinates: MNI [-16, -32, -22]; Cluster size: 34 voxels *Studies on TBA during explicit emotion processing of faces:* Decreased TBA in SCZ vs. HC: 1) Anterior cingulate cortex R (BA 32); Coordinates: MNI [12, 36, 12]; Cluster size: 336 voxels 2) Dorsolateral frontal cortex R (BA 44); Coordinates: MNI [48, 12, 12]; Cluster size: 393 voxels 3) Ventral pallidum L; Coordinates: MNI [-6, 2, -10]; Cluster size: 26 voxels 4) Caudate body R;

		Coordinates: MNI [16, -4, 12]; Cluster size: 213 voxels 5) Amygdala/Hippocampus R; Coordinates: MNI [12, -6, -18]; Cluster size: 37 voxels 6) Superior temporal gyrus R (BA 22); Coordinates: MNI [48, -24, -6]; Cluster size: 82 voxels 7) Middle temporal gyrus R (BA 21); Coordinates: MNI [60, -48, 10]; Cluster size: 110 voxels 8) Fusiform gyrus R (BA 20, 37); Coordinates: MNI [46, -52, -22]; Cluster size: 74 voxels 9) Fusiform gyrus L (BA 19); Coordinates: MNI [-30, -74, -16]; Cluster size: 82 voxels 10) Fusiform gyrus R (BA 19); Coordinates: MNI [32, -78, -14]; Cluster size: 365 voxels 11) Occipital pole (BA 18); Coordinates: MNI [-8, -102, -10]; Cluster size: 197 voxels Increased TBA in SCZ vs. HC: 1) Superior temporal gyrus L (BA 21); Coordinates: MNI [-44, 4, -18; Cluster size: 266 voxels 2) Precentral gyrus R (BA 6); Coordinates: MNI [50, 0, 28]; Cluster size: 215 voxels 3) Parietal lobule L (BA 2); Coordinates: MNI [-36, -44, 54; Cluster size: 204 voxels 4) Cuneus L (BA 19); Coordinates: MNI [-4, -88, 32]; Cluster size: 650 voxels
Townsend et al. (2022)	Decreased CM in anterior cingulate cortex and orbitofrontal cortex in SCZ	Decreased CM in SCZ vs. HC: 1) Cingulate/Paracingulate gyrus L; Coordinates: MNI [0, 24, 34]; Cluster size: 309 voxels; */† 2) Inferior orbital frontal gyrus L; Coordinates: MNI [-42, 24, -4]; Cluster size: 62 voxels; */†
Vitolo et al. (2018)	Decreased WM and FA in fornix, cingulum, inferior fronto-occipital fasciculus, inferior longitudinal fasciculus, superior longitudinal fasciculus, arcuate fasciculus, uncinate fasciculus, internal capsule, optic radiation, corticospinal tract, corpus callosum, and cerebellar tracts in SCZ Correlation of decreased WM in fornix and genu of corpus callosum, along with decreased FA in anterior cingulum and superior longitudinal fasciculus, with shorter illness duration in SCZ	Decreased WM in SCZ vs. HC: 1) Arcuate fasciculus L; Coordinates: Tal [-46, -49, 35] → MNI [-46, -51, 36]; Cluster size: 24480 voxels 2) Arcuate fasciculus R; Coordinates: Tal [49, -10, 29] → MNI [51, -11, 29]; Cluster size: 23307 voxels 3) Anterior Commissure L; Coordinates: Tal [-10, 5, -1] → MNI [-10, 8, -5]; Cluster size: 16636 voxels 4) Anterior segment of arcuate fasciculus R; Coordinates: Tal [50, -10, 29] → MNI [52, -11, 29]; Cluster size: 8780 voxels 5) Cingulum L; Coordinates: Tal [-4, -4, 27] → MNI [-5, -4, 28]; Cluster size: 42476 voxels 6) Cingulum R; Coordinates: Tal [20, -37, 5] → MNI [21, -37, 1]; Cluster size: 38840 voxels 7) Corpus Callosum R;

		Coordinates: Tal [17, -28, 17] → MNI [18, -29, 16]; Cluster size: 114544 voxels 8) Cortico-ponto-cerebellum tract L; Coordinates: Tal [-22, -24, 8] → MNI [-23, -24, 5]; Cluster size: 2176 voxels 9) Corticospinal tract L; Coordinates: Tal [-22, -28, 8] → MNI [-23, -28, 5]; Cluster size: 29175 voxels 10) Corticospinal tract R; Coordinates: Tal [17, 2, 5] → MNI [18, 5, 2]; Cluster size: 23730 voxels 11) Fornix R; Coordinates: Tal [17, -28, 17] → MNI [18, -29, 16]; Cluster size: 26318 voxels 12) Inferior fronto-occipital fasciculus L; Coordinates: Tal [-28, -1, 0] → MNI [-29, 1, -4]; Cluster size: 22154 voxels 13) Inferior fronto-occipital fasciculus R; Coordinates: Tal [18, 26, 5] → MNI [19, 29, 3]; Cluster size: 23185 voxels 14) Inferior longitudinal fasciculus L; Coordinates: Tal [-23, -7, -7] → MNI [-24, -5, -13]; Cluster size: 20131 voxels 15) Inferior longitudinal fasciculus R; Coordinates: Tal [40, -1, 0] → MNI [42, 1, -6]; Cluster size: 16338 voxels 16) Inferior cerebellar pedunculus L; Coordinates: Tal [-2, -51, -16] → MNI [-3, -51, -24]; Cluster size: 5648 voxels 17) Inferior cerebellar pedunculus R; Coordinates: Tal [11, -25, -31] → MNI [12, -23, -41]; Cluster size: 5302 voxels 18) Internal capsule R; Coordinates: Tal [10, -25, -31] → MNI [11, -23, -41]; Cluster size: 63671 voxels 19) Optic radiation L; Coordinates: Tal [-22, -24, 5] → MNI [-23, -23, 2]; Cluster size: 7923 voxels 20) Optic radiation R; Coordinates: Tal [40, -55, 1] → MNI [40, -55, -4]; Cluster size: 5982 voxels 21) Posterior segment of arcuate fasciculus L; Coordinates: Tal [-51, -42, -7] → MNI [-55, -41, -14]; Cluster size: 11088 voxels 22) Posterior segment of arcuate fasciculus R; Coordinates: Tal [56, -34, 11] → MNI [57, -34, 8]; Cluster size: 12107 voxels 23) Superior longitudinal fasciculus I L; Coordinates: Tal [-16, 35, 41] → MNI [-17, 34, 45]; Cluster size: 109025 voxels 24) Superior longitudinal fasciculus I R; Coordinates: Tal [22, 50, 14] → MNI [23, 52, 15]; Cluster size: 98037 voxels 25) Superior longitudinal fasciculus II L; Coordinates: Tal [-26, 50, 14] → MNI [-26, -52, 15]; Cluster size: 112229 voxels 26) Superior longitudinal fasciculus II R; Coordinates: Tal [25, 51, 14] → MNI [26, 53, 15]; Cluster size: 117581 voxels 27) Superior longitudinal fasciculus III L; Coordinates: Tal [-43, -46, 35] → MNI [-43, -48, 36]; Cluster size: 72219 voxels 28) Superior longitudinal fasciculus III R; Coordinates: Tal [50, -10, 29] → MNI [52, -11, 29]; Cluster size: 119900 voxels 29) Superior cerebellar pedunculus R; Coordinates: Tal [8, -25, -11] → MNI [9, -24, -18]; Cluster size: 8113 voxels

		30) Uncinate fasciculus L; Coordinates: Tal [-21, 23, 2] → MNI [-22, 26, 0]; Cluster size: 12282 voxels 31) Uncinate fasciculus R; Coordinates: Tal [17, 4, 1] → MNI [18, 7, -2]; Cluster size: 13022 voxels Decreased FA in SCZ vs. HC: 1) Arcuate fasciculus L; Coordinates: Tal [-34, -40, -1] → MNI [-36, -40, -7]; Cluster size: 24480 voxels 2) Arcuate fasciculus R; Coordinates: Tal [44, -38, -1] → MNI [46, -38, -8]; Cluster size: 23307 voxels 3) Anterior commissure L; Coordinates: Tal [-25, 8, -25] → MNI [-25, 13, -32]; Cluster size: 16636 voxels 4) Anterior segment of arcuate fasciculus L; Coordinates: Tal [-51, -7, 15] → MNI [-54, -6, 14]; Cluster size: 5391 voxels 5) Cingulum L; Coordinates: Tal [-19, -43, 39] → MNI [-19, -46, 42]; Cluster size: 42476 voxels 6) Cingulum R; Coordinates: Tal [18, 35, 32] → MNI [19, 35, 34]; Cluster size: 38840 voxels 7) Corpus Callosum R; Coordinates: Tal [17, 35, 35] → MNI [17, 34, 38]; Cluster size: 114544 voxels 8) Cortico-ponto cerebellum tract L; Coordinates: Tal [-16, -37, -32] → MNI [-17, -36, -42]; Cluster size: 2176 voxels 9) Cortico-ponto-cerebellum tract R; Coordinates: Tal [25, -17, 5] → MNI [26, -16, 2]; Cluster size: 766 voxels 10) Corticospinal tract L; Coordinates: Tal [-19, -1, 17] → MNI [-20, 0, 17]; Cluster size: 29175 voxels 11) Corticospinal tract R; Coordinates: Tal [29, -19, 5] → MNI [30, -18, 2]; Cluster size: 23730 voxels 12) Fornix L; Coordinates: Tal [-29, 10, -27] → MNI [-29, 16, -34]; Cluster size: 26318 voxels 13) Inferior fronto-occipital fasciculus L; Coordinates: Tal [-31, -22, -7] → MNI [-33, -21, -13]; Cluster size: 22154 voxels 14) Inferior fronto-occipital fasciculus R; Coordinates: Tal [41, -31, -7] → MNI [43, -30, -14]; Cluster size: 23185 voxels 15) Inferior longitudinal fasciculus L; Coordinates: Tal [-34, -40, -1] → MNI [-36, -40, -7]; Cluster size: 20131 voxels 16) Inferior longitudinal fasciculus R; Coordinates: Tal [41, -31, -7] → MNI [43, -30, -14]; Cluster size: 16338 voxels 17) Inferior cerebellar pedunculus L; Coordinates: Tal [-7, -33, -22] → MNI [-8, -32, -31]; Cluster size: 5648 voxels 18) Inferior cerebellar pedunculus R; Coordinates: Tal [14, -38, -31] → MNI [15, -37, -41]; Cluster size: 5302 voxels 19) Internal capsule L; Coordinates: Tal [-19, -1, 17] → MNI [-20, 0, 17]; Cluster size: 63671 voxels 20) Long segment of arcuate fasciculus L;

		Coordinates: Tal [-34, -40, -1] → MNI [-36, -40, -7]; Cluster size: 7639 voxels 21) Optic radiation L; Coordinates: Tal [-34, -40, -1] → MNI [-36, -40, -7]; Cluster size: 7923 voxels 22) Optic radiation R; Coordinates: Tal [29, -19, 5] → MNI [30, -18, 2]; Cluster size: 5982 voxels 23) Posterior segment of arcuate fasciculus L; Coordinates: Tal [-34, -40, -1] → MNI [-36, -40, -7]; Cluster size: 11088 voxels 24) Posterior segment of arcuate fasciculus R; Coordinates: Tal [41, -34, -4] → MNI [43, -33, -11], Cluster size: 12107 voxels 25) Superior longitudinal fasciculus I L; Coordinates: Tal [-19, -43, 39] → MNI [-19, -46, 42]; Cluster size: 109025 voxels 26) Superior longitudinal fasciculus I R; Coordinates: Tal [20, 35, 35] → MNI [20, 34, 38]; Cluster size: 98037 voxels 27) Superior longitudinal fasciculus II L; Coordinates: Tal [-20, -4, 53] → MNI [-20, -8, 58]; Cluster size: 112229 voxels 28) Superior longitudinal fasciculus II R; Coordinates: Tal [20, 35, 35] → MNI [20, 34, 38]; Cluster size: 117581 voxels 29) Superior longitudinal fasciculus III L; Coordinates: Tal [-49, -37, 14] → MNI [-52, -38, 12]; Cluster size: 72219 voxels 30) Superior longitudinal fasciculus III R; Coordinates: Tal [23, 27, 31] → MNI [24, 26, 32]; Cluster size: 119900 voxels 31) Superior cerebellar pedunculus L; Coordinates: Tal [-7, -31, -22] → MNI [-8, -30, -31]; Cluster size: 8012 voxels 32) Superior cerebellar pedunculus R; Coordinates: Tal [13, -24, -7] → MNI [14, -23, -13]; Cluster size: 8113 voxels 33) Uncinate fasciculus L; Coordinates: Tal [-25, 9, -21] → MNI [-25, 14, -28]; Cluster size: 12282 voxels 34) Uncinate fasciculus R; Coordinates: Tal [16, 27, 2] → MNI [17, 30, 0]; Cluster size: 13022 voxels <u>Meta-regression analysis:</u> *Effects of clinical variables on WM reduction in SCZ:* Negative correlation between age in SCZ and WM in: 1) Arcuate fasciculus L; Coordinates: Tal [-29, -27, 18] → MNI [-30, -28, 16]; Cluster size: 137 voxels 2) Corpus callosum (splenium) L; Coordinates: Tal [-14, -86, -1] → MNI [-14, -89, -7]; Cluster size: 29 voxels Positive correlation between age in SCZ and WM in: 1) Inferior longitudinal fasciculus L; Coordinates: Tal [-35, -62, 4] → MNI [-36, -63, 0]; Cluster size: 175 voxels 2) Corpus callosum (genu) R; Coordinates: Tal [12, 17, 11] → MNI [13, 19, 10]; Cluster size: 16 voxels Negative correlation between illness duration in SCZ and WM in: 1) Internal capsule L;

		Coordinates: Tal [-25, -30, 6] → MNI [-26, -30, 3]; Cluster size: 1313 voxels 2) Arcuate fasciculus R; Coordinates: Tal [47, -6, 31] → MNI [49, -7, 31]; Cluster size: 73 voxels Positive correlation between illness duration in SCZ and WM in: 1) Fornix R; Coordinates: Tal [6, -1, -2] → MNI [7, 1, -7]; Cluster size: 39 voxels 2) Corpus callosum (genu) L; Coordinates: Tal [-3, 15, 12] → MNI [-3, 17, 11]; Cluster size: 25 voxels Negative correlation between male percentage in SCZ and WM in: 1) Uncinate fasciculus L; Coordinates: Tal [-29, -1, -2] → MNI [-30, 2, -7]; Cluster size: 208 voxels 2) Superior longitudinal fasciculus III R; Coordinates: Tal [51, -6, 33] → MNI [53, -7, 33]; Cluster size: 69 voxels 3) Cingulum L; Coordinates: Tal [-18, -30, 3] → MNI [-19, -30, -1]; Cluster size: 44 voxels Positive correlation between male percentage in SCZ and WM in: 1) Corticospinal tract R; Coordinates: Tal [18, 6, 10] → MNI [19, 8, 8]; Cluster size: 525 voxels 2) Anterior commissure L; Coordinates: Tal [-7, 9, -1] → MNI [-7, 12, -5]; Cluster size: 52 voxels *Effects of clinical variables on FA reduction in SCZ:* Negative correlation between age in SCZ and FA in: 1) Corpus callosum (splenium) R; Coordinates: Tal [17, -49, 25] → MNI [17, -51, 25]; Cluster size: 2102 voxels 2) Corticospinal tract R; Coordinates: Tal [27, -35, 45] → MNI [26, -38, 49]; Cluster size: 76 voxels Positive correlation between age in SCZ and FA in: 1) Corticospinal tract L; Coordinates: Tal [-24, -17, 36] → MNI [-25, -19, 38]; Cluster size: 560 voxels 2) Cingulum R; Coordinates: Tal [10, 36, 9] → MNI [11, 39, 9]; Cluster size: 323 voxels 3) WM of superior temporal gyrus R (near superior longitudinal fasciculus III); Coordinates: Tal [44, -26, 2] → MNI [46, -25, -2]; Cluster size: 81 voxels 4) Superior longitudinal fasciculus III L; Coordinates: Tal [-31, 46, 3] → MNI [-32, 49, 3]; Cluster size: 11 voxels Negative correlation between illness duration in SCZ and FA in: 1) Uncinate fasciculus R; Coordinates: Tal [27, 6, 5] → MNI [28, 9, 1]; Cluster size: 394 voxels 2) Uncinate fasciculus L; Coordinates: Tal [-27, -1, 3] → MNI [-28, 1, 0]; Cluster size: 120 voxels 3) Inferior longitudinal fasciculus L; Coordinates: Tal [-42, -27, -10] → MNI [-45, -26, -16]; Cluster size: 100 voxels 4) Inferior fronto-occipital fasciculus R; Coordinates: Tal [40, -35, -6] → MNI [42, -34, -13]; Cluster size: 91 voxels

		5) Cingulum (posterior) R; Coordinates: Tal [4, 0, 34] → MNI [4, -1, 36]; Cluster size: 11 voxels Positive correlation between illness duration in SCZ and FA in: 1) Cingulum (anterior) R; Coordinates: Tal [7, 36, 5] → MNI [8, 39, 5]; Cluster size: 167 voxels 2) WM of median cingulate gyrus R (near superior longitudinal fasciculus I); Coordinates: Tal [8, 15, 39] → MNI [8, 14, 42]; Cluster size: 19 voxels 3) Superior longitudinal fasciculus III L; Coordinates: Tal [-31, 46, 3] → MNI [-32, 49, 3]; Cluster size: 19 voxels Negative correlation between male percentage of SCZ in SCZ and FA in: 1) Superior longitudinal fasciculus II R; Coordinates: Tal [32, 3, 37] → MNI [32, 2, 39]; Cluster size: 154 voxels 2) WM of inferior temporal gyrus L (near posterior segment of arcuate fasciculus); Coordinates: Tal [-44, -51, -8] → MNI [-47, -50, -15]; Cluster size: 112 voxels 3) Superior longitudinal fasciculus III L; Coordinates: Tal [-52, -6, 15] → MNI [-55, -5, 14]; Cluster size: 112 voxels 4) Superior longitudinal fasciculus III R; Coordinates: Tal [44, 25, 19] → MNI [46, 26, 18]; Cluster size: 78 voxels 5) WM of superior temporal gyrus R (above inferior longitudinal fasciculus); Coordinates: Tal [48, 1, -5] → MNI [51, 5, -12]; Cluster size: 48 voxels 6) Superior longitudinal fasciculus III L; Coordinates: Tal [-48, -34, 17] → MNI [-50, -35, 15]; Cluster size: 26 voxels 7) Posterior segment of arcuate fasciculus R; Coordinates: Tal [42, -59, 16] → MNI [42, -61, 14]; Cluster size: 23 voxels 8) Corpus callosum (body) L; Coordinates: Tal [-12, -9, 25] → MNI [-13, -9, 26]; Cluster size: 10 voxels Positive correlation between male percentage in SCZ and FA in: 1) Corpus callosum (genu) R; Coordinates: Tal [18, 28, 15] → MNI [19, 30, 15]; Cluster size: 1915 voxels 2) Inferior fronto-occipital fasciculus R; Coordinates: Tal [36, -35, -4] → MNI [38, -34, -11]; Cluster size: 785 voxels 3) Superior longitudinal fasciculus III R; Coordinates: Tal [28, -35, 45] → MNI [27, -38, 49]; Cluster size: 181 voxels 4) Superior cerebellar pedunculus L; Coordinates: Tal [-5, -30, -20] → MNI [-6, -29, -29]; Cluster size: 128 voxels 5) Optic radiation L; Coordinates: Tal [-27, -19, -7] → MNI [-28, -18, -13]; Cluster size: 119 voxels 6) Long segment of arcuate fasciculus L; Coordinates: Tal [-33, -22, 30] → MNI [-34, -23, 31]; Cluster size: 110 voxels
Vucurovic et al. (2020)	Decreased TBA in middle temporal gyrus/temporoparietal junction in SCZ during cognitive processing of theory of mind (i.e., intention/belief attribution)	Decreased TBA in SCZ vs. HC during cognitive processing of theory of mind: 1) Middle temporal gyrus L (BA 39); Coordinates: Tal [-47, -69, 13] → MNI [-48, -70, 10]; Cluster size: 1408 mm^3 Decreased TBA in SCZ vs. HC during emotion processing (empathy):

	Decreased TBA in inferior frontal gyrus/ventrolateral prefrontal cortex during emotion processing (empathy, i.e., emotional attribution)	1) Inferior frontal gyrus R (BA 45); Coordinates: Tal [47, 25, 9] → MNI [49, 27, 5]; Cluster size: 664 mm^3
Wang et al. (2021)	Decreased TBA in dorsolateral/dorsomedial prefrontal cortex, precuneus, basal ganglia, and cerebellum, as well as increased TBA in anterior cingulate cortex, posterior cingulate cortex, and middle temporal gyrus, along with precentral gyrus and occipital cortex, in SCZ during cognitive processing of working memory Correlation of symptomatology in SCZ with decreased TBA in dorsolateral prefrontal cortex, as well as increased TBA in posterior cingulate cortex, during cognitive processing of working memory	Decreased TBA in SCZ vs. HC during cognitive processing of working memory: 1) Cerebellum R; Coordinates: MNI [8, -64 -36]; Cluster size: 3382 voxels; #(38/38)/† 2) Supplementary motor area R (BA 8); Coordinates: MNI [6, 24, 50]; Cluster size: 880 voxels; #(37/38)/† 3) Middle frontal gyrus L (BA 6); Coordinates: MNI [-38, 8, 52]; Cluster size: 587 voxels; #(38/38)/† 4) Striatum R; Coordinates: MNI [26, 12, 6]; Cluster size: 579 voxels; #(37/38)/† 5) Caudate nucleus R; Coordinates: MNI [12, 4, 10]; Cluster size: 211 voxels; #(38/38)/† 6) Precuneus L (BA 7); Coordinates: MNI [-6, -70, 50]; Cluster size: 171 voxels; #(38/38)/† Increased TBA in SCZ vs. HC during cognitive processing of working memory: 1) Anterior cingulate/Paracingulate gyri L (BA 10); Coordinates: MNI [-4, 48, 6] Cluster size: 3899 voxels; #(38/38)/† 2) Posterior cingulate gyrus L; Coordinates: MNI [0, -42, 22]; Cluster size: 620 voxels; #(38/38)/† 3) Precentral gyrus R (BA 6); Coordinates: MNI [20, -26, 66)]; Cluster size: 329 voxels; #(38/38)/† 4) Temporal pole/Middle temporal gyrus R (BA 36); Coordinates: MNI [24, 12, -42]; Cluster size: 259 voxels; #(38/38)/† 5) Temporal pole/Middle temporal gyrus L (BA 36); Coordinates: MNI [-28, 8, -38]; Cluster size: 105 voxels; #(38/38)/† 6) Superior occipital gyrus R (BA 18); Coordinates: MNI [22, -96, 18]; Cluster size: 57 voxels; #(38/38)/† <u>Subgroup meta-analysis:</u> *Studies on TBA during cognitive processing of working memory in stable SCZ:* Decreased TBA in stable SCZ vs. HC: 1) Cerebellum R; Coordinates: MNI [12, -64, -36]; Cluster size: 1795 voxels 2) Superior frontal gyrus (medial) R (BA 8); Coordinates: MNI [10, 24, 50]; Cluster size: 512 voxels 3) Striatum R; Coordinates: MNI [24, 4, 8]; Cluster size: 32 voxels Increased TBA in stable SCZ vs. HC: 1) Undefined (BA 36);

		Coordinates: MNI [24, 8, -48]; Cluster size: 790 voxels 2) Temporal pole/Middle temporal gyrus L (BA 36); Coordinates: MNI [-26, 4, -38]; Cluster size: 196 voxels *Studies on TBA during cognitive processing of verbal working memory in SCZ:* Decreased TBA in SCZ vs. HC: 1) Cerebellum R; Coordinates: MNI [2, -72, -28]; Cluster size: 3285 voxels 2) Caudate nucleus R; Coordinates: MNI [12, 6, 16]; Cluster size: 1320 voxels 3) Fronto-insular tract R; Coordinates: MNI [28, 14, 6]; Cluster size: 827 voxels 4) Superior frontal gyrus (medial) R (BA 8); Coordinates: MNI [8, 28, 44]; Cluster size: 725 voxels 5) Precentral gyrus L (BA 6); Coordinates: MNI [-42, 6, 42]; Cluster size: 639 voxels 6) Striatum L; Coordinates: MNI [-18, 6, 0]; Cluster size: 19 voxels Increased TBA in SCZ vs. HC: 1) Corpus callosum R; Coordinates: MNI [6, 38, -20]; Cluster size: 4256 voxels 2) Posterior cingulate gyrus L; Coordinates: MNI [-2, -42, 22]; Cluster size: 1072 voxels 3) Supplementary motor area R (BA 4); Coordinates: MNI [4, -24, 58]; Cluster size: 418 voxels 4) Temporal pole/Middle temporal gyrus R (BA 36); Coordinates: MNI [22, 12. -42]; Cluster size: 292 voxels 5) Temporal pole/Middle temporal gyrus L (BA 36); Coordinates: MNI [-28, 8, -38]; Cluster size: 224 voxels 6) Superior occipital gyrus R (BA 18); Coordinates: MNI [18, -96, 26]; Cluster size: 65 voxels <u>Meta-regression analysis:</u> *Effects of clinical variables on TBA in SCZ during cognitive processing of working memory:* Positive correlation between symptoms (PANSS total score) and TBA in: 1) Posterior cingulate gyrus L; Coordinates: MNI [0, -42, 22]; Cluster size: 45 voxels Negative correlation between symptoms (PANSS total score) and TBA in: 1) Middle frontal gyrus L; Coordinates: MNI [-38, 8, 54]; Cluster size: 39 voxels
Weng et al. (2022)	Decreased TBA in medial prefrontal cortex in SCZ during cognitive processing of theory of mind	Decreased TBA in SCZ vs. HC during cognitive processing of theory of mind: 1) Superior frontal gyrus (medial) L (BA 10); Coordinates: MNI [-4, 62, 20]; Cluster size: 459 voxels

		2) Cuneus L (BA 18); Coordinates: MNI [0, -72, 22]; Cluster size: 209 voxels 3) Precentral gyrus R (BA 4); Coordinates: MNI [48, -10, 40]; Cluster size: 13 voxels Increased TBA in SCZ vs. HC during cognitive processing of theory of mind: 1) Superior longitudinal fasciculus L; Coordinates: MNI [-44, -46, 38]; Cluster size: 20 voxels
Wu et al. (2019)	Decreased TBA in dorsolateral prefrontal cortex and insula, as well as increased TBA in anterior cingulate cortex, posterior cingulate cortex, and temporoparietal junction, in SCZ during cognitive processing of working memory	Decreased TBA in SCZ vs. HC during cognitive processing of working memory: 1) Middle frontal gyrus R (BA 9); Coordinates: Tal [44, 14, 32] → MNI [45, 13, 32]; Cluster size: 2368 mm^3 2) Inferior frontal gyrus L (BA 9); Coordinates: Tal [-46, 10, 22] → MNI [-48, 11, 22]; Cluster size: 1560 mm^3 3) Inferior frontal gyrus R (BA 47); Coordinates: Tal [30, 20, -4] → MNI [32, 24, -9]; Cluster size: 1008 mm^3 4) Claustrum L; Coordinates: Tal [-30, 18, -2] → MNI [-31, 22, -6]; Cluster size: 768 mm^3 Increased TBA in SCZ vs. HC during cognitive processing of working memory: 1) Inferior parietal lobule L (BA 40); Coordinates: Tal [-52, -54, 40] → MNI [-52, -57, 42]; Cluster size: 1408 mm^3 2) Superior frontal gyrus L (BA 6); Coordinates: Tal [-6, 10, 50] → MNI [-7, 7, 55]; Cluster size: 1056 mm^3 3) Anterior cingulate gyrus L (BA 32); Coordinates: Tal [0, 38, -2] → MNI [0, 42, -3]; Cluster size: 784 mm^3 4) Posterior cingulate gyrus L (BA 31); Coordinates: Tal [-8, -32, 32] → MNI [-9, -34, 34]; Cluster size: 544 mm^3
Yao et al. (2013)	Decreased FA in frontal and temporal WM, involving fornix, cingulum, inferior fronto-occipital fasciculus, inferior longitudinal fasciculus, uncinate fasciculus, and corpus callosum, in first-episode SCZ	Decreased FA in first-episode SCZ vs. HC: 1) Frontal WM R (anterior cingulum, genu of corpus callosum, uncinate fasciculus); Coordinates: Tal [12, 36, 12] → MNI [13, 38, 13]; Cluster size: 328 mm^3 2) Temporal WM L (fornix, inferior longitudinal fasciculus, inferior fronto-occipital fasciculus, splenium of corpus callosum); Coordinates: Tal [-40, -16, -16] →MNI [-42, -14, -23]; Cluster size: 296 mm^3
Zeng et al. (2022)	Decreased TBA in striatum (extending to insula), anterior cingulate cortex, superior temporal gyrus, and precentral gyrus in SCZ during emotion processing of positive stimuli (reward anticipation) Decreased TBA in medial prefrontal cortex and dorsolateral prefrontal cortex, as well as increased TBA in striatum	Decreased TBA in SCZ vs. HC during emotion processing of positive stimuli (reward anticipation): 1) Striatum R/L; Coordinates: MNI [-8, 4, 6]; Cluster size: 2956 voxels; #(16/17) 2) Anterior cingulate cortex/Median cingulate cortex R/L; Coordinates: MNI [0, 12, 24]; Cluster size: 1931 voxels; #(16/17) 3) Precentral gyrus R; Coordinates: MNI [50, 4, 36]; Cluster size: 244 voxels; #(15/17) 4) Superior temporal gyrus R; Coordinates: MNI [62, 0, -4]; Cluster size: 30 voxels; #(15/17)

	(extending to insula), parahippocampal gyrus, postcentral gyrus, middle cingulate cortex, and cerebellum, in SCZ during emotion processing of positive stimuli (reward outcome) Correlation of negative symptomatology in SCZ with decreased TBA in ventral striatum during emotion processing of positive stimuli	Decreased TBA in SCZ vs. HC during emotion processing of positive stimuli (reward outcome): 1) Medial prefrontal cortex L; Coordinates: MNI [-10, 52, 6]; Cluster size: 817 voxels; #(9/10) 2) Dorsolateral prefrontal cortex L; Coordinates: MNI [-24, 56, 20]; Cluster size: 422 voxels; #(9/10) 3) Dorsolateral prefrontal cortex R; Coordinates: MNI [22, 20, 62]; Cluster size: 143 voxels; #(9/10) Increased TBA in SCZ vs. HC during emotion processing of positive stimuli (reward outcome): 1) Striatum R; Coordinates: MNI [28, 10, -14]; Cluster size: 590 voxels; #(9/10) 2) Striatum L; Coordinates: MNI [-22, 0, 2]; Cluster size: 439 voxels; #(10/10) 3) Cerebellum L; Coordinates: MNI [-8, -36, -18]; Cluster size: 194 voxels; #(9/10) 4) Parahippocampal gyrus R; Coordinates: MNI [30, -4, -26]; Cluster size: 176 voxels; #(10/10) 5) Postcentral gyrus R; Coordinates: MNI [52, -18, 56]; Cluster size: 31 voxels; #(10/10) 6) Middle cingulate cortex R; Coordinates: MNI [8, 34, 30]; Cluster size: 20 voxel; #(9/10) <u>Meta-regression analysis:</u> *Effects of clinical variables on TBA in SCZ during emotion processing of reward anticipation:* Negative correlation between negative symptoms (PANSS negative score) and TBA in: 1) Ventral striatum R; Coordinates: MNI [16, 14, -6] Positive correlation between percentage of medicated SCZ (2° generation antipsychotics) and TBA in: 1) Ventral striatum R; Coordinates: MNI [16, 2, 0] *Effects of clinical variables on TBA in SCZ during emotion processing of reward outcome:* Negative correlation between positive symptoms (PANSS positive score) and TBA in: 1) Medial prefrontal cortex L; Coordinates: MNI [0, 46, -10] Positive correlation between percentage of medicated SCZ (2° generation antipsychotics) and TBA in: 1) Medial prefrontal cortex L; Coordinates: MNI [0, 46, -10]
Zhang et al. (2016)	Decreased TBA in anterior cingulate cortex, midbrain, striatum, and thalamus during emotion processing of positive stimuli (consummatory and anticipatory	Decreased TBA in SCZ vs. HC during emotion processing of positive stimuli (consummatory reward): 1) Midbrain (red nucleus) R; Coordinates: Tal [4, -22, -6] → MNI [5, -21, -12]; Cluster size: 696 mm^3 2) Putamen L;

	reward) in SCZ	Coordinates: Tal [-22, 10, 12] → MNI [-23, 12, 11]; Cluster size: 592 mm^3 3) Thalamus (pulvinar) L; Coordinates: Tal [-12, -24, 4] → MNI [-13, -24, 1]; Cluster size: 520 mm^3 4) Caudate head L; Coordinates: Tal [-6, 8, 2] → MNI [-6, 11, 0]; Cluster size: 400 mm^3 Decreased TBA in SCZ vs. HC during emotion processing of positive stimuli (anticipatory reward): 1) Putamen L; Coordinates: Tal [-14, 8, -2] → MNI [-14, 11, -6]; Cluster size: 2408 mm^3 2) Caudate head R; Coordinates: Tal [10, 10, -4] → MNI [10, 13, -8]; Cluster size: 1048 mm^3 3) Anterior cingulate cortex L (BA 32); Coordinates: Tal [0, 46, 8] → MNI [0, 50, 10]; Cluster size: 640 mm^3 Decreased TBA in SCZ vs. HC during emotion processing: 1) Thalamus (ventral lateral nucleus) R; Coordinates: Tal [16, -16, 18] → MNI [17, -16, 17]; Cluster size: 448 mm^3
Zhao et al. (2021)	Decreased FA and WM in corpus callosum, anterior/posterior corona radiata, external capsule, and uncinate fasciculus in SCZ Correlation of positive symptomatology in SCZ with altered FA/WM in corpus callosum, along with altered FA in inferior longitudinal fasciculus and superior longitudinal fasciculus; Correlation of negative symptomatology in SCZ with altered FA/WM in corpus callosum and insular area, along with altered FA in inferior longitudinal fasciculus, superior longitudinal fasciculus, and uncinate fasciculus	Decreased FA in SCZ vs. HC: 1) Corpus callosum/Anterior corona radiata L; Coordinates: MNI [-18, 34, 2]; Cluster size: 10828 voxels; #(48/48)/† 2) Posterior thalamic radiation (inferior longitudinal fasciculus) R; Coordinates: MNI [30, -62, 4]; Cluster size: 47 voxels: #(44/48)/† Decreased WM in SCZ vs. HC: 1) Corpus callosum (body)/Posterior corona radiata R/L; Coordinates: MNI [-10, -24, 24]; Cluster size: 4221 voxels; #(24/24)/† 2) External capsule/Uncinate fasciculus L; Coordinates: MNI [-26, 4, -10]; Cluster size: 54 voxels; #(20/24)/† 3) External capsule/Uncinate fasciculus (inferior fronto-occipital fasciculus) R; Coordinates: MNI [28, 0, -10]; Cluster size: 25 voxels; #(20/24)/† <u>Subgroup meta-analysis:</u> *Studies on combined FA and WM in SCZ:* Decreased FA and WM in SCZ vs. HC: 1) Corpus callosum (genu/body)/Anterior corona radiata L/R; Coordinates: MNI [-10, -10, 30]; Cluster size: 6632 voxels 2) Anterior limb of internal capsule R; Coordinates: MNI [10, -2, -6]; Cluster size: 83 voxels *Studies on FA an/or WM in SCZ matched for age and sex with HC:* Decreased FA in SCZ vs. HC: 1) Corpus callosum (genu/body/splenium)/Anterior corona radiata L; Coordinates: MNI [-18, 26, 16]; Cluster size: 7615 voxels

		2) Superior corona radiata R; Coordinates: MNI [26, -12, 38]; Cluster size: 27 voxels Decreased WM in SCZ vs. HC: 1) Corpus callosum (body)/Retrolenticular part of internal capsule/Posterior thalamic radiation L; Coordinates: MNI [-4, -22, 2]; Cluster size: 683 voxels 2) Corpus callosum (genu/body) R; Coordinates: MNI [10, 20, 16]; Cluster size: 184 voxels 3) External capsule L; Coordinates: MNI [-30, -2, -8]; Cluster size: 11 voxels Decreased FA and WM in SCZ vs. HC: 1) Corpus callosum (genu/body)/Anterior corona radiata L/R; Coordinates: MNI [-14, -26, 22]; Cluster size: 4420 voxels 2) Corpus callosum (genu)/Anterior corona radiata R; Coordinates: MNI [12, 22, -10]; Cluster size: 61 voxels *Studies on FA and/or WM in chronic SCZ:* Decreased FA in chronic SCZ vs. HC: 1) Corpus callosum (genu/body)/Anterior corona radiata L/R; Coordinates: MNI [-18, 32, 2]; Cluster size: 7831 voxels 2) Posterior thalamic radiation R; Coordinates: MNI [30, -60, 6]; Cluster size: 127 voxels 3) Fornix R; Coordinates: MNI [2, 0, 6]; Cluster size: 30 voxels Decreased WM in chronic SCZ vs. HC: 1) External capsule/Corpus callosum (genu) L; Coordinates: MNI [-24, 2, -8]; Cluster size: 156 voxels 2) Anterior limb of internal capsule R; Coordinates: MNI [14, 16, -10]; Cluster size: 145 voxels 3) External capsule/Uncinate fasciculus R; Coordinates: MNI [28, 0, -8]; Cluster size: 56 voxels Decreased FA and WM in chronic SCZ vs. HC: 1) Corpus callosum (genu)/Internal capsule/Anterior corona radiata/External capsule R; Coordinates: MNI [8, 24, -8]; Cluster size: 156 voxels <u>Meta-regression analysis:</u> *Effects of clinical variables on FA reduction in SCZ:* Negative correlation between age of illness onset in SCZ and FA in: 1) Corpus callosum R; Coordinates: MNI [2, 26, 12]; Cluster size: 1577 voxels 2) Corpus callosum L; Coordinates: MNI [-12, -24, 30]; Cluster size: 260 voxels Positive correlation between illness duration in SCZ and FA in: 1) Corticospinal tract R; Coordinates: MNI [18, -4, 8]; Cluster size: 78 voxels

		2) Corpus callosum L; Coordinates: MNI [-20, -28, 36]; Cluster size: 31 voxels Negative correlation between illness duration in SCZ and FA in: 1) WM near striatum L; Coordinates: MNI [-28, 26, 16]; Cluster size: 41 voxels 2) Corpus callosum L; Coordinates: MNI [-22, -4, 36]; Cluster size: 15 voxels Positive correlation between percentage of medicated SCZ and FA in: 1) Corpus callosum L; Coordinates: MNI [-2, 20, 18]; Cluster size: 33 voxels Negative correlation between percentage of medicated SCZ and FA in: 1) Corpus callosum L; Coordinates: MNI [-28, -62, 16]; Cluster size: 180 voxels 2) Corpus callosum R; Coordinates: MNI [20, -28, 32]; Cluster size: 125 voxels 3) Corpus callosum R/L; Coordinates: MNI [0, 0, 8]; Cluster size: 125 voxels Positive correlation between positive symptoms (PANSS positive score) and FA in: 1) Corpus callosum L; Coordinates: MNI [-30, 26, 18]; Cluster size: 101 voxels 2) Superior longitudinal fasciculus II R; Coordinates: MNI [32, -48, 32]; Cluster size: 12 voxels Negative correlation between positive symptoms (PANSS positive score) and FA in: 1) Inferior longitudinal fasciculus L; Coordinates: MNI [-44, -16, -22]; Cluster size: 20 voxels 2) Corpus callosum L; Coordinates: MNI [-6, -10, 24]; Cluster size: 14 voxels Positive correlation between negative symptoms (PANSS negative score) and FA in: 1) Corpus callosum L; Coordinates: MNI [-30, 28, 18]; Cluster size: 109 voxels 2) Superior longitudinal fasciculus II R; Coordinates: MNI [32, -46, 30]; Cluster size: 43 voxels 3) Fronto-insular tract R; Coordinates: MNI [32, -16, 6]; Cluster size: 24 voxels Negative correlation between negative symptoms (PANSS negative score) and FA in: 1) Inferior longitudinal fasciculus R; Coordinates: MNI [44, -36, -14]; Cluster size: 56 voxels 2) Uncinate fasciculus L; Coordinates: MNI [-20, 18, -12]; Cluster size: 22 voxels *Effects of clinical variables on WM reduction in SCZ:* Positive correlation between age of illness onset in SCZ and WM in: 1) Cingulum L; Coordinates: MNI [-8, 14, 24]; Cluster size: 204 voxels Negative correlation between age of illness onset in SCZ and WM in:

		1) Inferior longitudinal fasciculus R; Coordinates: MNI [48, -34, -10]; Cluster size: 13 voxels Positive correlation between illness duration in SCZ and WM in: 1) Corpus callosum L; Coordinates: MNI [-30, -38, 2]; Cluster size: 111 voxels Negative correlation between illness duration in SCZ and WM in: 1) Superior longitudinal fasciculus II R; Coordinates: MNI [32, -26, 40]; Cluster size: 91 voxels Positive correlation between percentage of medicated SCZ and WM in: 1) Anterior thalamic radiation L; Coordinates: MNI [-22, -24, 12]; Cluster size: 723 voxels Negative correlation between percentage of medicated SCZ and WM in: 1) Precentral gyrus L; Coordinates: MNI [-28, -18, 60]; Cluster size: 27 voxels Positive correlation between positive symptoms (PANSS positive score) and WM in: 1) Corpus callosum R; Coordinates: MNI [20, 50, 18]; Cluster size: 105 voxels Negative correlation between positive symptoms (PANSS positive score) and WM in: 1) Corpus callosum L; Coordinates: MNI [-22, -26, 10]; Cluster size: 573 voxels Positive correlation between negative symptoms (PANSS negative score) and WM in: 1) Corpus callosum R; Coordinates: MNI [16, -24, 62]; Cluster size: 94 voxels 2) Corpus callosum L; Coordinates: MNI [-20, -18, 60]; Cluster size: 11 voxels Negative correlation between negative symptoms (PANSS negative score) and WM in: 1) WM near insula R; Coordinates: MNI [34, -16, 12]; Cluster size: 134 voxels
STRUCTURAL-FUNCTIONAL BRAIN CORRELATES OF SYMPTOMS OF SCHIZOPHRENIA		
Study	**Main Results**	**Specific Results**
Jardri et al. (2011)	Activation in superior/middle temporal gyrus, insula, precentral gyrus, inferior frontal cortex, inferior parietal lobule, and hippocampus/parahippocampal area in SCZ during experience of auditory verbal hallucinations	Activation in SCZ during auditory (verbal) hallucinatory experience: 1) Broca's convolution L (BA 44); Coordinates: Tal [-48, 10, 7] → MNI [-50, 13, 5]; Cluster size: 1312 mm^3 2) Anterior insula L (BA 13); Coordinates: Tal [-42, 0, 6] → MNI [-44, 2, 3]; Cluster size: 1240 mm^3 3) Precentral gyrus L (BA 6); Coordinates: Tal [-54, 0, 14] → MNI [-57, 2, 13]; Cluster size: 488 mm^3 4) Hippocampus/Parahippocampal gyrus L (BA 27); Coordinates: Tal [-24, -32, -4] → MNI [-26, -31, -10]; Cluster size: 1664 mm^3 5) Anterior insula R (BA 13); Coordinates: Tal [44, 6, -4] → MNI [47, 10, -10]; Cluster size: 964 mm^3 6) Frontal operculum R (BA 47);

		Coordinates: Tal [42, 12, -10] → MNI [44, 17, -17]; Cluster size: 265 mm^3 7) Superior temporal gyrus/Middle temporal gyrus L (BA 21, 22); Coordinates: Tal [-54, -44, 16] → MNI [-56, -45, 14]; Cluster size: 800 mm^3 8) Supramarginal gyrus L (BA 40); Coordinates: Tal [-52, -20, 15] → MNI [-55, -20, 14]; Cluster size: 304 mm^3
Kompus et al. (2011)§	*Decreased TBA in superior temporal gyrus, anterior cingulate cortex, superior frontal gyrus, hippocampus, and thalamus in SCZ during auditory perception* Activation in superior temporal gyrus, insula, postcentral gyrus, middle temporal gyrus, inferior parietal lobule, inferior frontal gyrus, superior frontal gyrus, hippocampus, and cerebellum in SCZ during auditory verbal hallucinations Decreased TBA during auditory perception and activation during auditory verbal hallucinations in superior temporal gyrus/primary auditory cortex (left-side) in SCZ	*Decreased TBA in SCZ vs. HC during auditory perception:* *1) Superior temporal gyrus L (BA 22, 41);* *Coordinates: Tal [-54, -8, 0] → MNI [-57, -6, -4]; Cluster size: 1824 mm^3* *2) Anterior cingulate cortex L (BA 24);* *Coordinates: Tal [-10, 0, 40] → MNI [-11, -2, 43]; Cluster size: 520 mm^3* *3) Thalamus R;* *Coordinates: Tal [12, -22, 18] → MNI [12, -22, 16]; Cluster size: 520 mm^3* *4) Superior frontal gyrus R (BA 10);* *Coordinates: Tal [24, 50, 14] → MNI [25, 52, 15]; Cluster size: 456 mm^3* *5) Retrosplenial cortex/Hippocampus L;* *Coordinates: Tal [-12, -38, 10] → MNI [-13, -39, 7]; Cluster size: 200 mm^3* Activation in SCZ during auditory (verbal) hallucinatory experience: 1) Insula L (BA 13); Coordinates: Tal [-44, -2, 6] → MNI [-46, 0, 3]; Cluster size: 2656 mm^3 2) Hippocampus L; Coordinates: Tal [-24, -32, -4] → MNI [-26, -31, -10]; Cluster size: 1064 mm^3 3) Postcentral gyrus L (BA 2); Coordinates: Tal [-50, -24, 40] → MNI [-51, -26, 43]; Cluster size: 1016 mm^3 4) Inferior parietal lobule R (BA 40); Coordinates: Tal [32, -40, 48] → MNI [31, -44, 53]; Cluster size: 960 mm^3 5) Superior temporal gyrus L (BA 42); Coordinates: Tal [-52, -22, 16] → MNI [-55, -22, 15]; Cluster size: 952 mm^3 6) Inferior frontal gyrus R (BA 44); Coordinates: Tal [40, 12, 16] → MNI [42, 14, 13]; Cluster size: 408 mm^3 7) Middle temporal gyrus R (BA 21); Coordinates: Tal [54, -32, -4] → MNI [57, -31, -11]; Cluster size: 368 mm^3 8) Cerebellum R; Coordinates: Tal [20, -46, -16] → MNI [21, -45, -24]; Cluster size: 248 mm^3 9) Superior frontal gyrus R (BA 10); Coordinates: Tal [26, 42, 26] → MNI [27, 42, 28]; Cluster size: 240 mm^3 10) Middle temporal gyrus R (BA 22); Coordinates: Tal [58, -44, 14] → MNI [59, -45, 11]; Cluster size: 200 mm^3 <u>Subgroup meta-analysis:</u> *Studies on combination between auditory perception and auditory hallucinations in SCZ:* Decreased TBA during auditory perception and activation during auditory (verbal) hallucinatory experience in SCZ:

		1) Superior temporal gyrus L; Coordinates: Tal [-52, -22, 13] → MNI [-55, -22, 11]; Cluster size: 184 mm^3
Kuhn and Gallinat (2012)	Activation in parietal operculum, postcentral gyrus, and inferior frontal gyrus in SCZ during auditory verbal hallucinations *Decreased TBA in superior temporal gyrus, middle temporal gyrus, anterior cingulate cortex, and premotor cortex in SCZ during auditory perception (and imagery)*	Activation in SCZ during auditory (verbal) hallucinatory experience: 1) Parietal operculum L (BA 43, 40); Coordinates: Tal [-55, -19, 16] → MNI [-58, -19, 15]; Cluster size: 334 mm^3 2) Postcentral gyrus L (BA 3); Coordinates: Tal [-49, -17, 41] → MNI [-50, -19, 44]; Cluster size: 256 mm^3 3) Postcentral gyrus R (BA 3); Coordinates: Tal [36, -32, 50] → MNI [35, -36, 55]; Cluster size: 216 mm^3 4) Inferior frontal gyrus L (BA 44); Coordinates: Tal [-48, 2, 6] → MNI [-51, 5, 3]; Cluster size: 208 mm^3 *Decreased TBA in SCZ with hallucinations vs. SCZ without hallucinations and HC during auditory perception (and imagery):* *1) Middle temporal gyrus L (BA 21);* *Coordinates: Tal [-56, -30, 0] → MNI [-60, -29, -5]; Cluster size: 424* mm^3 *2) Premotor cortex L (BA 6);* *Coordinates: Tal [-10, 3, 56] → MNI [-11, -1, 62]; Cluster size: 376* mm^3 *3) Anterior cingulate gyrus L (BA 32);* *Coordinates: Tal [-4, 26, 31] → MNI [-5, 26, 33]; Cluster size: 160* mm^3 *4) Superior temporal gyrus L (BA 22);* *Coordinates: Tal [-44, -22, 0] → MNI [-47, -21, -5]; Cluster size: 152* mm^3 *5) Anterior cingulate gyrus L (BA 32);* *Coordinates: Tal [-42, 2, 18] → MNI [-44, 4, 17]; Cluster size: 152* mm^3 *6) Anterior cingulate gyrus L (BA 24);* *Coordinates: Tal [-9, 4, 37] → MNI [-10, 3, 40]; Cluster size: 112* mm^3
Palaniyappan et al. (2012)	Correlation of auditory hallucinations in SCZ with decreased GM in insula/superior temporal gyrus	Negative correlation between auditory hallucinations (severity) in SCZ and GM in: 1) Insula L (extending to superior temporal gyrus and inferior frontal gyrus L); Coordinates: Tal [-42, -4, 2] → MNI [-44, -2, -1]; Cluster size: 717 voxels; #(7/7) 2) Superior temporal gyrus R (extending to insula R); Coordinates: Tal [58, -6, 10] → MNI [62, -5, 7]; Cluster size: 318 voxels; #(6/7)
Wensing et al. (2017)	Correlation of formal thought deficits in SCZ with altered TBA in superior/middle temporal gyrus during verbal processing	Correlation between formal thought deficits (disorganized speech severity) in SCZ and altered TBA during verbal processing in: 1) Superior temporal gyrus L; Coordinates: MNI [-54, -32, 9]; Cluster size: 114 voxels 2) Middle temporal gyrus L; Coordinates: MNI [-46, -54, 3]; Cluster size: 72 voxels
Zhao et al. (2014)	Correlation of motor deficits in first-episode SCZ with decreased GM in precentral gyrus, postcentral gyrus, inferior frontal gyrus, inferior parietal	Negative correlation between motor deficits (severity) in first-episode SCZ and GM in: 1) Precentral gyrus L (BA 6); Coordinates: Tal [-56, -6, 40] → MNI [-57, -8, 43]; Cluster size: 424 mm^3 2) Thalamus R;

	lobule, and thalamus (along with decreased WM in temporal lobe)	Coordinates: Tal [2, -12, 14] → MNI [2, -12, 13]; Cluster size: 308 mm^3 3) Precentral gyrus L (BA 4); Coordinates: Tal [-46, -8, 50] → MNI [-46, -11, 54]; Cluster size: 296 mm^3 4) Inferior frontal gyrus L (BA 45); Coordinates: Tal [-54, 20, 20] → MNI [-56, 21, 20]; Cluster size: 280 mm^3 5) Precentral gyrus R (BA 6); Coordinates: Tal [56, -4, 40] → MNI [57, -6, 42]; Cluster size: 280 mm^3 6) Postcentral gyrus L (BA 2); Coordinates: Tal [-48, -26, 52] → MNI [-48, -29, 57]; Cluster size: 224 mm^3 7) Inferior parietal lobule L (BA 40); Coordinates: Tal [-50, -40, 44] → MNI [-50, -43, 47]; Cluster size: 184 mm^3 Negative correlation between motor deficits (severity) in first-episode SCZ and WM in: 1) WM near middle temporal gyrus R; Coordinates: Tal [44, -68, 22] → MNI [43, -71, 21]; Cluster size: 288 mm^3
Zmigrod et al. (2016)	Activation in superior temporal gyrus, insula, postcentral/precentral gyrus, middle temporal gyrus, inferior frontal gyrus, medial frontal gyrus, parahippocampal gyrus, thalamus, and cerebellum in SCZ during auditory verbal hallucinations Activation in lingual gyrus, cuneus, and cerebellum in SCZ during visual hallucinations Activation in superior temporal gyrus and inferior frontal gyrus in SCZ during auditory verbal hallucinations but not during visual hallucinations Activation in lingual gyrus in SCZ during visual hallucinations but not during auditory verbal hallucinations	Activation in SCZ (and other non-SCZ with hallucinations) during auditory (verbal) hallucinatory experience: 1) Postcentral gyrus L (BA 3): Coordinates: MNI [-46, -18, 44]; Cluster size: 2104 mm^3 2) Superior temporal gyrus R (BA 22): Coordinates: MNI [54, 12, -6]; Cluster size: 1608 mm^3 3) Precentral gyrus L (BA 6): Coordinates: MNI [-56, 4, 12]; Cluster size: 1392 mm^3 4) Postcentral gyrus R (BA 2): Coordinates: MNI [60, -22, 44]; Cluster size: 1048 mm^3 5) Cerebellum R: Coordinates: MNI [26, -54, -20]; Cluster size: 1024 mm^3 6) Thalamus L: Coordinates: MNI [-12, -20, 4]; Cluster size: 888 mm^3 7) Parahippocampal gyrus L (BA 27): Coordinates: MNI [-26, -32, -4]; Cluster size: 792 mm^3 8) Superior temporal gyrus L (BA 13): Coordinates: MNI [-58, -46, 20]; Cluster size: 792 mm^3 9) Inferior frontal gyrus R (BA 44): Coordinates: MNI [56, 16, 8]; Cluster size: 752 mm^3 10) Medial frontal gyrus R (BA 6): Coordinates: MNI [6, 6, 60]; Cluster size: 664 mm^3 11) Cerebellum R: Coordinates: MNI [26, -62, -46]; Cluster size: 560 mm^3 12) Insula R (BA 13): Coordinates: MNI [40, 0, 12]; Cluster size: 352 mm^3 13) Medial frontal gyrus L (BA 32): Coordinates: MNI [0, 12, 46]; Cluster size: 344 mm^3 14) Middle temporal gyrus R (BA 21):

		Coordinates: MNI [60, -32, -6]; Cluster size: 224 mm^3 15) Thalamus R: Coordinates: MNI [18, -10, 2]; Cluster size: 216 mm^3 Activation in SCZ (and other non-SCZ with hallucinations) during visual hallucinatory experience: 1) Lingual gyrus R (BA 19): Coordinates: MNI [12, -62, 4]; Cluster size: 1672 mm^3 2) Cuneus R (BA 18): Coordinates: MNI [4, -76, 30]; Cluster size: 1360 mm^3 3) Lingual gyrus R (BA 19): Coordinates: MNI [20, -60, -4]; Cluster size: 1056 mm^3 4) Lingual gyrus L (BA 19): Coordinates: MNI [-14, -62, 4]; Cluster size: 904 mm^3 5) Cuneus L (BA 19): Coordinates: MNI [-14, -80, 40]; Cluster size: 760 mm^3 6) Cerebellum R: Coordinates: MNI [32, -84, -16]; Cluster size: 736 mm^3 7) Cuneus L (BA 23): Coordinates: MNI [-4, -76, 16]; Cluster size: 648 mm^3 Subgroup meta-analysis: *Studies on activation in SCZ (and other non-SCZ with hallucinations) during auditory (verbal) hallucinatory experience but not during visual hallucinatory experience:* Activation in SCZ (and other non-SCZ with hallucinations) specifically during auditory hallucinations: 1) Superior temporal gyrus R (BA 22): Coordinates: MNI [55, 13, -4]; Cluster size: 1496 mm^3 2) Superior temporal gyrus L (BA 13): Coordinates: MNI [-56, -44, 23]; Cluster size: 736 mm^3 3) Inferior frontal gyrus R (BA 45): Coordinates: MNI [52, 25, 2]; Cluster size: 512 mm^3 *Studies on activation in SCZ (and other non-SCZ with hallucinations) during visual hallucinatory experience but not during auditory (verbal) hallucinatory experience:* Activation in SCZ (and other non-SCZ with hallucinations) specifically during visual hallucinations: 1) Lingual gyrus R (BA 18): Coordinates: MNI [12, -72, 6]; Cluster size: 1128 mm^3 2) Lingual gyrus R (BA 19): Coordinates: MNI [22, -66, -4]; Cluster size: 1008 mm^3 3) Lingual gyrus L (BA 19): Coordinates: MNI [-18, -63, 4]; Cluster size: 904 mm^3 4) Middle occipital gyrus R (BA 18): Coordinates: MNI [36, -86, -8]; Cluster size: 624 mm^3

Notes:
Jackknife sensitivity analysis; * Analysis of heterogeneity (Q test, non-significant); † Publication bias (Egger's test, non-significant)
§ Study reported in multiple sections of the table (data/results in italics are not considered in the current section of the table).
Abbreviations: CHR, clinical high risk for schizophrenia; SCZ, schizophrenia; HC, healthy controls; MNI, Montreal neurological institute; Tal, Talairach; BA, Brodmann area; GM, grey matter; WM, white matter; FA, fractional anisotropy; ALFF, amplitude of low-frequency fluctuations; ReHo, regional homogeneity; FC, functional connectivity; CM, cerebral metabolism; CBF, cerebral blood flow; CP; combined parameters; TBA, task-based activation; PANSS, positive and negative syndrome scale.

Supplementary Table 3

STRUCTURAL-FUNCTIONAL BRAIN ALTERATIONS IN PRODROME OF SCHIZOPHRENIA							
ALTERATIONS OF GREY MATTER STRUCTURE IN PRODROME OF SCHIZOPHRENIA (sMRI)							
Brain Network	*Brain Region*	*MNI coordinates (x, y, z)*	*CS*	*↓/↑*	*Parameter*	*Subjects CHR / HC (n)*	*Study*
DMN	Paracingulate gyrus [Anterior cingulate cortex R]	5, 41, -7	800	↓	GM	580/621	Liloia et al. (2021)
	Frontal medial cortex R [Gyrus rectus R]	4, 38, -18	480	↓	GM	743/588	Ding et al. (2019)
	Frontal medial cortex L	-10, 34, -12	11	↓	GM	599/620	Luna et al. (2022)
	Frontal pole R [Superior frontal gyrus R]	10, 56, 14	287	↓	GM	743/588	Ding et al. (2019)
LN	Frontal pole L [Superior frontal gyrus L]	-20, 52, -14	136	↓	GM	743/588	Ding et al. (2019)
	Temporal pole L	-18, 6, -34	164	↑	GM	743/588	Ding et al. (2019)
	Fusiform gyrus R	22, 0, -50	202	↑	GM	743/588	Ding et al. (2019)
CEN	Anterior cingulate gyrus R [Median cingulate R]	6, -14, 30	234	↑	GM	743/588	Ding et al. (2019)
SUBCORTICAL STRUCTURES	Thalamus R	8, -18, 20	60	↑	GM	743/588	Ding et al. (2019)
ALTERATIONS OF TASK-BASED BRAIN ACTIVATION IN PRODROME OF SCHIZOPHRENIA (TB-fMRI/PET)							
Brain Network	*Brain Region*	*MNI coordinates (x, y, z)*	*CS*	*↓/↑*	*Parameter*	*Subjects CHR / HC (n)*	*Study*
CEN	Anterior cingulate gyrus L/R [Superior frontal gyrus L/R]	0, 32, 26	102	↓	TBA (Cognitive and emotion processing)	519/503	Luna et al. (2022)

	Superior frontal gyrus L/R	0, 32, 46	16	↓	TBA (Cognitive and emotion processing)	519/503	Luna et al. (2022)
	Middle frontal gyrus R [Inferior frontal gyrus R]	50, 26, 30	34	↓	TBA (Cognitive and emotion processing)	519/503	Luna et al. (2022)
VN	Cuneal cortex R [Precuneus R]	14, -80, 30	114	↓	TBA (Cognitive and emotion processing)	519/503	Luna et al. (2022)
STRUCTURAL-FUNCTIONAL BRAIN ALTERATIONS IN SCHIZOPHRENIA							
ALTERATIONS OF GREY MATTER STRUCTURE IN SCHIZOPHRENIA (sMRI)							
FIRST-EPISODE PSYCHOSIS / EARLY-STAGE SCHIZOPHRENIA							
Brain Network	*Brain Region*	*MNI coordinates (x, y, z)*	*CS*	↓/↑	*Parameter*	*Subjects SCZ / HC (n)*	*Study*
SMN	Heschl's gyrus L [Transverse temporal gyrus L]	-49, -17, 8	1032	↓	GM	1636/1953	Liloia et al. (2021)
	Heschl’s gyrus L [Transverse temporal gyrus L]	-49, -17, 8	288	↓	GM	555/621	Olabi et al. (2012)
	Planum polare L [Superior temporal gyrus L]	-48, -10, 0	1839	↓	GM	NS/5216	Picó-Pérez et al. (2022)
	Planum polare R [Insula/Superior temporal gyrus R]	42, -19, -2	652	↓	GM	431/2180	Bora et al. (2011)
	Planum temporale L [Superior temporal gyrus L]	-61, -26, 10	272	↓	GM	555/621	Olabi et al. (2012)
	Planum temporale R [Superior temporal gyrus R]	50, -24, 7	400	↓	GM	555/621	Olabi et al. (2012)
	Temporal pole L [Superior temporal gyrus L]	-59, 6, -9	216	↓	GM	555/621	Olabi et al. (2012)
	Parietal opercular cortex R [Transverse temporal gyrus R]	50, -24, 14	1624	↓	GM	1636/1953	Liloia et al. (2021)

	Postcentral gyrus L [Precentral gyrus L]	-50, -10, 24	1776	↓	GM	1636/1953	Liloia et al. (2021)
	Postcentral gyrus L	-63, -18, 19	184	↓	GM	555/621	Olabi et al. (2012)
	Postcentral gyrus R	54, -23, 47	216	↓	GM	555/621	Olabi et al. (2012)
	Insula R	36, -14, 10	136	↓	GM	555/621	Olabi et al. (2012)
	Anterior cingulate gyrus L	-9, -6, 41	152	↓	GM	555/621	Olabi et al. (2012)
SN	Insula L	-33, 25, 2	1096	↓	GM	1636/1953	Liloia et al. (2021)
	Insula R	38, 10, 7	216	↓	GM	555/621	Olabi et al. (2012)
	Frontal opercular cortex L [Insula L]	-37, 23, 4	376	↓	GM	555/621	Olabi et al. (2012)
	Paracingulate gyrus R [Dorsal anterior cingulate gyrus R]	15, 18, 32	106	↓	GM	431/2180	Bora et al. (2011)
	Supplementary motor cortex R [Medial frontal gyrus R]	6, 3, 53	112	↓	GM	555/621	Olabi et al. (2012)
DMN	Anterior cingulate gyrus L	-2, 38, -5	784	↓	GM	1636/1953	Liloia et al. (2021)
	Paracingulate gyrus R [Medial frontal gyrus R]*	14, 33, 39	136	↓	GM	555/621	Olabi et al. (2012)
	Precuneus L [Cingulate gyrus L]	-1, -45, 41	112	↓	GM	555/621	Olabi et al. (2012)
	Superior temporal gyrus R [Middle temporal gyrus R]	53, -5, -15	1296	↓	GM	1636/1953	Liloia et al. (2021)
	Middle temporal gyrus R	57, -25, -8	272	↓	GM	555/621	Olabi et al. (2012)
	Inferior temporal gyrus L	-49, -12, -25	152	↓	GM	555/621	Olabi et al. (2012)

CEN	Frontal pole L [Middle frontal gyrus L]	-30, 53, 4	200	↓	GM	555/621	Olabi et al. (2012)
LN	Subcallosal cortex R [Caudate R/L]	3, 17, -3	1624	↓	GM	555/621	Olabi et al. (2012)
	Frontal orbital cortex L [Superior temporal gyrus L]	-32, 20, -28	152	↓	GM	555/621	Olabi et al. (2012)
	Frontal orbital cortex L [Inferior frontal gyrus L]	-22, 32, -9	184	↓	GM	555/621	Olabi et al. (2012)
	Parahippocampal gyrus L [Amygdala L]	-20, -1, -25	752	↓	GM	1636/1953	Liloia et al. (2021)
	Parahippocampal gyrus L [Uncus L]	-18, 1, -30	1272	↓	GM	555/621	Olabi et al. (2012)
	Parahippocampal gyrus R [Amygdala/Uncus R]	21, -1, -30	168	↓	GM	555/621	Olabi et al. (2012)
CHRONIC-STAGE SCHIZOPHRENIA†							
Brain Network	*Brain Region*	*MNI coordinates (x, y, z)*	*CS*	*↓/↑*	*Parameter*	*Subjects SCZ / HC (n)*	*Study*
SMN	Heschl’s gyrus L [Rolandic opercular gyrus L]	-44, -22, 12	648	↓	GM	1207/1328	Fornara et al. (2017)
	Heschl’s gyrus L [Superior temporal gyrus L]	-48, -22, 10		↓	GM	4789/5216	Picó-Pérez et al. (2022)
	Heschl’s gyrus R	46, -20, 4	32	↓	GM	6311/6745	Brandl et al. (2018)
	Planum polare L [Superior temporal gyrus L]	-54, -4, 2	832	↓	GM	1207/1328	Fornara et al. (2017)
	Planum polare R [Superior temporal gyrus R]	52, -6, -6	330	↓	GM	486/485	Gao et al. (2018)
	Planum polare R [Superior temporal pole R]	56, 4, 0	72	↓	GM	1207/1328	Fornara et al. (2017)
	Planum temporale R [Superior temporal gyrus R]	62, -20, 12	272	↓	GM	1207/1328	Fornara et al. (2017)

	Planum temporale R [Superior temporal gyrus R]	60, -12, 4		↓	GM	4789/5216	Picó-Pérez et al. (2022)
	Temporal pole R	54, 6, -8		↓	GM	4789/5216	Picó-Pérez et al. (2022)
	Central opercular cortex R [Transverse temporal gyrus R]	52, -18, 12	27240	↓	GM	3517/3676	Huang et al. (2021)
	Central opercular cortex R	48, -2, 6	2580	↓	GM	6311/6745	Brandl et al. (2018)
	Central opercular cortex R [Superior temporal gyrus R]	50, -4, 2	224	↓	GM	1207/1328	Fornara et al. (2017)
	Central opercular cortex R	60, -8, 8		↓	GM	4789/5216	Picó-Pérez et al. (2022)
	Parietal opercular cortex R	52, -22, 16	256	↓	GM	3795/4315	Goodkind et al. (2015)
	Parietal opercular cortex R [Rolandic opercular gyrus R]	50, -20, 16	216	↓	GM	1207/1328	Fornara et al. (2017)
	Postcentral gyrus L	-60, -12, 28		↓	GM	4789/5216	Picó-Pérez et al. (2022)
	Postcentral gyrus R	50, -18, 40		↓	GM	4789/5216	Picó-Pérez et al. (2022)
	Insula R	36, -4, 4	41	↓	GM	6311/6745	Brandl et al. (2018)
	Anterior cingulate gyrus L	-10, -14, 42	648	↓	GM	3517/3676	Huang et al. (2021)
SN	Insula L	-35, 21, 4	4928	↓	GM	2120/2563	Liloia et al. (2021)
	Insula L	-36, -2, -2	6415	↓	GM	6311/6745	Brandl et al. (2018)
	Insula L	-28, 18, 8	21	↓	GM	6311/6745	Brandl et al. (2018)
	Insula L [Claustrum L]	-36, 16, -2	41240	↓	GM	3517/3676	Huang et al. (2021)

	Insula L	-42, 16, -8	1768	↓	GM	1207/1328	Fornara et al. (2017)
	Insula R	42, 17, -2	3056	↓	GM	2120/2563	Liloia et al. (2021)
	Insula R	42, 14, -2	2465	↓	GM	6311/6745	Brandl et al. (2018)
	Insula R	36, 20, 4	464	↓	GM	1207/1328	Fornara et al. (2017)
	Insula R	42, 12, -6		↓	GM	4789/5216	Picó-Pérez et al. (2022)
	Central opercular cortex L	-44, 8, 0	4409	↓	GM	6311/6745	Brandl et al. (2018)
	Central opercular cortex L [Insular cortex L]	-38, 8, 14	8	↓	GM	1207/1328	Fornara et al. (2017)
	Central opercular cortex L	-52, -4, 8		↓	GM	4789/5216	Picó-Pérez et al. (2022)
	Central opercular cortex R [Insula/Inferior frontal cortex R]	49, 5, 2	1047	↓	GM	1999/2180	Bora et al. (2011)
	Frontal opercular cortex L [Insula/inferior frontal cortex L]	-44, 11, 4	1339	↓	GM	1999/2180	Bora et al. (2011)
	Frontal opercular cortex R [Insula R]	44, 12, 1	1053	↓	GM	3795/4315	Goodkind et al. (2015)
	Temporal pole R	40, 6, -20	72	↓	GM	1207/1328	Fornara et al. (2017)
	Paracingulate gyrus L [Supplementary motor area R]	0, 14, 46	256	↓	GM	1207/1328	Fornara et al. (2017)
	Frontal orbital cortex R [Insular cortex R]	44, 18, -8	840	↓	GM	1207/1328	Fornara et al. (2017)
	Inferior frontal gyrus R	54, 10, 10		↓	GM	4789/5216	Picó-Pérez et al. (2022)
	Middle frontal gyrus L	-30, 32, 26	1160	↓	GM	3517/3676	Huang et al. (2021)

	Posterior cingulate gyrus L	-4, -26, 44		↓	GM	4789/5216	Picó-Pérez et al. (2022)
	Posterior cingulate gyrus R	4, -20, 44		↓	GM	4789/5216	Picó-Pérez et al. (2022)
	Paracingulate gyrus L [Supplementary motor area L]	-4, 10, 50		↓	GM	4789/5216	Picó-Pérez et al. (2022)
	Paracingulate gyrus R [Supplementary motor area R]	4, 12, 46		↓	GM	4789/5216	Picó-Pérez et al. (2022)
	Supramarginal gyrus L	-56, -40, 36	293	↓	GM	486/485	Gao et al. (2018)
	Supramarginal gyrus L	-58, -48, 30		↓	GM	4789/5216	Picó-Pérez et al. (2022)
	Supramarginal gyrus R	60, -24, 44		↓	GM	4789/5216	Picó-Pérez et al. (2022)
DMN	Anterior cingulate gyrus L	-2, 44, 6	3115	↓	GM	6311/6745	Brandl et al. (2018)
	Paracingulate gyrus L [Anterior cingulate cortex L]	-6, 48, -8	25600	↓	GM	3517/3676	Huang et al. (2021)
	Paracingulate gyrus L [Anterior medial prefrontal cortex L]	-6, 48, -8	476	↓	GM	3795/4315	Goodkind et al. (2015)
	Paracingulate gyrus L [Ventromedial prefrontal cortex L]	-2, 48, -6	1330	↓	GM	6311/6745	Brandl et al. (2018)
	Paracingulate gyrus L [Middle frontal gyrus (pars orbitalis) L]	-6, 46, -8	608	↓	GM	1207/1328	Fornara et al. (2017)
	Paracingulate gyrus L [Rostral medial frontal cortex/Anterior cingulate cortex L]	-4, 51, -1	467	↓	GM	1999/2180	Bora et al. (2011)
	Paracingulate gyrus L [Dorsal anterior cingulate cortex R/L]	0, 36, 32	114	↓	GM	6311/6745	Brandl et al. (2018)
	Paracingulate gyrus L [Superior frontal gyrus/Dorsomedial prefrontal cortex L]	-2, 52, 14		↓	GM	4789/5216	Picó-Pérez et al. (2022)
	Paracingulate gyrus L [Anterior cingulate gyrus L]	-8, 44, -4		↓	GM	4789/5216	Picó-Pérez et al. (2022)

	Paracingulate gyrus R [Superior frontal gyrus/Dorsomedial prefrontal cortex R]	4, 52, 14		↓	GM	4789/5216	Picó-Pérez et al. (2022)
	Frontal medial cortex L [Rectus gyrus L]	-10, 52, -14	10	↓	GM	1207/1328	Fornara et al. (2017)
	Frontal medial cortex L	-6, 50, -10		↓	GM	4789/5216	Picó-Pérez et al. (2022)
	Frontal medial cortex R	5, 41, -15	1656	↓	GM	2120/2563	Liloia et al. (2021)
	Frontal medial cortex R	6, 50, -18		↓	GM	4789/5216	Picó-Pérez et al. (2022)
	Frontal orbital cortex L [Insula L]	-42, 22, -14	1629	↓	GM	3795/4315	Goodkind et al. (2015)
	Frontal orbital cortex L	-44, 24, -14		↓	GM	4789/5216	Picó-Pérez et al. (2022)
	Frontal orbital cortex R	38, 24, -12		↓	GM	4789/5216	Picó-Pérez et al. (2022)
	Superior frontal gyrus L	-14, 32, 50	64	↓	GM	1207/1328	Fornara et al. (2017)
	Superior frontal gyrus L	-2, 44, 38	48	↓	GM	1207/1328	Fornara et al. (2017)
	Frontal pole L [Superior frontal gyrus (pars medialis) L]	-4, 58, 6	760	↓	GM	1207/1328	Fornara et al. (2017)
	Frontal pole L [Inferior frontal gyrus (pars orbitalis) L]	-36, 38, -14	40	↓	GM	1207/1328	Fornara et al. (2017)
	Frontal pole L [Middle frontal gyrus L]	-38, 50, -8		↓	GM	4789/5216	Picó-Pérez et al. (2022)
	Inferior frontal gyrus L	-50, 30, -6	128	↓	GM	1207/1328	Fornara et al. (2017)
	Inferior frontal gyrus L	-52, 16, 12		↓	GM	4789/5216	Picó-Pérez et al. (2022)
	Frontal opercular cortex L [Inferior frontal gyrus L]	-46, 16, 0	649	↓	GM	486/485	Gao et al. (2018)

	Posterior cingulate gyrus L	-8, -52, 28		↓	GM	4789/5216	Picó-Pérez et al. (2022)
	Posterior cingulate gyrus R	4, -50, 24		↓	GM	4789/5216	Picó-Pérez et al. (2022)
	Precuneus L [Posterior cingulate cortex L]	-6, -60, 18	4360	↓	GM	3517/3676	Huang et al. (2021)
	Precuneus L	-4, -58, 20		↓	GM	4789/5216	Picó-Pérez et al. (2022)
	Precuneus R	14, -64, 26		↓	GM	4789/5216	Picó-Pérez et al. (2022)
	Middle temporal gyrus L	-56, -2, -30	624	↓	GM	3517/3676	Huang et al. (2021)
	Middle temporal gyrus R	64, -28, -2	168	↓	GM	1207/1328	Fornara et al. (2017)
	Middle temporal gyrus R	54, -4, -20	136	↓	GM	1207/1328	Fornara et al. (2017)
	Superior temporal gyrus L [Middle temporal gyrus L]	-54, -40, 2	16	↓	GM	1207/1328	Fornara et al. (2017)
	Superior temporal gyrus L [Middle temporal gyrus L]	-60, -32, 2		↓	GM	4789/5216	Picó-Pérez et al. (2022)
	Superior temporal gyrus R [Middle temporal gyrus R]	64, -30, 0		↓	GM	4789/5216	Picó-Pérez et al. (2022)
	Temporal pole L	-48, 12, -26	152	↓	GM	1207/1328	Fornara et al. (2017)
	Temporal pole R	42, 14, -28	304	↓	GM	1207/1328	Fornara et al. (2017)
	Angular gyrus L	-50, -58, 26		↓	GM	4789/5216	Picó-Pérez et al. (2022)
	Lateral occipital cortex (superior division) R [Angular gyrus R]	50, -62, 34		↓	GM	4789/5216	Picó-Pérez et al. (2022)
CEN	Middle frontal gyrus L [Precentral gyrus L]	-46, 12, 34	1096	↓	GM	1207/1328	Fornara et al. (2017)

	Inferior frontal gyrus L	-50, 10, 10	688	↓	GM	1207/1328	Fornara et al. (2017)
	Inferior frontal gyrus L	-40, 24, 16	80	↓	GM	1207/1328	Fornara et al. (2017)
	Inferior frontal gyrus L	-52, 14, 30		↓	GM	4789/5216	Picó-Pérez et al. (2022)
	Inferior frontal gyrus R	54, 20, 24	88	↓	GM	1207/1328	Fornara et al. (2017)
	Frontal pole L [Superior frontal gyrus L]	-28, 58, 8	1984	↓	GM	3517/3676	Huang et al. (2021)
	Frontal pole L [Middle frontal gyrus L]	-32, 54, 22	192	↓	GM	1207/1328	Fornara et al. (2017)
	Frontal pole L [Superior frontal gyrus L]	-30, 54, 2	8	↓	GM	1207/1328	Fornara et al. (2017)
	Frontal pole L [Middle frontal gyrus L]	-36, 54, 10		↓	GM	4789/5216	Picó-Pérez et al. (2022)
	Frontal pole R [Superior frontal gyrus R]	30, 60, -2	1600	↓	GM	3517/3676	Huang et al. (2021)
	Frontal pole R [Superior frontal gyrus R]	26, 60, 2	112	↓	GM	1207/1328	Fornara et al. (2017)
	Frontal pole R [Superior frontal gyrus (pars orbitalis) R]	32, 62, -2	8	↓	GM	1207/1328	Fornara et al. (2017)
	Frontal pole R [Middle frontal gyrus R]	46, 46, 8		↓	GM	4789/5216	Picó-Pérez et al. (2022)
	Frontal pole R [Superior frontal gyrus R]	32, 60, -4		↓	GM	4789/5216	Picó-Pérez et al. (2022)
	Frontal pole R [Middle frontal gyrus R]	44, 52, -4		↓	GM	4789/5216	Picó-Pérez et al. (2022)
	Frontal orbital cortex L [Insula L]	-32, 24, -4		↓	GM	4789/5216	Picó-Pérez et al. (2022)
	Paracingulate gyrus R [Dorsal anterior cingulate cortex R]	6, 38, 24	430	↓	GM	3795/4315	Goodkind et al. (2015)

	Paracingulate gyrus R [Dorsal medial frontal cortex/Anterior cingulate cortex R/L]	4, 25, 44	493	↓	GM	1999/2180	Bora et al. (2011)
	Anterior cingulate gyrus R	6, 34, 18		↓	GM	4789/5216	Picó-Pérez et al. (2022)
	Supramarginal gyrus L [Inferior parietal gyrus L]	-50, -46, 48		↓	GM	4789/5216	Picó-Pérez et al. (2022)
DAN	Superior frontal gyrus L	-22, 4, 66	160	↓	GM	1207/1328	Fornara et al. (2017)
	Middle frontal gyrus R	48, 8, 38	864	↓	GM	3517/3676	Huang et al. (2021)
	Inferior frontal gyrus R	52, 14, 24		↓	GM	4789/5216	Picó-Pérez et al. (2022)
	Precentral gyrus R	46, 8, 32	152	↓	GM	1207/1328	Fornara et al. (2017)
	Precentral gyrus R	50, 8, 30		↓	GM	4789/5216	Picó-Pérez et al. (2022)
	Middle temporal gyrus L [Middle occipital gyrus L]	-56, -62, -2	1448	↓	GM	3517/3676	Huang et al. (2021)
	Inferior temporal gyrus L [Inferior occipital gyrus L]	-48, -62, -12		↓	GM	4789/5216	Picó-Pérez et al. (2022)
	Inferior temporal gyrus L	-50, -58, -12		↓	GM	4789/5216	Picó-Pérez et al. (2022)
	Inferior temporal gyrus L [Fusiform gyrus L]	-48, -58, -20		↓	GM	4789/5216	Picó-Pérez et al. (2022)
	Supramarginal gyrus R [Inferior parietal gyrus R]	42, -40, 50		↓	GM	4789/5216	Picó-Pérez et al. (2022)
	Lateral occipital cortex (superior division) R [Middle occipital gyrus R]	38, -72, 38		↓	GM	4789/5216	Picó-Pérez et al. (2022)
VN	Cuneus L	-4, -72, 20	96	↓	GM	1207/1328	Fornara et al. (2017)
	Occipital pole R [Cuneus R]	8, -88, 14		↓	GM	4789/5216	Picó-Pérez et al. (2022)

	Intracalcarine cortex L [Cuneus L]	-2, -86, 0		↓	GM	4789/5216	Picó-Pérez et al. (2022)
	Lateral occipital cortex (inferior division) L [Middle occipital gyrus L]	-44, -70, 0		↓	GM	4789/5216	Picó-Pérez et al. (2022)
	Lateral occipital cortex (inferior division) R [Inferior temporal gyrus R]	52, -64, -4	552	↓	GM	3517/3676	Huang et al. (2021)
	Lateral occipital cortex (inferior division) R [Middle temporal gyrus R]	54, -64, 2	160	↓	GM	1207/1328	Fornara et al. (2017)
	Lateral occipital cortex (inferior division) R [Inferior occipital gyrus R]	38, -84, -8		↓	GM	4789/5216	Picó-Pérez et al. (2022)
	Lateral occipital cortex (superior division) R [Superior occipital gyrus R]	28, -82, 28		↓	GM	4789/5216	Picó-Pérez et al. (2022)
	Temporal occipital fusiform gyrus L	-26, -54, -16	771	↓	GM	486/485	Gao et al. (2018)
	Inferior temporal gyrus R	50, -60, -16		↓	GM	4789/5216	Picó-Pérez et al. (2022)
	Parahippocampal gyrus L [Lingual gyrus L]	-14, -40, -10		↓	GM	4789/5216	Picó-Pérez et al. (2022)
	Parahippocampal gyrus R	26, -34, -14		↓	GM	4789/5216	Picó-Pérez et al. (2022)
	Precuneus L [Calcarine cortex L]	-4, -64, 14	96	↓	GM	1207/1328	Fornara et al. (2017)
	Posterior cingulate gyrus L [Lingual gyrus L]	-16, -40, -4	208	↓	GM	1207/1328	Fornara et al. (2017)
	Posterior cingulate gyrus R [Lingual gyrus R]	14, -50, 4	592	↓	GM	1207/1328	Fornara et al. (2017)
	Posterior cingulate gyrus R [Lingual gyrus R]	16, -38, -2	112	↓	GM	1207/1328	Fornara et al. (2017)
LN	Subcallosal cortex L [Subgenual anterior cingulate cortex L]	-4, 10, -10	282	↓	GM	3795/4315	Goodkind et al. (2015)
	Subcallosal cortex L	-8, 18, -14		↓	GM	4789/5216	Picó-Pérez et al. (2022)

	Frontal medial cortex R	4, 40, -24	506	↓	GM	3795/4315	Goodkind et al. (2015)
	Frontal medial cortex R [Rectus gyrus R]	4, 38, -24	1200	↓	GM	1207/1328	Fornara et al. (2017)
	Frontal pole L [Superior frontal gyrus R]	6, 60, -22	155	↑	GM	486/485	Gao et al. (2018)
	Temporal pole L	-44, 6, -12		↓	GM	4789/5216	Picó-Pérez et al. (2022)
	Inferior temporal gyrus L	-48, -18, -34	480	↓	GM	1207/1328	Fornara et al. (2017)
	Inferior temporal gyrus R	46, -14, -30	46	↓	GM	1207/1328	Fornara et al. (2017)
	Temporal fusiform gyrus L	-36, -12, -38	216	↓	GM	1207/1328	Fornara et al. (2017)
	Temporal fusiform gyrus R [Uncus L]	-36, -14, -38	1032	↓	GM	3517/3676	Huang et al. (2021)
	Temporal fusiform gyrus R [Uncus R]	40, -14, -38	760	↓	GM	3517/3676	Huang et al. (2021)
	Temporal fusiform gyrus R	42, -14, -38	608	↓	GM	1207/1328	Fornara et al. (2017)
	Parahippocampal gyrus L [Fusiform gyrus L]	-30, -2, -32	40	↓	GM	1207/1328	Fornara et al. (2017)
SUBCORTICAL STRUCTURES	Hippocampus L	-22, -16, -14		↓	GM	4789/5216	Picó-Pérez et al. (2022)
	Hippocampus L [Parahippocampal gyrus L]	-28, -18, -22		↓	GM	4789/5216	Picó-Pérez et al. (2022)
	Hippocampus R [Parahippocampal gyrus R]	30, -20, -14	664	↓	GM	3517/3676	Huang et al. (2021)
	Hippocampus R [Parahippocampal gyrus R]	24, -6, -28		↓	GM	4789/5216	Picó-Pérez et al. (2022)
	Amygdala L	-20, -4, -18	1056	↓	GM	2120/2563	Liloia et al. (2021)

	Amygdala L [Hippocampus L]	-20, -6, -18	640	↓	GM	1207/1328	Fornara et al. (2017)
	Amygdala L	-22, -2, -24	470	↓	GM	6311/6745	Brandl et al. (2018)
	Amygdala R [Parahippocampal gyrus R]	18, -4, -22	2920	↓	GM	3517/3676	Huang et al. (2021)
	Amygdala R	17, -1, -23	680	↓	GM	2120/2563	Liloia et al. (2021)
	Amygdala R [Parahippocampal gyrus R]	20, -2, -22	280	↓	GM	1207/1328	Fornara et al. (2017)
	Caudate L	-6,10, 2	9946	↓	GM	6311/6745	Brandl et al. (2018)
	Caudate L	-6, 10, 4		↓	GM	4789/5216	Picó-Pérez et al. (2022)
	Caudate R	8, 16, 2		↓	GM	4789/5216	Picó-Pérez et al. (2022)
	Accumbens L [Caudate L]	-4, 9, -8	1224	↓	GM	2120/2563	Liloia et al. (2021)
	Putamen L	-20, 10, 2	223	↑	GM	3795/4315	Goodkind et al. (2015)
	Pallidum L	-12, -2, 0	14083	↓	GM	6311/6745	Brandl et al. (2018)
	Pallidum R [Striatum R]*	12, 4, -4	176	↑	GM	3795/4315	Goodkind et al. (2015)
	Thalamus L	-3, -15, 3	2312	↓	GM	2120/2563	Liloia et al. (2021)
	Thalamus L	-3, -15, 1	544	↓	GM	1999/2180	Bora et al. (2011)
	Thalamus L	0, -14, 4	740	↓	GM	6311/6745	Brandl et al. (2018)
	Thalamus L	-2, -12, 4		↓	GM	4789/5216	Picó-Pérez et al. (2022)

	Thalamus R	4, -16, 2	14496	↓	GM	3517/3676	Huang et al. (2021)
	Thalamus R	2, -12, 4	960	↓	GM	1207/1328	Fornara et al. (2017)
	Thalamus R	2, -14, 4	486	↓	GM	3795/4315	Goodkind et al. (2015)
	Thalamus R	14, -14, 14		↓	GM	4789/5216	Picó-Pérez et al. (2022)
	Brainstem R [Lingual gyrus R]	6, -34, -6	466	↑	GM	486/485	Gao et al. (2018)
	Cerebellum L	-4, -48, -32	79	↑	GM	6311/6745	Brandl et al. (2018)
	Cerebellum L	-14, -62, -18		↓	GM	4789/5216	Picó-Pérez et al. (2022)
	Cerebellum R	6, -66, -32	4530	↑	GM	6311/6745	Brandl et al. (2018)
	Cerebellum R [Pons R]	14, -42, -34	1249	↑	GM	6311/6745	Brandl et al. (2018)
	Cerebellum R [Pons R]	20, -42, -38	523	↑	GM	6311/6745	Brandl et al. (2018)
	Cerebellum R	4, -44, -20	39	↑	GM	6311/6745	Brandl et al. (2018)
	Cerebellum R	18, -36, -20	32	↑	GM	6311/6745	Brandl et al. (2018)
	Cerebellum R	26, -40, -24		↓	GM	4789/5216	Picó-Pérez et al. (2022)

ALTERATIONS OF WHITE MATTER STRUCTURE IN SCHIZOPHRENIA (sMRI/dMRI)							
FIRST-EPISODE PSYCHOSIS / EARLY-STAGE SCHIZOPHRENIA							
	White Matter Tract	*MNI coordinates (x, y, z)*	*CS*	↓/↑	*Parameter*	*Subjects SCZ / HC (n)*	*Study*
	[Temporal WM L]	-36, -59, -3	159	↓	WM	217/934	Bora et al. (2011)
	[Temporal WM R (inferior fronto-occipital fasciculus, inferior longitudinal fasciculus, fornix)]	37, -34, -2	1029	↓	WM	217/934	Bora et al. (2011)
	[Temporal WM and retrolenticular internal/external capsule L (inferior fronto-occipital fasciculus, inferior longitudinal fasciculus, cingulum/hippocampus, fornix)]	-29, -49, 9	900	↓	FA	127/681	Bora et al. (2011)
	[Temporal WM L (fornix, inferior longitudinal fasciculus, inferior fronto-occipital fasciculus, splenium of corpus callosum)]	-42, -14, -23	296	↓	FA	271/297	Yao et al. (2013)
	[Posterior limb of internal capsule R]	15, -7, -1	45	↓	FA	127/681	Bora et al. (2011)
	[Frontal WM R (anterior cingulum, genu of corpus callosum, uncinate fasciculus)]	13, 38, 13	328	↓	FA	271/297	Yao et al. (2013)
CHRONIC-STAGE SCHIZOPHRENIA†							
	White Matter Tract	*MNI coordinates (x, y, z)*	*CS*	↓/↑	*Parameter*	*Subjects SCZ / HC (n)*	*Study*
	[Fornix R]	18, -29, 16	26318	↓	WM	978/934	Vitolo et al. (2018)
	[Cingulum L]	-5, -4, 28	42476	↓	WM	978/934	Vitolo et al. (2018)
	[Cingulum R]	21, -37, 1	38840	↓	WM	978/934	Vitolo et al. (2018)
	[Inferior longitudinal fasciculus L]	-24, -5, -13	20131	↓	WM	978/934	Vitolo et al. (2018)
	[Inferior longitudinal fasciculus R]	42, 1, -6	16338	↓	WM	978/934	Vitolo et al. (2018)

	[Inferior fronto-occipital fasciculus L]	-29, 1, -4	22154	↓	WM	978/934	Vitolo et al. (2018)
	[Inferior fronto-occipital fasciculus R]	19, 29, 3	23185	↓	WM	978/934	Vitolo et al. (2018)
	[Superior longitudinal fasciculus I L]	-17, 34, 45	109025	↓	WM	978/934	Vitolo et al. (2018)
	[Superior longitudinal fasciculus II L]	-26, -52, 15	112229	↓	WM	978/934	Vitolo et al. (2018)
	[Superior longitudinal fasciculus III L]	-43, -48, 36	72219	↓	WM	978/934	Vitolo et al. (2018)
	[Superior longitudinal fasciculus I R]	23, 52, 15	98037	↓	WM	978/934	Vitolo et al. (2018)
	[Superior longitudinal fasciculus II R]	26, 53, 15	117581	↓	WM	978/934	Vitolo et al. (2018)
	[Superior longitudinal fasciculus III R]	52, -11, 29	119900	↓	WM	978/934	Vitolo et al. (2018)
	[Arcuate fasciculus L]	-46, -51, 36	24480	↓	WM	978/934	Vitolo et al. (2018)
	[Posterior segment of arcuate fasciculus L]	-55, -41, -14	11088	↓	WM	978/934	Vitolo et al. (2018)
	[Arcuate fasciculus R]	51, -11, 29	23307	↓	WM	978/934	Vitolo et al. (2018)
	[Anterior segment of arcuate fasciculus R]	52, -11, 29	8780	↓	WM	978/934	Vitolo et al. (2018)
	[Posterior segment of arcuate fasciculus R]	57, -34, 8	12107	↓	WM	978/934	Vitolo et al. (2018)
	[Uncinate fasciculus R]	-22, 26, 0	12282	↓	WM	978/934	Vitolo et al. (2018)
	[Uncinate fasciculus R]	18, 7, -2	13022	↓	WM	978/934	Vitolo et al. (2018)
	[Corticospinal tract L]	-23, -28, 5	29175	↓	WM	978/934	Vitolo et al. (2018)

	[Corticospinal tract R]	18, 5, 2	23730	↓	WM	978/934	Vitolo et al. (2018)
	[Internal capsule L]	-17, 5, -2	248	↓	WM	712/639	Di et al. (2009)
	[Anterior limb of internal capsule L/R (anterior thalamic radiation)]	13, 2, 8	409	↓	WM	903/934	Bora et al. (2011)
	[Internal capsule R]	11, -23, -41	63671	↓	WM	978/934	Vitolo et al. (2018)
	[Internal capsule R]	17, 7, 6	352	↓	WM	712/639	Di et al. (2009)
	[External capsule/Uncinate fasciculus L]	-26, 4, -10	54	↓	WM	1068/1073	Zhao et al. (2021)
	[External capsule/Uncinate fasciculus (inferior frontal occipital fasciculus) R]	28, 0, -10	25	↓	WM	1068/1073	Zhao et al. (2021)
	[Optic radiation L]	-23, -23, 2	7923	↓	WM	978/934	Vitolo et al. (2018)
	[Optic radiation R]	40, -55, -4	5982	↓	WM	978/934	Vitolo et al. (2018)
	[Anterior Commissure L]	-10, 8, -5	16636	↓	WM	978/934	Vitolo et al. (2018)
	[Corpus callosum (body)/Posterior corona radiata L/R]	-10, -24, 24	4221	↓	WM	1068/1073	Zhao et al. (2021)
	[Corpus Callosum R]	18, -29, 16	114544	↓	WM	978/934	Vitolo et al. (2018)
	[Cortico-ponto-cerebellum tract L]	-23, -24, 5	2176	↓	WM	978/934	Vitolo et al. (2018)
	[Inferior cerebellar pedunculus L]	-3, -51, -24	5648	↓	WM	978/934	Vitolo et al. (2018)
	[Inferior cerebellar pedunculus R]	12, -23, -41	5302	↓	WM	978/934	Vitolo et al. (2018)
	[Superior cerebellar pedunculus R]	9, -24, -18	8113	↓	WM	978/934	Vitolo et al. (2018)

	[Temporal WM R (inferior frontal occipital fasciculus, inferior longitudinal fasciculus)]	37, -34, -2	93	↓	WM	903/934	Bora et al. (2011)
	[Frontal WM L]	-8, 53, -1	336	↓	WM	712/639	Di et al. (2009)
	[Frontal WM R]	21, 47, 28	544	↓	WM	712/639	Di et al. (2009)
	[Fornix L]	-29, 16, -34	26318	↓	FA	1220/1237	Vitolo et al. (2018)
	[Cingulum L]	-19, -46, 42	42476	↓	FA	1220/1237	Vitolo et al. (2018)
	[Cingulum R]	19, 35, 34	38840	↓	FA	1220/1237	Vitolo et al. (2018)
	[Cingulum R]	10, -38, 20	156	↓	FA	754/775	Dong et al. (2017)
	[Inferior longitudinal fasciculus L]	-36, -40, -7	20131	↓	FA	1220/1237	Vitolo et al. (2018)
	[Inferior longitudinal fasciculus R]	43, -30, -14	16338	↓	FA	1220/1237	Vitolo et al. (2018)
	[Inferior fronto-occipital fasciculus L]	-33, -21, -13	22154	↓	FA	1220/1237	Vitolo et al. (2018)
	[Inferior fronto-occipital fasciculus R]	43, -30, -14	23185	↓	FA	1220/1237	Vitolo et al. (2018)
	[Superior longitudinal fasciculus L]	-34, -52, 30	43	↓	FA	754/775	Dong et al. (2017)
	[Superior longitudinal fasciculus I L]	-19, -46, 42	109025	↓	FA	1220/1237	Vitolo et al. (2018)
	[Superior longitudinal fasciculus II L]	-20, -8, 58	112229	↓	FA	1220/1237	Vitolo et al. (2018)
	[Superior longitudinal fasciculus III L]	-52, -38, 12	72219	↓	FA	1220/1237	Vitolo et al. (2018)
	[Superior longitudinal fasciculus R]	26, -10, 44	24	↓	FA	754/775	Dong et al. (2017)

	[Superior longitudinal fasciculus I R]	20, 34, 38	98037	↓	FA	1220/1237	Vitolo et al. (2018)
	[Superior longitudinal fasciculus II R]	20, 34, 38	117581	↓	FA	1220/1237	Vitolo et al. (2018)
	[Superior longitudinal fasciculus III R]	24, 26, 32	119900	↓	FA	1220/1237	Vitolo et al. (2018)
	[Arcuate fasciculus L]	-36, -40, -7	24480	↓	FA	1220/1237	Vitolo et al. (2018)
	[Anterior segment of arcuate fasciculus L]	-54, -6, 14	5391	↓	FA	1220/1237	Vitolo et al. (2018)
	[Posterior segment of arcuate fasciculus L]	-36, -40, -7	11088	↓	FA	1220/1237	Vitolo et al. (2018)
	[Long segment of arcuate fasciculus L]	-36, -40, -7	7639	↓	FA	1220/1237	Vitolo et al. (2018)
	[Arcuate fasciculus R]	46, -38, -8	23307	↓	FA	1220/1237	Vitolo et al. (2018)
	[Posterior segment of arcuate fasciculus R]	43, -33, -11	12107	↓	FA	1220/1237	Vitolo et al. (2018)
	[Uncinate fasciculus L]	-25, 14, -28	12282	↓	FA	1220/1237	Vitolo et al. (2018)
	[Uncinate fasciculus R]	17, 30, 0	13022	↓	FA	1220/1237	Vitolo et al. (2018)
	[Corticospinal tract L]	-20, 0, 17	29175	↓	FA	1220/1237	Vitolo et al. (2018)
	[Corticospinal tract R]	30, -18, 2	23730	↓	FA	1220/1237	Vitolo et al. (2018)
	[Internal capsule L]	-20, 0, 17	63671	↓	FA	1220/1237	Vitolo et al. (2018)
	[Anterior thalamic radiation/Caudate nucleus L]	-4, -20, 18	92	↓	FA	754/775	Dong et al. (2017)
	[Anterior thalamic radiation R]	12, 0, 4	19	↓	FA	754/775	Dong et al. (2017)

	[Posterior thalamic radiation (inferior longitudinal fasciculus) R]	30, -62, 4	47	↓	FA	1543/1612	Zhao et al. (2021)
	[Optic radiation L]	-36, -40, -7	7923	↓	FA	1220/1237	Vitolo et al. (2018)
	[Optic radiation R]	30, -18, 2	5982	↓	FA	1220/1237	Vitolo et al. (2018)
	[Anterior commissure L]	-25, 13, -32	16636	↓	FA	1220/1237	Vitolo et al. (2018)
	[Genu of corpus callosum L/R and anterior cingulate/medial frontal area (forceps minor, cingulum, inferior frontal occipital fasciculus R)]	19, 26, 9	2501	↓	FA	699/681	Bora et al. (2011)
	[Corpus callosum/Anterior corona radiata L]	-18, 34, 2	10828	↓	FA	1543/1612	Zhao et al. (2021)
	[Corpus callosum L]	-26, -60, 14	56	↓	FA	754/775	Dong et al. (2017)
	[Corpus callosum R]	22, -14, 36	21	↓	FA	754/775	Dong et al. (2017)
	[Corpus Callosum R]	17, 34, 38	114544	↓	FA	1220/1237	Vitolo et al. (2018)
	[Cortico-ponto cerebellum tract L]	-17, -36, -42	2176	↓	FA	1220/1237	Vitolo et al. (2018)
	[Cortico-ponto cerebellum tract R]	26, -16, 2	766	↓	FA	1220/1237	Vitolo et al. (2018)
	[Inferior cerebellar pedunculus L]	-8, -32, -31	5648	↓	FA	1220/1237	Vitolo et al. (2018)
	[Inferior cerebellar pedunculus R]	15, -37, -41	5302	↓	FA	1220/1237	Vitolo et al. (2018)
	[Superior cerebellar pedunculus L]	-8, -30, -31	8012	↓	FA	1220/1237	Vitolo et al. (2018)
	[Superior cerebellar pedunculus R]	14, -23, -13	8113	↓	FA	1220/1237	Vitolo et al. (2018)
	[Temporal WM and retrolenticular internal/external capsule L (inferior frontal occipital fasciculus, inferior longitudinal fasciculus, cingulum, fornix)]	-34, -25, -7	349	↓	FA	699/681	Bora et al. (2011)

	[Temporal WM L (splenium of corpus callosum, fornix/stria terminalis, inferior longitudinal fasciculus, inferior fronto-occipital fasciculus)]	-32, -31, -8	2264	↓	FA	407/383	Wright and Bullmore (2009)
	[Temporal WM R (inferior frontal occipital fasciculus, inferior longitudinal fasciculus, fornix)]	40, -31, -10	154	↓	FA	699/681	Bora et al. (2011)
	[Frontal WM L (genu of corpus callosum, cingulum, anterior thalamic radiation, corticobulbar tract, inferior fronto-occipital fasciculus)]	-12, 37, 10	2368	↓	FA	407/383	Wright and Bullmore (2009)
	[Frontal WM/Genu of corpus callosum (forceps minor)/Anterior thalamic radiation/Inferior fronto-occipital fasciculus/Uncinate fasciculus L]	-20, 34, 8	356	↓	FA	754/775	Dong et al. (2017)
ALTERATIONS OF INTRINSIC BRAIN ACTIVITY IN SCHIZOPHRENIA (RS-fMRI/PET/SPECT)							
FIRST-EPISODE PSYCHOSIS / EARLY-STAGE SCHIZOPHRENIA							
Brain Network	*Brain Region*	*MNI coordinates (x, y, z)*	*CS*	*↓/↑*	*Parameter*	*Subjects SCZ / HC (n)*	*Study*
DMN	Frontal medial cortex L#	-2, 48, -12	1551	↓	ALFF	402/1179	Gong et al. (2019)
	Frontal medial cortex L	-2, 54, -12	1609	↓	ALFF	583/1179	Gong et al. (2019)
	Precuneus R#	4, -54, 16	281	↓	ALFF	402/1179	Gong et al. (2019)
	Precuneus R	2, -52, 18	628	↓	ALFF	583/1179	Gong et al. (2019)
	Lateral occipital cortex (superior division) R [Inferior parietal gyrus/Angular gyrus R]#	48, -60, 26	853	↓	ALFF	402/1179	Gong et al. (2019)
CEN	Angular gyrus L [Inferior parietal gyrus L]	-42, -52, 46	21	↓	ALFF	583/1179	Gong et al. (2019)
	Angular gyrus R [Inferior parietal gyrus R]	50, -48, 46	1294	↓	ALFF	583/1179	Gong et al. (2019)
VN	Lateral occipital cortex (inferior division) R [Middle occipital gyrus R]	36, -82, 8	46	↑	ALFF	583/1179	Gong et al. (2019)

	Occipital fusiform gyrus L [Middle occipital gyrus L]	-34, -72, -8	20	↑	ALFF	583/1179	Gong et al. (2019)
SUBCORTICAL STRUCTURES	Putamen L#	-22, 8, 2	1870	↑	ALFF	402/1179	Gong et al. (2019)
	Putamen L	-22, 4, 0	1837	↑	ALFF	583/1179	Gong et al. (2019)
	Putamen R#	26, 6, -4	2749	↑	ALFF	402/1179	Gong et al. (2019)
	Putamen R	28, 6, 0	2223	↑	ALFF	583/1179	Gong et al. (2019)
CHRONIC-STAGE SCHIZOPHRENIA†							
Brain Network	*Brain Region*	*MNI coordinates (x, y, z)*	*CS*	*↓/↑*	*Parameter*	*Subjects SCZ / HC (n)*	*Study*
SN	Insula R	38, 14, -14	339	↓	CP (ALFF/CBF)	403/ 428	Gao et al. (2018)
SMN	Postcentral gyrus L	-50, -18, 44	296	↓	ALFF	1249/1179	Gong et al. (2019)
	Postcentral gyrus R	46, -20, 44	2615	↓	ALFF	1249/1179	Gong et al. (2019)
	Precuneus L	-2, -44, 60	641	↓	ALFF	1249/1179	Gong et al. (2019)
	Precuneus R	3, -44, 69	528	↓	ALFF/ReHo/FC/CM/CBF	285/282	Kuhn and Gallinat (2013)
DMN	Paracingulate gyrus L [Ventromedial prefrontal cortex L]	-4, 40, -9	272	↓	ALFF/ReHo/FC/CM/CBF	285/282	Kuhn and Gallinat (2013)
	Frontal orbital cortex L	-42, 24, -4	62	↓	CM	234/120	Townsend et al. (2022)
	Posterior cingulate gyrus R [Precuneus R]	10, -48, 28	248	↓	ALFF/ReHo/FC/CM/CBF	285/282	Kuhn and Gallinat (2013)

	Precuneus L	-6, -70, 35	488	↓	ALFF/ReHo/FC/CM/CBF	285/282	Kuhn and Gallinat (2013)
	Precuneus R	4, -54, 16	185	↓	ALFF	1249/1179	Gong et al. (2019)
	Angular gyrus L [Inferior parietal gyrus L]	-48, -54, 42	214	↓	ALFF	1249/1179	Gong et al. (2019)
	Paracingulate gyrus R [Anterior cingulate cortex R]	8, 40, 26	145	↑	ALFF	1249/1179	Gong et al. (2019)
	Frontal pole R [Inferior frontal gyrus R]	50, 36, -4	841	↑	ALFF	1249/1179	Gong et al. (2019)
	Inferior frontal gyrus R	48, 20, 14	41	↑	ALFF	1249/1179	Gong et al. (2019)
	Inferior temporal gyrus L	-50, 0, -36	233	↑	ALFF	1249/1179	Gong et al. (2019)
CEN	Paracingulate gyrus L	0, 24, 34	309	↓	CM	234/120	Townsend et al. (2022)
	Lateral occipital cortex (superior division) R [Angular gyrus R]	40, -60, 52	331	↓	CP (ALFF/ CBF)	403/ 428	Gao et al. (2018)
	Posterior cingulate gyrus L	-1, -29, 26	384	↓	ALFF/ReHo/FC/CM/CBF	285/282	Kuhn and Gallinat (2013)
DAN	Precentral gyrus R [Inferior frontal gyrus R]	46, 10, 30	893	↓	CP (ALFF/CBF)	403/ 428	Gao et al. (2018)
VN	Intracalcarine cortex R	18, -68, 12	12	↓	ALFF	1249/1179	Gong et al. (2019)
	Lateral occipital cortex (superior division) R [Superior occipital gyrus R]	26, -86, 34	37	↓	ALFF	1249/1179	Gong et al. (2019)
	Lingual gyrus L	-11, -57, 2	1296	↑	ALFF/ReHo/FC/CM/CBF	285/282	Kuhn and Gallinat (2013)
	Lingual gyrus R	11, -55, 2	1200	↑	ALFF/ReHo/FC/CM/CBF	285/282	Kuhn and Gallinat (2013)

	Occipital fusiform gyrus L [Inferior occipital gyrus L]	-34, -76, -12	168	↑	CP (ALFF/CBF)	403/ 428	Gao et al. (2018)
LN	Frontal pole L [Ventromedial prefrontal cortex L]	-10, 48, -20	312	↓	ALFF/ReHo/FC/CM/CBF	285/282	Kuhn and Gallinat (2013)
SUBCROTICAL STRUCTURES	Hippocampus L	-21, -10, -24	264	↓	ALFF/ReHo/FC/CM/CBF	285/282	Kuhn and Gallinat (2013)
	Putamen L	-28, -2, 4	2761	↑	CP (ALFF/CBF)	403/ 428	Gao et al. (2018)
	Putamen R	26, 4, 2	4830	↑	ALFF	1249/1179	Gong et al. (2019)
	Putamen R	26, -2, 8	212	↑	CP (ALFF/CBF)	403/ 428	Gao et al. (2018)
ALTERATIONS OF TASK-BASED BRAIN ACTIVATION IN SCHIZOPHRENIA (TB-fMRI/PET)							
FIRST-EPISODE PSYCHOSIS / EARLY-STAGE SCHIZOPHRENIA							
Brain Network	*Brain Region*	*MNI coordinates (x, y, z)*	*CS*	↓/↑	*Parameter*	*Subjects SCZ / HC (n)*	*Study*
SN	Inferior frontal gyrus R [Insula R]	41, 10, 16	16	↓	TBA (Cognitive processing of attention)	290/316	Casale et al. (2016)
CEN	Middle frontal gyrus R	48, 30, 28	80	↓	TBA (Cognitive processing of attention)	290/316	Casale et al. (2016)
	Frontal orbital cortex L [Insula L]	-28, 22, -10	72	↓	TBA (Cognitive processing of working memory)	290/316	Casale et al. (2016)
	Supramarginal gyrus R [Inferior parietal lobule R]	52, -46, 48	56	↓	TBA (Cognitive processing of attention)	290/316	Casale et al. (2016)
DAN	Lateral occipital cortex (superior division) R [Superior parietal gyrus R]	22, -66, 50	220	↓	TBA (Cognitive processing)	NS/3723	Picó-Pérez et al. (2022)

EARLY-ONSET SCHIZOPHRENIA							
Brain Network	*Brain Region*	*MNI coordinates (x, y, z)*	*CS*	↓/↑	*Parameter*	*Subjects SCZ / HC (n)*	*Study*
DMN	Precuneus L	-4, -60, 28	433	↑	TBA (Cognitive processing)	118/99	Arsalidou et al. (2020)
CEN	Frontal pole L [Inferior frontal gyrus L]	-52, 38, 12	290	↑	TBA (Cognitive processing)	118/99	Arsalidou et al. (2020)
DAN	Precuneus R	4, -50, 46	164	↓	TBA (Cognitive processing)	118/99	Arsalidou et al. (2020)
VN	Occipital fusiform gyrus L	-38, -68, -12	709	↓	TBA (Cognitive processing)	118/99	Arsalidou et al. (2020)
SUBCORTICAL STRUCTURES	Cerebellum L	10, -80, -22	147	↑	TBA (Cognitive processing)	118/99	Arsalidou et al. (2020)
CHRONIC-STAGE SCHIZOPHRENIA†							
PERCEPTION							
Brain Network	*Brain Region*	*MNI coordinates (x, y, z)*	*CS*	↓/↑	*Parameter*	*Subjects SCZ / HC (n)*	*Study*
SMN	Supplementary motor cortex L [Anterior cingulate cortex L]	-11, -2, 43	520	↓	TBA (Auditory perception)	204/170	Kompus et al. (2011)
DMN	Superior temporal gyrus L	-57, -6, -4	1824	↓	TBA (Auditory perception)	204/170	Kompus et al. (2011)
CEN	Frontal pole L [Superior frontal gyrus L]	25, 52, 15	456	↓	TBA (Auditory perception)	204/170	Kompus et al. (2011)
SUBCORTICAL STRUCTURES	Hippocampus L*	-13, -39, 7	200	↓	TBA (Auditory perception)	204/170	Kompus et al. (2011)
	Thalamus R	12, -22, 16	520	↓	TBA (Auditory perception)	204/170	Kompus et al. (2011)

EMOTION PROCESSING							
Brain Network	*Brain Region*	*MNI coordinates (x, y, z)*	*CS*	↓/↑	*Parameter*	*Subjects SCZ / HC (n)*	*Study*
SMN	Heschl's gyrus R [Superior temporal gyrus R]	50, -20, 4	89	↓	TBA (Emotion processing: perception)	450/422	Taylor et al. (2012)
SN	Anterior cingulate gyrus R	2, 26, 30	560	↓	TBA (Emotion processing: emotion recognition)	199/215	Jáni et al. (2018)
	Inferior frontal gyrus R [Dorsolateral frontal cortex R]	48, 12, 12	118	↓	TBA (Emotion processing: perception)	450/422	Taylor et al. (2012)
DMN	Anterior cingulate gyrus R*	16, 32, 14	347	↓	TBA (Emotion processing: perception)	450/422	Taylor et al. (2012)
	Frontal pole R [Inferior frontal gyrus R]	48, 34, -6	5611	↓	TBA (Emotion processing: emotion recognition)	199/ 215	Jáni et al. (2018)
	Inferior frontal gyrus R	49, 27, 5	664	↓	TBA (Emotion processing: empathy)	240/242	Vucurovic et al. (2020)
	Precuneus L [Cingulum L]	-10, -58, 40	11	↑	TBA (Emotion processing: emotion recognition)	199/ 215	Jáni et al. (2018)
CEN	Superior frontal gyrus R [Medial frontal cortex R]	4, 22, 52	122	↓	TBA (Emotion processing: perception)	450/422	Taylor et al. (2012)
	Superior frontal gyrus R	9, 19, 56	288	↓	TBA (Emotion processing: faces)	268/243	Li et al. (2010)
DAN	Precentral gyrus R*	50, 0, 28	215	↑	TBA (Emotion processing: perception)	450/422	Taylor et al. (2012)
	Precentral gyrus R [Middle frontal gyrus R]	44, -4, 56	65	↑	TBA (Emotion processing: emotion recognition)	199/215	Jáni et al. (2018)
	Postcentral gyrus L	-46, -32, 48	1243	↑	TBA (Emotion processing: emotion recognition)	199/ 215	Jáni et al. (2018)
	Superior parietal lobule L	-36, -44, 54	204	↑	TBA (Emotion processing: perception)	450/422	Taylor et al. (2012)

VN	Occipital pole L	-10, -100, -6	146	↓	TBA (Emotion processing: perception)	450/422	Taylor et al. (2012)
	Lateral occipital cortex (superior division) L [Occipital pole L]*	-34, -70, 16	34	↓	TBA (Emotion processing: experience)	450/422	Taylor et al. (2012)
	Lateral occipital cortex (inferior division) L [Middle occipital gyrus L]	47, -73, -1	208	↓	TBA (Emotion processing: faces)	268/243	Li et al. (2010)
	Lateral occipital cortex (inferior division) R [Occipital pole R]	32, -86, -10	413	↓	TBA (Emotion processing: perception)	450/422	Taylor et al. (2012)
	Occipital fusiform gyrus L	-34, -76, -12	340	↓	TBA (Emotion processing: perception)	450/422	Taylor et al. (2012)
	Occipital fusiform gyrus L	-39, -65, -21	1768	↓	TBA (Emotion processing: faces)	268/243	Li et al. (2010)
	Occipital fusiform gyrus L	-36, -70, -8	343	↓	TBA (Emotion processing: faces)	906/888	McTeague et al. (2020)
	Occipital fusiform gyrus R	38, -64, -18	408	↓	TBA (Emotion processing: faces)	268/243	Li et al. (2010)
	Occipital fusiform gyrus R	32, -78, -6	416	↓	TBA (Emotion processing: faces)	906/888	McTeague et al. (2020)
	Temporal occipital fusiform gyrus R	38, -44, -18	12	↓	TBA (Emotion processing: perception)	450/422	Taylor et al. (2012)
	Temporal occipital fusiform gyrus R	41, -49, -23	408	↓	TBA (Emotion processing: faces)	268/243	Li et al. (2010)
	Temporal fusiform gyrus R	28, -36, -18	32	↓	TBA (Emotion processing: perception)	450/422	Taylor et al. (2012)
	Cuneus L	-4, -88, 32	439	↑	TBA (Emotion processing: perception)	450/422	Taylor et al. (2012)
	Supracalcarine cortex R	8, -82, 16	301	↑	TBA (Emotion processing: faces)	906/888	McTeague et al. (2020)
	Lateral occipital cortex (superior division) L [Middle occipital gyrus L]	-28, -88, 22	12	↑	TBA (Emotion processing: emotion recognition)	199/ 215	Jáni et al. (2018)

LN	Temporal pole L [Superior temporal gyrus L]	-44, 4, -18	266	↑	TBA (Emotion processing: perception)	450/422	Taylor et al. (2012)
	Temporal pole R	34, 12, -24	59	↓	TBA (Emotion processing: perception)	450/422	Taylor et al. (2012)
SUBCORTICAL STRUCTURES	Hippocampus L	24, -12, -18	515	↓	TBA (Emotion processing: perception)	450/422	Taylor et al. (2012)
	Amygdala L	-22, -6, -20	305	↓	TBA (Emotion processing: perception)	450/422	Taylor et al. (2012)
	Amygdala L	-27, -8, -20	272	↓	TBA (Emotion processing: faces)	268/243	Li et al. (2010)
	Amygdala L	-23, -3, -15	464	↓	TBA (Emotion processing: faces)	268/243	Li et al. (2010)
	Amygdala R	27, -6, -19	368	↓	TBA (Emotion processing: faces)	268/243	Li et al. (2010)
	Amygdala R [Lentiform nucleus R]	24, -2, -13	424	↓	TBA (Emotion processing: faces)	268/243	Li et al. (2010)
	Thalamus L	-2, -18, 2	416	↓	TBA (Emotion processing: faces)	906/888	McTeague et al. (2020)
	Thalamus R	17, -16, 17	448	↓	TBA (Emotion processing)	436/412	Zhang et al. (2016)
	Thalamus R	10, -10, 12	21	↓	TBA (Emotion processing: perception)	450/422	Taylor et al. (2012)
	Thalamus R [Caudate R]*	16, -4, 12	18	↓	TBA (Emotion processing: perception)	450/422	Taylor et al. (2012)
	Brainstem L/R	0, -22, -6	51	↓	TBA (Emotion processing: perception)	450/422	Taylor et al. (2012)
	Brainstem R	4, -28, -12	62	↓	TBA (Emotion processing: perception)	450/422	Taylor et al. (2012)
	Cerebellum L	-16, -32, -22	11	↓	TBA (Emotion processing: perception)	450/422	Taylor et al. (2012)

EMOTION PROCESSING OF NEUTRAL STIMULI							
Brain Network	*Brain Region*	*MNI coordinates (x, y, z)*	*CS*	↓/↑	*Parameter*	*Subjects SCZ / HC (n)*	*Study*
SMN	Precentral gyrus L [Postcentral gyrus L]	-46, -12, 34	212	↑	TBA (Emotion processing of neutral stimuli)	304/290	Dugré et al. (2019)
CEN	Middle frontal gyrus R	48, 20, 38	360	↓	TBA (Emotion processing of neutral stimuli)	304/290	Dugré et al. (2019)
VN	Occipital fusiform gyrus R	36, -70, -10	300	↓	TBA (Emotion processing of neutral stimuli)	304/290	Dugré et al. (2019)
SUBCORTICAL STRUCTURES	Putamen L	-30, 2, -2	1338	↑	TBA (Emotion processing of neutral stimuli)	304/290	Dugré et al. (2019)
	Putamen R	32, 2, 2	924	↑	TBA (Emotion processing of neutral stimuli)	304/290	Dugré et al. (2019)
EMOTION PROCESSING OF NEGATIVE STIMULI							
Brain Network	*Brain Region*	*MNI coordinates (x, y, z)*	*CS*	↓/↑	*Parameter*	*Subjects SCZ / HC (n)*	*Study*
DMN	Anterior cingulate gyrus L	-2, 36, -6	2573	↑	TBA (Emotion processing of negative stimuli: threatening faces)	354/374	Dong et al. (2018)
CEN	Inferior frontal gyrus L	54, 18, 16	699	↓	TBA (Emotion processing of negative stimuli: threatening faces)	354/374	Dong et al. (2018)
VN	Temporal occipital fusiform gyrus R	30, -40, -24	514	↓	TBA (Emotion processing of negative stimuli: threatening faces)	354/374	Dong et al. (2018)
SUBCORTICAL STRUCTURES	Amygdala L*	-14, -8, -12	1615	↓	TBA (Emotion processing of negative stimuli: threatening faces)	354/374	Dong et al. (2018)

	Amygdala R*	22, -14, -8	1408	↓	TBA (Emotion processing of negative stimuli: threatening faces)	354/374	Dong et al. (2018)
	Thalamus R	4, -8, -2	393	↓	TBA (Emotion processing of negative stimuli: threatening faces)	354/374	Dong et al. (2018)
	Cerebellum L	-32, -38, -28	1811	↓	TBA (Emotion processing of negative stimuli; threatening faces)	354/374	Dong et al. (2018)

EMOTION PROCESSING OF POSITIVE STIMULI

Brain Network	*Brain Region*	*MNI coordinates (x, y, z)*	*CS*	↓/↑	*Parameter*	*Subjects SCZ / HC (n)*	*Study*
SMN	Superior temporal gyrus R	62, 0, -4	30	↓	TBA (Emotion processing of positive stimuli: reward anticipation)	368/428	Zeng et al. (2022)
	Postcentral gyrus R	52, -18, 56	31	↑	TBA (Emotion processing of positive stimuli: reward outcome)	368/428	Zeng et al. (2022)
SN	Anterior cingulate gyrus L/R	0, 12, 24	1931	↓	TBA (Emotion processing of positive stimuli: reward anticipation)	368/428	Zeng et al. (2022)
DMN	Paracingulate gyrus L/R [Anterior cingulate cortex L/R]	0, 50, 10	640	↓	TBA (Emotion processing of positive stimuli: anticipatory reward)	436/412	Zhang et al. (2016)
	Paracingulate gyrus L [Medial prefrontal cortex L]	-10, 52, 6	817	↓	TBA (Emotion processing of positive stimuli: reward outcome)	368/428	Zeng et al. (2022)
	Frontal pole L [Dorsolateral prefrontal cortex L]	-24, 56, 20	422	↓	TBA (Emotion processing of positive stimuli: reward outcome)	368/428	Zeng et al. (2022)
CEN	Superior frontal gyrus R [Dorsolateral prefrontal cortex R]	22, 20, 62	143	↓	TBA (Emotion processing of positive stimuli; reward	368/428	Zeng et al. (2022)

					outcome)		
	Paracingulate gyrus R [Middle cingulate cortex R]	8, 34, 30	20	↑	TBA (Emotion processing of positive stimuli; reward outcome)	368/428	Zeng et al. (2022)
DAN	Precentral gyrus R	50, 4, 36	244	↓	TBA (Emotion processing of positive stimuli: reward anticipation)	368/428	Zeng et al. (2022)
SUBCORTICAL STRUCTURES	Amygdala R [Parahippocampal gyrus R]	30, -4, -26	176	↑	TBA (Emotion processing of positive stimuli: reward outcome)	368/428	Zeng et al. (2022)
	Caudate L	-6, 11, 0	400	↓	TBA (Emotion processing of positive stimuli; consummatory reward)	436/412	Zhang et al. (2016)
	Caudate L	-8, 4, 6	2956	↓	TBA (Emotion processing of positive stimuli: reward anticipation)	368/428	Zeng et al. (2022)
	Caudate R	10, 12, -2	181	↓	TBA (Emotion processing of positive stimuli: reward)	471/482	Chase et al. (2018)
	Accumbens R	10, 13, -8	1048	↓	TBA (Emotion processing of positive stimuli: anticipatory reward)	436/412	Zhang et al. (2016)
	Putamen L	-14, 11, -6	2408	↓	TBA (Emotion processing of positive stimuli; anticipatory reward)	436/412	Zhang et al. (2016)
	Putamen L*	-23, 12, 11	592	↓	TBA (Emotion processing of positive stimuli: consummatory reward)	436/412	Zhang et al. (2016)
	Putamen L	-22, 0, 2	439	↑	TBA (Emotion processing of positive stimuli: reward outcome)	368/428	Zeng et al. (2022)
	Putamen R*	28, 10, -14	590	↑	TBA (Emotion processing of positive stimuli: reward outcome)	368/428	Zeng et al. (2022)

	Thalamus L	-13, -24, 1	520	↓	TBA (Emotion processing of positive stimuli: consummatory reward)	436/412	Zhang et al. (2016)
	Brainstem R	5, -21, -12	696	↓	TBA (Emotion processing of positive stimuli: consummatory reward)	436/412	Zhang et al. (2016)
	Brainstem L [Cerebellum L]	-8, -36, -18	194	↑	TBA (Emotion processing of positive stimuli: reward outcome)	368/428	Zeng et al. (2022)
COGNITIVE PROCESSING							
Brain Network	*Brain Region*	*MNI coordinates (x, y, z)*	*CS*	↓/↑	*Parameter*	*Subjects SCZ / HC (n)*	*Study*
DMN	Frontal orbital cortex R [Insula/Ventrolateral prefrontal cortex R]	44, 28, -12	309	↓	TBA (Cognitive processing)	2906/2622	McTeague et al. (2017)
	Frontal pole R [Inferior frontal gyrus R]	48, 36, -8	157	↓	TBA (Cognitive processing)	3446/3723	Picó-Pérez et al. (2022)
	Middle frontal gyrus L	-44, 14, 40	121	↓	TBA (Cognitive processing)	1086/1182	Alústiza et al. (2017)
CEN	Middle frontal gyrus L	-48, 24, 26	686	↓	TBA (Cognitive processing)	2906/2622	McTeague et al. (2017)
	Middle frontal gyrus R	52, 26, 34	443	↓	TBA (Cognitive processing)	1086/1182	Alústiza et al. (2017)
	Middle frontal gyrus R	26, 18, 52	22	↓	TBA (Cognitive processing)	1086/1182	Alústiza et al. (2017)
	Superior frontal gyrus L/R [Dorsomedial prefrontal cortex/Supplementary motor area L/R]	0, 24, 52	704	↓	TBA (Cognitive processing)	3446/3723	Picó-Pérez et al. (2022)
	Paracingulate gyrus L	-4, 30, 30	2004	↓	TBA (Cognitive processing)	1086/1182	Alústiza et al. (2017)
	Supramarginal gyrus L [Inferior parietal gyrus L]	-44, -46, 52	598	↓	TBA (Cognitive processing)	1086/1182	Alústiza et al. (2017)

DAN	Precentral gyrus L	-30, -8, 54	106	↑	TBA (Cognitive processing)	1086/1182	Alústiza et al. (2017)
	Precentral gyrus R	26, -8, 50	18	↑	TBA (Cognitive processing)	1086/1182	Alústiza et al. (2017)
VN	Lateral occipital cortex (superior division) R [Middle occipital gyrus R]	30, -80, 28	171	↑	TBA (Cognitive processing)	1086/1182	Alústiza et al. (2017)
SUBCORTICAL STRUCTURES	Thalamus R	8, -18, 6	263	↓	TBA (Cognitive processing)	1086/1182	Alústiza et al. (2017)
	Cerebellum L	-28, -68, -34	280	↓	TBA (Cognitive processing)	1086/1182	Alústiza et al. (2017)
COGNITIVE PROCESSING OF EPISODIC MEMORY							
Brain Network	*Brain Region*	*MNI coordinates (x, y, z)*	*CS*	*↓/↑*	*Parameter*	*Subjects SCZ / HC (n)*	*Study*
SMN	Postcentral gyrus L [Precentral gyrus L]	-27, -31, 74	1296	↑	TBA (Cognitive processing of episodic memory: retrieval)	248/231	Ragland et al. (2009)
	Precentral gyrus L	-47, -10, 43	2704	↑	TBA (Cognitive processing of episodic memory: encoding)	248/231	Ragland et al. (2009)
SN	Frontal opercular cortex L [Inferior frontal gyrus L]*	-37, 28, 11	1424	↓	TBA (Cognitive processing of episodic memory: encoding)	248/231	Ragland et al. (2009)
	Anterior cingulate gyrus L	-3, 5, 41	1368	↑	TBA (Cognitive processing of episodic memory: encoding)	248/231	Ragland et al. (2009)
DMN	Subcallosal cortex R [Anterior cingulate gyrus R]	5, 30, -8	888	↓	TBA (Cognitive processing of episodic memory: retrieval)	248/231	Ragland et al. (2009)
	Posterior cingulate gyrus R	4, -38, 33	896	↓	TBA (Cognitive processing of episodic memory: encoding)	248/231	Ragland et al. (2009)
	Precuneus R [Posterior cingulate gyrus R]	10, -54, 19	520	↓	TBA (Cognitive processing of episodic memory: retrieval)	248/231	Ragland et al. (2009)

	Middle temporal gyrus L	-60, -42, -6	560	↓	TBA (Cognitive processing of episodic memory: retrieval)	248/231	Ragland et al. (2009)
	Angular gyrus R [Inferior parietal gyrus R]	49, -51, 38	1056	↓	TBA (Cognitive processing of episodic memory: encoding)	248/231	Ragland et al. (2009)
	Paracingulate gyrus R [Medial frontal gyrus R]	13, 47, 11	1168	↑	TBA (Cognitive processing of episodic memory: retrieval)	248/231	Ragland et al. (2009)
	Frontal pole R [Middle frontal gyrus R]	36, 41, -21	600	↑	TBA (Cognitive processing of episodic memory: retrieval)	248/231	Ragland et al. (2009)
CEN	Middle frontal gyrus L	-39, 31, 41	888	↓	TBA (Cognitive processing of episodic memory: retrieval)	248/231	Ragland et al. (2009)
	Inferior frontal gyrus L	-42, 23, 20	3048	↓	TBA (Cognitive processing of episodic memory: retrieval)	248/231	Ragland et al. (2009)
	Inferior frontal gyrus R*	41, 31, 10	2760	↓	TBA (Cognitive processing of episodic memory: encoding)	248/231	Ragland et al. (2009)
	Superior frontal gyrus R	6, 34, 53	1104	↓	TBA (Cognitive processing of episodic memory: encoding)	248/231	Ragland et al. (2009)
	Frontal pole R [Superior frontal gyrus R]	23, 50, 15	4608	↓	TBA (Cognitive processing of episodic memory: encoding)	248/231	Ragland et al. (2009)
	Precentral gyrus L*	-37, -2, 29	1064	↓	TBA (Cognitive processing of episodic memory: retrieval)	248/231	Ragland et al. (2009)
DAN	Inferior temporal gyrus L [Middle temporal gyrus L]	-47, -41, -15	352	↑	TBA (Cognitive processing of episodic memory: encoding)	248/231	Ragland et al. (2009)
	Middle temporal gyrus R	61, -58, -6	336	↑	TBA (Cognitive processing of episodic memory: retrieval)	248/231	Ragland et al. (2009)
	Supramarginal gyrus L [Postcentral gyrus L]	-45, -30, 38	344	↑	TBA (Cognitive processing of episodic memory:	248/231	Ragland et al. (2009)

					encoding)		
VN	Occipital pole R [Cuneus R]	16, -89, 6	2568	↓	TBA (Cognitive processing of episodic memory: retrieval)	248/231	Ragland et al. (2009)
	Occipital fusiform gyrus R [Lingual gyrus R]	18, -88, -6	1192	↓	TBA (Cognitive processing of episodic memory: encoding)	248/231	Ragland et al. (2009)
	Temporal occipital fusiform gyrus L [Parahippocampal gyrus L]	-30, -50, -10	304	↑	TBA (Cognitive processing of episodic memory: encoding)	248/231	Ragland et al. (2009)
SUBCORTICAL STRUCTURES	Hippocampus R [Thalamus R]*	27, -30, 3	792	↑	TBA (Cognitive processing of episodic memory: retrieval)	248/231	Ragland et al. (2009)
	Thalamus L*	-5, -8, 18	1496	↓	TBA (Cognitive processing of episodic memory: retrieval)	248/231	Ragland et al. (2009)
	Thalamus R	8, -24, 8	1448	↓	TBA (Cognitive processing of episodic memory: retrieval)	248/231	Ragland et al. (2009)
	Cerebellum L	-25, -59, -53	1488	↓	TBA (Cognitive processing of episodic memory: retrieval)	248/231	Ragland et al. (2009)
	Cerebellum R	29, -79, -45	624	↓	TBA (Cognitive processing of episodic memory: retrieval)	248/231	Ragland et al. (2009)
COGNITIVE PROCESSING OF WORKING MEMORY							
Brain Network	*Brain Region*	*MNI coordinates (x, y, z)*	*CS*	↓/↑	*Parameter*	*Subjects SCZ / HC (n)*	*Study*
SMN	Precentral gyrus R	20, -26, 66	329	↑	TBA (Cognitive processing of working memory)	1126/1139	Wang et al. (2021)
SN	Supplementary motor cortex L [Superior frontal gyrus L]	-7, 7, 55	1056	↑	TBA (Cognitive processing of working memory)	971/1028	Wu et al. (2019)
DMN	Middle frontal gyrus L	-38, 8, 52	587	↓	TBA (Cognitive processing of working memory)	1126/1139	Wang et al. (2021)
	Anterior cingulate gyrus L/R	0, 42, -3	784	↑	TBA (Cognitive processing of	971/1028	Wu et al. (2019)

					working memory)		
	Paracingulate gyrus L	-4, 48, 6	3899	↑	TBA (Cognitive processing of working memory)	1126/1139	Wang et al. (2021)
	Posterior cingulate gyrus L	0, -42, 22	620	↑	TBA (Cognitive processing of working memory)	1126/1139	Wang et al. (2021)
	Posterior cingulate gyrus L	-9, -34, 34	544	↑	TBA (Cognitive processing of working memory)	971/1028	Wu et al. (2019)
	Angular gyrus L [Inferior parietal lobule L]	-52, -57, 42	1408	↑	TBA (Cognitive processing of working memory)	971/1028	Wu et al. (2019)
CEN	Middle frontal gyrus R	45, 13, 32	2368	↓	TBA (Cognitive processing of working memory)	971/1028	Wu et al. (2019)
	Inferior frontal gyrus L	-48, 11, 22	1560	↓	TBA (Cognitive processing of working memory)	971/1028	Wu et al. (2019)
	Superior frontal gyrus R [Supplementary motor area R]	6, 24, 50	880	↓	TBA (Cognitive processing of working memory)	1126/1139	Wang et al. (2021)
	Frontal orbital cortex R [Inferior frontal gyrus R]	32, 24, -9	1008	↓	TBA (Cognitive processing of working memory)	971/1028	Wu et al. (2019)
	Insula L [Claustrum L]	-31, 22, -6	768	↓	TBA (Cognitive processing of working memory)	971/1028	Wu et al. (2019)
	Precuneus L	-6, -70, 50	171	↓	TBA (Cognitive processing of working memory)	1126/1139	Wang et al. (2021)
VN	Occipital pole R [Superior occipital gyrus R]	22, -96, 18	57	↑	TBA (Cognitive processing of working memory)	1126/1139	Wang et al. (2021)
LN	Temporal pole L	-28, 8, -38	105	↑	TBA (Cognitive processing of working memory)	1126/1139	Wang et al. (2021)
	Temporal pole R	24, 12, -42	259	↑	TBA (Cognitive processing of working memory)	1126/1139	Wang et al. (2021)
SUBCORTICAL STRUCTURES	Caudate R*	12, 4, 10	211	↓	TBA (Cognitive processing of working memory)	1126/1139	Wang et al. (2021)

	Putamen R	26, 12, 6	579	↓	TBA (Cognitive processing of working memory)	1126/1139	Wang et al. (2021)
	Cerebellum R	8, -64 -36	3382	↓	TBA (Cognitive processing of working memory)	1126/1139	Wang et al. (2021)
COGNITIVE PROCESSING OF TIMING							
Brain Network	*Brain Region*	*MNI coordinates (x, y, z)*	*CS*	↓/↑	*Parameter*	*Subjects SCZ / HC (n)*	*Study*
SMN	Planum polare R [Precentral gyrus R]	51, -4, 1	1208	↓	TBA (Cognitive processing of timing: time estimation)	29/35	Ortuño et al. (2011)
SN	Paracingulate gyrus L [Anterior cingulate gyrus L]	-10, 25, 30	392	↓	TBA (Cognitive processing of timing: time estimation)	29/35	Ortuño et al. (2011)
DMN	Frontal pole R [Superior frontal gyrus R]	17, 38, 37	560	↓	TBA (Cognitive processing of timing: time estimation)	29/35	Ortuño et al. (2011)
	Frontal pole R [Superior frontal gyrus R]	15, 70, 11	128	↓	TBA (Cognitive processing of timing: time estimation)	29/35	Ortuño et al. (2011)
	Frontal orbital cortex R [Inferior frontal gyrus R]	36, 26, -18	75	↑	TBA (Cognitive processing of timing)	200/195	Alústiza et al. (2017)
	Temporal pole R	48, 14, -28	31	↑	TBA (Cognitive processing of timing)	200/195	Alústiza et al. (2017)
CEN	Middle frontal gyrus R	36, 34, 42	224	↓	TBA (Cognitive processing of timing: time estimation)	29/35	Ortuño et al. (2011)
	Paracingulate gyrus R [Supplementary motor area R]	4, 16, 52	296	↓	TBA (Cognitive processing of timing)	200/195	Alústiza et al. (2017)
	Lateral occipital cortex (superior division) R [Parietal cortex R]	45, -74, 35	504	↓	TBA (Cognitive processing of timing: time estimation)	29/35	Ortuño et al. (2011)
DAN	Lateral occipital cortex (superior division) L [Superior parietal gyrus L]	-22, -72, 44	593	↑	TBA (Cognitive processing of timing)	200/195	Alústiza et al. (2017)
	Lateral occipital cortex (superior division) R [Superior parietal gyrus R]	30, -68, 54	36	↑	TBA (Cognitive processing of timing)	200/195	Alústiza et al. (2017)

VN	Occipital pole L [Superior occipital gyrus L]	-14, -98, 12	636	↓	TBA (Cognitive processing of timing)	200/195	Alústiza et al. (2017)
	Occipital pole R [Inferior occipital gyrus R]	28, -92, -12	567	↓	TBA (Cognitive processing of timing)	200/195	Alústiza et al. (2017)
SUBCORTICAL STRUCTURES	Caudate R	12, 10, 6	1366	↓	TBA (Cognitive processing of timing)	200/195	Alústiza et al. (2017)
	Putamen R	29, -13, -5	1408	↓	TBA (Cognitive processing of timing: time estimation)	29/35	Ortuño et al. (2011)
	Putamen R	20, 6, 6	60	↓	TBA (Cognitive processing of timing)	200/195	Alústiza et al. (2017)
	Thalamus R	9, -6, 9	488	↓	TBA (Cognitive processing of timing: time estimation)	29/35	Ortuño et al. (2011)
COGNITIVE PROCESSING OF EXECUTIVE FUNCTIONS							
Brain Network	*Brain Region*	*MNI coordinates (x, y, z)*	*CS*	*↓/↑*	*Parameter*	*Subjects SCZ / HC (n)*	*Study*
SMN	Precentral gyrus L	-56, 5, 31	752	↑	TBA (Cognitive processing of executive functions)	594/623	Minzenberg et al. (2009)
	Precentral gyrus L [Superior frontal gyrus L]	-9, -20, 76	440	↑	TBA (Cognitive processing of executive functions)	594/623	Minzenberg et al. (2009)
SN	Anterior cingulate gyrus R	2, 17, 37	1704	↓	TBA (Cognitive processing of executive functions)	594/623	Minzenberg et al. (2009)
	Insula R	40, 19, 0	1136	↑	TBA (Cognitive processing of executive functions)	594/623	Minzenberg et al. (2009)
	Paracingulate gyrus L [Cingulate gyrus L]	-3, 9, 44	2208	↑	TBA (Cognitive processing of executive functions)	594/623	Minzenberg et al. (2009)
DMN	Paracingulate gyrus R [Medial frontal gyrus R]	7, 45, 20	1480	↓	TBA (Cognitive processing of executive functions)	594/623	Minzenberg et al. (2009)
	Frontal medial cortex R	9, 50, -12	424	↑	TBA (Cognitive processing of executive functions)	594/623	Minzenberg et al. (2009)

	Superior frontal gyrus L	-2, 54, 28	1320	↑	TBA (Cognitive processing of executive functions)	594/623	Minzenberg et al. (2009)
	Middle temporal gyrus R [Superior temporal gyrus R]*	39, -36, 2	584	↑	TBA (Cognitive processing of executive functions)	594/623	Minzenberg et al. (2009)
CEN	Middle frontal gyrus L	-39, 30, 32	3096	↓	TBA (Cognitive processing of executive functions)	594/623	Minzenberg et al. (2009)
	Middle frontal gyrus R*	32, 22, 44	712	↓	TBA (Cognitive processing of executive functions)	594/623	Minzenberg et al. (2009)
	Frontal orbital cortex L [Claustrum L]	-29, 28, -3	880	↓	TBA (Cognitive processing of executive functions)	594/623	Minzenberg et al. (2009)
	Insula R [Claustrum R]*	27, 25, -1	1776	↓	TBA (Cognitive processing of executive functions)	594/623	Minzenberg et al. (2009)
	Frontal pole L [Inferior frontal gyrus L]	-41, 38, 11	656	↑	TBA (Cognitive processing of executive functions)	594/623	Minzenberg et al. (2009)
	Supramarginal gyrus L [Inferior parietal lobule L]	-54, -46, 44	1200	↑	TBA (Cognitive processing of executive functions)	594/623	Minzenberg et al. (2009)
DAN	Precentral gyrus L [Middle frontal gyrus L]	-30, -9, 48	664	↓	TBA (Cognitive processing of executive functions)	594/623	Minzenberg et al. (2009)
	Lateral occipital cortex (superior division) R [Inferior parietal lobule R]	35, -62, 46	792	↓	TBA (Cognitive processing of executive functions)	594/623	Minzenberg et al. (2009)
VN	Lateral occipital cortex (inferior division) R [Middle occipital gyrus R]	-43, -71, 2	416	↓	TBA (Cognitive processing of executive functions)	594/623	Minzenberg et al. (2009)
	Lingual gyrus R	14, -76, 2	800	↑	TBA (Cognitive processing of executive functions)	594/623	Minzenberg et al. (2009)
SUBCORTICAL STRUCTURES	Amygdala R	19, -2, -19	592	↑	TBA (Cognitive processing of executive functions)	594/623	Minzenberg et al. (2009)
	Putamen R*	21, -3, 13	448	↓	TBA (Cognitive processing of executive functions)	594/623	Minzenberg et al. (2009)
	Thalamus L	-5, -13, 8	1736	↓	TBA (Cognitive processing of	594/623	Minzenberg et al.

					executive functions)		(2009)
COGNITIVE PROCESSING OF THEORY OF MIND							
Brain Network	*Brain Region*	*MNI coordinates (x, y, z)*	*CS*	↓/↑	*Parameter*	*Subjects SCZ / HC (n)*	*Study*
SMN	Planum polare R [Insula R]	50, -2, 0	1340	↓	TBA (Cognitive processing of theory of mind)	262/279	Jáni et al. (2018)
	Central opercular cortex R [Premotor cortex R]	54, -14, 18	1101	↓	TBA (Cognitive processing of theory of mind)	308/315	Kronbichler et al. (2017)
	Postcentral gyrus R [Precentral gyrus R]	46, -12, 34	14	↓	TBA (Cognitive processing of theory of mind)	262/279	Jáni et al. (2018)
	Precentral gyrus R	48, -10, 40	13	↓	TBA (Cognitive processing of theory of mind)	427/405	Weng et al. (2022)
DMN	Paracingulate gyrus L [Medial prefrontal cortex L]	-2, 52, 18	1573	↓	TBA (Cognitive processing of theory of mind)	308/315	Kronbichler et al. (2017)
	Superior frontal gyrus R	8, 52, 28	580	↓	TBA (Cognitive processing of theory of mind)	262/279	Jáni et al. (2018)
	Frontal pole L [Superior frontal gyrus L]	-4, 62, 20	459	↓	TBA (Cognitive processing of theory of mind)	427/405	Weng et al. (2022)
	Angular gyrus R	54, -52, 26	98	↓	TBA (Cognitive processing of social cognition)	1755/1819	Picó-Pérez et al. (2022)
	Superior frontal gyrus R*	18, 24, 46	375	↑	TBA (Cognitive processing of theory of mind)	262/279	Jáni et al. (2018)
CEN	Middle frontal gyrus L [Inferior frontal gyrus L]	-44, 16, 34	203	↑	TBA (Cognitive processing of theory of mind)	262/279	Jáni et al. (2018)
	Supramarginal gyrus L [Inferior parietal cortex L]	-42, -48, 38	486	↑	TBA (Cognitive processing of theory of mind)	308/315	Kronbichler et al. (2017)
	Supramarginal gyrus L [Superior longitudinal fasciculus L]	-44, -46, 38	20	↑	TBA (Cognitive processing of theory of mind)	427/405	Weng et al. (2022)

	Supramarginal gyrus R [Inferior parietal cortex R]	58, -40, 40	405	↑	TBA (Cognitive processing of theory of mind)	308/315	Kronbichler et al. (2017)
	Supramarginal gyrus R [Inferior parietal lobule R]	64, -40, 38	258	↑	TBA (Cognitive processing of theory of mind)	262/279	Jáni et al. (2018)
	Supramarginal gyrus R*	-44, -46, 36	143	↑	TBA (Cognitive processing of theory of mind)	262/279	Jáni et al. (2018)
	Precuneus R*	16, -60, 38	183	↑	TBA (Cognitive processing of theory of mind)	262/279	Jáni et al. (2018)
DAN	Lateral occipital cortex (superior division) L [Lateral occipitotemporal cortex L]	-48, -72, 22	27	↓	TBA (Cognitive processing of theory of mind)	308/315	Kronbichler et al. (2017)
VN	Cuneus L	0, -84, 22	569	↓	TBA (Cognitive processing of theory of mind)	262/279	Jáni et al. (2018)
	Cuneus L	0, -72, 22	209	↓	TBA (Cognitive processing of theory of mind)	427/405	Weng et al. (2022)
	Intracalcarine cortex L [Medial occipitoparietal cortex L]	-4, -76, 14	128	↓	TBA (Cognitive processing of theory of mind)	308/315	Kronbichler et al. (2017)
	Lateral occipital cortex (inferior division) L [Middle temporal gyrus L]	-48, -70, 10	1408	↓	TBA (Cognitive processing of theory of mind)	274/286	Vucurovic et al. (2020)
	Lateral occipital cortex (inferior division) L [Middle temporal gyrus L]	-46, -66, 12	1080	↓	TBA (Cognitive processing of theory of mind)	292/305	Arioli et al. (2021)
	Lingual gyrus R	12, -58, 2	99	↓	TBA (Cognitive processing of theory of mind)	308/315	Kronbichler et al. (2017)
	Lingual gyrus R	12, -60, 4	71	↓	TBA (Cognitive processing of theory of mind)	262/279	Jáni et al. (2018)
	Posterior cingulate gyrus L	-18, -44, -2	24	↓	TBA (Cognitive processing of theory of mind)	308/315	Kronbichler et al. (2017)
LN	Frontal orbital cortex L	-30, 22, -24	30	↓	TBA (Cognitive processing of theory of mind)	308/315	Kronbichler et al. (2017)

STRUCTURAL-FUNCTIONAL BRAIN CORRELATES OF SYMPTOMS OF SCHIZOPHRENIA							
AUDITORY HALLUCINATIONS							
Brain Network	*Brain Region*	*MNI coordinates (x, y, z)*	*CS*	↓/↑	*Parameter*	*Subjects SCZ / HC (n)*	*Study*
SMN	Central opercular cortex L [Supramarginal gyrus L]	-55, -20, 14	304	↑	Activation during auditory hallucinations	68	Jardri et al. (2011)
	Central opercular cortex L [Parietal operculum L]	-58, -19, 15	334	↑	Activation during auditory hallucinations	85	Kuhn and Gallinat (2012)
	Central opercular cortex R [Insula R]	40, 0, 12	352	↑	Activation during auditory hallucinations	161	Zmigrod et al. (2016)
	Temporal pole R [Insula R]	47, 10, -10	964	↑	Activation during auditory hallucinations	68	Jardri et al. (2011)
	Supramarginal gyrus L [Superior temporal gyrus L]	-56, -45, 14	800	↑	Activation during auditory hallucinations	68	Jardri et al. (2011)
	Postcentral gyrus L	-46, -18, 44	2104	↑	Activation during auditory hallucinations	161	Zmigrod et al. (2016)
	Postcentral gyrus L	-50, -19, 44	256	↑	Activation during auditory hallucinations	85	Kuhn and Gallinat (2012)
	Precentral gyrus L	-57, 2, 13	488	↑	Activation during auditory hallucinations	68	Jardri et al. (2011)
SN	Central opercular cortex L [Insula L]	-46, 0, 3	2656	↑	Activation during auditory hallucinations	88	Kompus et al. (2011)
	Central opercular cortex L [Insula L]	-44, 2, 3	1240	↑	Activation during auditory hallucinations	68	Jardri et al. (2011)
	Central opercular cortex L [Superior temporal gyrus L]	-55, -22, 15	952	↑	Activation during auditory hallucinations	88	Kompus et al. (2011)
	Central opercular cortex L [Inferior frontal gyrus L]	-51, 5, 3	208	↑	Activation during auditory hallucinations	85	Kuhn and Gallinat (2012)

	Frontal opercular cortex R [Inferior frontal gyrus R]	42, 14, 13	408	↑	Activation during auditory hallucinations	88	Kompus et al. (2011)
	Middle temporal gyrus R	59, -45, 11	200	↑	Activation during auditory hallucinations	88	Kompus et al. (2011)
	Temporal pole R [Superior temporal gyrus R]	54, 12, -6	1608	↑	Activation during auditory hallucinations	161	Zmigrod et al. (2016)
	Supramarginal gyrus L [Superior temporal gyrus L]	-58, -46, 20	792	↑	Activation during auditory hallucinations	161	Zmigrod et al. (2016)
	Precentral gyrus L	-56, 4, 12	1392	↑	Activation during auditory hallucinations	161	Zmigrod et al. (2016)
	Frontal pole R [Superior frontal gyrus R]	27, 42, 28	240	↑	Activation during auditory hallucinations	88	Kompus et al. (2011)
	Paracingulate gyrus L [Medial frontal gyrus L]	0, 12, 46	344	↑	Activation during auditory hallucinations	161	Zmigrod et al. (2016)
	Supplementary motor cortex R [Medial frontal gyrus R]	6, 6, 60	664	↑	Activation during auditory hallucinations	161	Zmigrod et al. (2016)
DMN	Middle temporal gyrus R	60, -32, -6	224	↑	Activation during auditory hallucinations	161	Zmigrod et al. (2016)
	Middle temporal gyrus R	57, -31, -11	368	↑	Activation during auditory hallucinations	88	Kompus et al. (2011)
CEN	Inferior frontal gyrus L [Broca's convolution L]	-50, 13, 5	1312	↑	Activation during auditory hallucinations	68	Jardri et al. (2011)
	Inferior frontal gyrus R	56, 16, 8	752	↑	Activation during auditory hallucinations	161	Zmigrod et al. (2016)
DAN	Postcentral gyrus L	-51, -26, 43	1016	↑	Activation during auditory hallucinations	88	Kompus et al. (2011)
	Postcentral gyrus R	35, -36, 55	216	↑	Activation during auditory hallucinations	85	Kuhn and Gallinat (2012)
	Supramarginal gyrus R [Postcentral gyrus R]	60, -22, 44	1048	↑	Activation during auditory hallucinations	161	Zmigrod et al. (2016)
	Superior parietal lobule R [Inferior parietal lobule R]	31, -44, 53	960	↑	Activation during auditory hallucinations	88	Kompus et al. (2011)

LN	Temporal pole R [Frontal operculum R]	44, 17, -17	265	↑	Activation during auditory hallucinations	68	Jardri et al. (2011)
SUBCORTICAL STRUCTURES	Hippocampus L	-26, -31, -10	1664	↑	Activation during auditory hallucinations	68	Jardri et al. (2011)
	Hippocampus L	-26, -31, -10	1064	↑	Activation during auditory hallucinations	88	Kompus et al. (2011)
	Hippocampus L [Parahippocampal gyrus L]*	-26, -32, -4	792	↑	Activation during auditory hallucinations	161	Zmigrod et al. (2016)
	Thalamus L	-12, -20, 4	888	↑	Activation during auditory hallucinations	161	Zmigrod et al. (2016)
	Thalamus R*	18, -10, 2	216	↑	Activation during auditory hallucinations	161	Zmigrod et al. (2016)
	Cerebellum R	26, -54, -20	1024	↑	Activation during auditory hallucinations	161	Zmigrod et al. (2016)
	Cerebellum R	26, -62, -46	560	↑	Activation during auditory hallucinations	161	Zmigrod et al. (2016)
	Cerebellum R	21, -45, -24	248	↑	Activation during auditory hallucinations	88	Kompus et al. (2011)
SN	Supplementary motor cortex L [Anterior cingulate gyrus L]	-10, 3, 40	112	↓	TBA (Auditory perception/imagery)	120/69	Kuhn and Gallinat (2012)
	Supplementary motor cortex L [Premotor cortex L]*	-11, -1, 62	376	↓	TBA (Auditory perception/imagery)	120/69	Kuhn and Gallinat (2012)
DMN	Superior temporal gyrus L	-47, -21, -5	152	↓	TBA (Auditory perception/imagery)	120/69	Kuhn and Gallinat (2012)
	Middle temporal gyrus L	-60, -29, -5	424	↓	TBA (Auditory perception/imagery)	120/69	Kuhn and Gallinat (2012)
CEN	Inferior frontal gyrus L [Anterior cingulate gyrus L]	-44, 4, 17	152	↓	TBA (Auditory perception/imagery)	120/69	Kuhn and Gallinat (2012)
	Paracingulate gyrus L [Anterior cingulate gyrus L]	-5, 26, 33	160	↓	TBA (Auditory perception/imagery)	120/69	Kuhn and Gallinat (2012)

SMN	Central opercular cortex R [Superior temporal gyrus/Insula R]	62, -5, 7	318	↓	GM (Auditory hallucinations)	350	Palaniyappan et al. (2012)
SN	Insula L [Insula/Superior temporal gyrus/Inferior frontal gyrus L]	-44, -2, -1	717	↓	GM (Auditory hallucinations)	350	Palaniyappan et al. (2012)
VISUAL HALLUCINATIONS							
Brain Network	*Brain Region*	*MNI coordinates (x, y, z)*	*CS*	*↓/↑*	*Parameter*	*Subjects SCZ / HC (n)*	*Study*
VN	Cuneus R	4, -76, 30	1360	↑	Activation during visual hallucinations	16	Zmigrod et al. (2016)
	Intracalcarine cortex L [Cuneus L]	-4, -76, 16	648	↑	Activation during visual hallucinations	16	Zmigrod et al. (2016)
	Lateral occipital cortex (superior division) L [Cuneus L]	-14, -80, 40	760	↑	Activation during visual hallucinations	16	Zmigrod et al. (2016)
	Lingual gyrus L	-14, -62, 4	904	↑	Activation during visual hallucinations	16	Zmigrod et al. (2016)
	Lingual gyrus R	12, -62, 4	1672	↑	Activation during visual hallucinations	16	Zmigrod et al. (2016)
	Lingual gyrus R	20, -60, -4	1056	↑	Activation during visual hallucinations	16	Zmigrod et al. (2016)
	Occipital fusiform gyrus R [Cerebellum R]	32, -84, -16	736	↑	Activation during visual hallucinations	16	Zmigrod et al. (2016)
FORMAL THOUGHT DEFICITS							
Brain Network	*Brain Region*	*MNI coordinates (x, y, z)*	*CS*	*↓/↑*	*Parameter*	*Subjects SCZ / HC (n)*	*Study*
SMN	Planum temporale L [Superior temporal gyrus L]	-54, -32, 9	114	↓	TBA during verbal processing (Formal thought deficits)	165	Wensing et al. (2017)
SN	Middle temporal gyrus L*	-46, -54, 3	72	↓	TBA during verbal processing (Formal thought deficits)	165	Wensing et al. (2017)

MOTOR DEFICITS							
Brain Network	*Brain Region*	*MNI coordinates (x, y, z)*	*CS*	↓/↑	*Parameter*	*Subjects SCZ / HC (n)*	*Study*
SMN	Precentral gyrus L	-57, -8, 43	424	↓	GM (Motor deficits)	303	Zhao et al. (2014)
	Precentral gyrus L	-46, -11, 54	296	↓	GM (Motor deficits)	303	Zhao et al. (2014)
	Precentral gyrus R	57, -6, 42	280	↓	GM (Motor deficits)	303	Zhao et al. (2014)
	Postcentral gyrus L	-48, -29, 57	224	↓	GM (Motor deficits)	303	Zhao et al. (2014)
DMN	Inferior frontal gyrus L	-56, 21, 20	280	↓	GM (Motor deficits)	303	Zhao et al. (2014)
CEN	Supramarginal gyrus L [Inferior parietal lobule L]	-50, -43, 47	184	↓	GM (Motor deficits)	303	Zhao et al. (2014)
DAN	Lateral occipital cortex (superior division) R [WM near middle temporal gyrus R]	43, -71, 21	288	↓	WM (Motor deficits)	303	Zhao et al. (2014)
SUBCORTICAL STRUCTURES	Thalamus R	2, -12, 13	308	↓	GM (Motor deficits)	303	Zhao et al. (2014)

Notes:
Peak coordinates of each brain region are mapped onto the seven large-scale brain network parcellation proposed by Yeo et al. (2011). Brain regions are named in accordance with the Harvard-Oxford Cortical Structural Atlas and Harvard-Oxford Subcortical Structural Atlas (the name of brain regions from the studies is reported in square brackets when not perfectly matching the atlases' name)
* Peak in white matter (or ventricles)
# Medication-naïve
† Including mixed samples of patients in the chronic and early stages
Abbreviations: CHR, clinical high risk for schizophrenia; SCZ, schizophrenia; HC, healthy controls; n, sample size; NS, not specified; MNI, Montreal neurological institute; CS, cluster size; fMRI, functional magnetic resonance imaging; PET, positron emission tomography; SPECT, single photon emission computed tomography; sMRI, structural MRI; dMRI, diffusion MRI; R, right; L, left; SMN, somatomotor network; SN, salience network; DMN, default-mode network; CEN, central executive network; DAN, dorsal attention network; VN, visual network; LN, limbic network; GM, grey matter; WM, white matter; FA, fractional anisotropy; ALFF, amplitude of low-frequency fluctuations; ReHo, regional homogeneity; FC, functional connectivity; CM, cerebral metabolism; CBF, cerebral blood flow; CP, combined parameters; TBA, task-based activation; ↑, increase; ↓, decrease.

Supplementary Table 4

STRUCTURAL-FUNCTIONAL BRAIN ALTERATIONS IN PRODROME OF SCHIZOPHRENIA						
Alterations	**Study**	**Group**	**JK**	**H**	**PB**	**Main Findings**
Grey matter	Ding at al. (2019)		X	X	X	Decreased GM in medial prefrontal cortex, as well as increased GM in median cingulate, temporal pole, and thalamus, in CHR
	Liloia et al. (2021)					
	Luna et al. (2022)			X		Decreased GM in medial prefrontal cortex in CHR
Task-based activation	Fiorito at al. (2022)			X	X	No TBA alterations in CHR during emotion processing
	Luna et al. (2022)			X		Decreased TBA in medial/lateral prefrontal cortex and occipital cortex in CHR during cognitive or emotion processing
STRUCTURAL-FUNCTIONAL BRAIN ALTERATIONS IN SCHIZOPHRENIA						
Alterations	**Study**	**Group**	**JK**	**H**	**PB**	**Main findings**
Grey matter	Bora et al. (2011)	FE-C			X	Decreased GM in fronto-insular cortex/superior temporal gyrus, anterior cingulate cortex, and thalamus in SCZ; decreased GM in posterior insula/superior temporal gyrus and anterior cingulate cortex in first-episode SCZ
	Brandl et al. (2018)					
	Fornara et al. (2017)					
	Gao et al. (2018)		X		X	Decreased GM in superior temporal gyrus, inferior frontal gyrus, insula, supramarginal gyrus, and fusiform gyrus, as well as increased GM in frontal pole and brainstem, in SCZ
	Goodkind et al. (2015)					
	Huang et al. (2021)		X			Decreased GM in insula, superior temporal gyrus, claustrum, anterior cingulate cortex, and thalamus in SCZ
	Liloia et al. (2021)	FE-C				
	Olabi et al. (2012)	FE				
	Picó-Pérez et al. (2022)	FE-C		X	X	Decreased GM in widespread areas in SCZ; decreased GM in superior temporal gyrus/insula/inferior frontal gyrus in early-stage SCZ
White matter	Bora et al. (2011)	FE-C			X	Decreased WM/FA in corpus callosum, anterior thalamic radiation, inferior frontal occipital fasciculus, inferior longitudinal fasciculus, cingulum, and fornix, in SCZ; decreased WM/FA in fornix, inferior longitudinal fasciculus, and inferior frontal occipital fasciculus in first-episode SCZ

	Di et al. (2009)					
	Dong et al. (2017)			X	X	Decreased FA in genu of corpus callosum, anterior thalamic radiation, uncinate fasciculus, inferior fronto-occipital fasciculus, superior longitudinal fasciculus, and cingulum in SCZ
	Ellison-Wright and Bullmore (2009)					
	Vitolo et al. (2018)					
	Yao et al. (2013)	FE				
	Zhao et al. (2021)					
Intrinsic brain activity	Gao et al. (2018)		X		X	Decreased CP in inferior frontal gyrus, angular gyrus, and insula, we well as increased CP in striatum and occipital cortex, in SCZ
	Gong et al. (2019)	FE-C	X		X	Decreased ALFF in postcentral gyrus, occipital cortex, precuneus, and inferior parietal lobule, as well as increased ALFF in anterior cingulate cortex, inferior frontal gyrus, inferior temporal gyrus, and putamen, in SCZ; decreased ALFF in medial prefrontal cortex, precuneus, and inferior parietal lobule (belonging to the default-mode network), as well as increased ALFF in putamen, in first-episode medication-naïve SCZ
	Kuhn and Gallinat (2013)					
	Townsend et al. (2022)			X	X	Decreased CM in anterior cingulate cortex and orbitofrontal cortex in SCZ
Task-based activation	Alústiza et al. (2017)		X		X	Decreased TBA in anterior cingulate cortex/supplementary motor area, middle frontal gyrus, inferior parietal lobule, thalamus, and cerebellum as well as increased TBA in occipital cortex and precentral gyrus, in SCZ during cognitive processing; decreased TBA in anterior cingulate cortex/supplementary motor area, occipital cortex, and striatum, as well as increased TBA in superior parietal gyrus, inferior frontal gyrus, and temporal pole in SCZ during cognitive processing of timing
	Arioli et al. (2021)					
	Arsalidou et al. (2020)		X			Decreased TBA in fusiform gyrus, increased TBA in inferior frontal gyrus, and altered TBA in precuneus and cerebellum in early-onset SCZ during cognitive processing
	Casale et al. (2016)	FE				
	Chase et al. (2018)					

	Dong et al. (2018)		X		X	Decreased TBA in amygdala-hippocampal complex, fusiform gyrus, inferior frontal gyrus, and thalamus, as well as increased TBA in medial prefrontal cortex, in chronic SCZ during emotion processing of negative stimuli
	Dugré et al. (2019)					
	Jáni et al. (2018)		X	X	X	Decreased TBA in inferior frontal gyrus/insula and anterior cingulate cortex, as well as increased TBA in posterior parietal cortex, occipital cortex, and middle frontal gyrus, in SCZ during emotion processing; decreased TBA in insula, superior frontal gyrus/anterior cingulate cortex, and occipital cortex, as well as increased TBA in inferior/superior frontal gyrus and posterior parietal cortex, in SCZ during cognitive processing of theory of mind
	Kompus et al. (2011)					
	Kronbichler et al. (2017)		X		X	Decreased TBA in medial prefrontal cortex, temporoparietal junction, premotor cortex, and occipital cortex, as well as increased TBA in posterior parietal cortex, in SCZ during cognitive processing of theory of mind
	Li et al. (2010)					
	McTeague et al. (2017)					
	McTeague et al. (2020)					
	Minzenberg et al. (2009)					
	Ortuño et al. (2011)					
	Picó-Pérez et al. (2022)	FE-C		X	X	Decreased TBA in dorsomedial/lateral prefrontal cortex and angular gyrus in SCZ during cognitive processing; decreased TBA in superior parietal gyrus in early-stage SCZ during cognitive processing
	Ragland et al. (2009)					
	Taylor et al. (2012)					
	Vucurovic et al. (2020)					
	Wang et al. (2021)		X		X	Decreased TBA in dorsolateral/dorsomedial prefrontal cortex, precuneus, basal ganglia, and cerebellum, as well as increased TBA in anterior cingulate cortex, posterior cingulate cortex, and middle temporal gyrus, along with precentral gyrus and occipital cortex, in SCZ during cognitive processing of working memory
	Weng et al. (2022)					
	Wu et al. (2019)					

Alterations	Study	Group	JK	H	PB	Main Findings
	Zeng et al. (2022)		X			Decreased TBA in striatum (extending to insula), anterior cingulate cortex, superior temporal gyrus, and precentral gyrus in SCZ during emotion processing of positive stimuli (reward anticipation); decreased TBA in medial prefrontal cortex and dorsolateral prefrontal cortex, as well as increased TBA in striatum (extending to insula), parahippocampal gyrus, postcentral gyrus, middle cingulate cortex, and cerebellum, in SCZ during emotion processing of positive stimuli (reward outcome)
	Zhang et al. (2016)					
STRUCTURAL-FUNCTIONAL BRAIN CORRELATES OF SYMPTOMS OF SCHIZOPHRENIA						
Alterations	**Study**	**Group**	**JK**	**H**	**PB**	**Main Findings**
Auditory hallucinations	Palaniyappan et al. (2012)		X			Correlation of auditory hallucinations in SCZ with decreased GM in insula/superior temporal gyrus
	Jardri et al. (2011)					
	Kompus et al. (2011)					
	Kuhn and Gallinat (2012)					
	Zmigrod et al. (2016)					
Visual hallucinations	Zmigrod et al. (2016)					
Formal thought disorder	Wensing et al. (2017)					
Motor deficits	Zhao et al. (2014)					

Abbreviations: JK, Jackknife sensitivity analysis; H, analyses of heterogeneity; PB, publication bias tests; CHR, clinical high risk for schizophrenia; SCZ, schizophrenia; FE, first episode of psychosis/early stage of schizophrenia; C, chronic stage of schizophrenia; GM, grey matter; WM, white matter; FA, fractional anisotropy; ALFF, amplitude of low-frequency fluctuations; CM, cerebral metabolism; CP, combined parameters; TBA, task-based activation.